

The authors thank both referees for very helpful and constructive comments, which have allowed us to clarify and improve the manuscript. Below we address the reviewer' comments, with the original comments in black, and our response in blue. We have revised the manuscript accordingly. Major changes include: (1) Added a figure (Fig. 8) comparing model prediction with more CLOUD data points (per request of Referee #1), and (2) Put the technical details related to the used thermodynamic and other data as well as QC calculations into a separate Appendix (per request of Referee #3). These changes do not affect the main conclusions of this manuscript.

All changes made to the manuscript have been marked with Track-Change tool in one of submitted files.

Anonymous Referee #1

Review of "H₂SO₄-H₂O-NH₃ ternary ion-mediated nucleation (TIMN): Kinetic-based model and comparison with CLOUD measurements" by F. Yu et al.

The manuscript presents a kinetic, quasi-unary molecular cluster and aerosol particle model to simulate ternary ion-mediated nucleation (TIMN) from sulfuric acid (H₂SO₄), water (H₂O) and ammonia (NH₃). This work extends the previously developed binary H₂SO₄-H₂O (BIMN) model (Yu, 2006b) to include also ammonia. This is done by using quantum chemical data for some H₂SO₄-H₂O-NH₃ molecular clusters (some of which have been previously published by the authors, and some of which are new but not yet published) and previously measured experimental thermodynamic data for bulk solutions, and implementing them in the model. Model results for the formation rate J_{1.7} of nanoparticles of 1.7 nm are compared to rates derived from particle measurements at the CLOUD aerosol chamber.

The manuscript is fairly clearly written and suits in the scope of ACP. However, the model details need further clarification, and some assumptions and approximations made in the model require justification and/or more discussion. Also, discussion of the results with respect to experiments and other nucleation parameterizations or models needs to be more balanced. After the authors have addressed these issues (as listed in detail below), the study can be considered for publication in ACP.

We appreciate the time and effort of the referee in providing the detailed comments. Please see below for our point-to-point replies and clarifications.

Specific comments:

The most important issues regarding the model can be summarized as follows:

The authors claim to present "the first comprehensive kinetically-based H₂SO₄-H₂O-NH₃ ternary ion-mediated nucleation (TIMN) model that is based on the thermodynamic data derived from both quantum-chemical calculations and laboratory measurements."

However, it turns out that the model is in fact quasi-unary, i.e. approximates the multicomponent chemical system as a one-compound system. Also, the quantum-chemical data is rather sparse, liquid thermodynamic data is used from quite small nanoparticle sizes onward, and the rest of the thermodynamics is in practice guessed by connecting quantum chemical and bulk data by an exponential function.

These facts and the related uncertainties should be clearly brought up and discussed. Considering the roughness of some approximations, the suggestion that the model is in excellent agreement with CLOUD data needs much more comparisons and more than a few data points from CLOUD.

We feel that the referee probably misunderstood the TIMN model. As shown in Figures 1 and 3 and discussed in the text, the model is multicomponent and does not approximate multicomponent systems by one-component system. First of all, the distributions of small

clusters of variable chemical composition were explicitly calculated (Figure 3) as a function of T, RH, and $[\text{NH}_3]$. Secondly, the compositions of neutral, positively charged and negatively charged clusters studied here are different. Thirdly, the model explicitly accounts for the formation and properties of both binary and ternary clusters and the interactions between neutral and charged clusters.

As for the amount of quantum-chemical data used to constrain the model, the TIMN model is constrained by a large amount of QC data available at the present time that was obtained using PW91PW91/6-311++G(3df,3pd) method. We have pointed out clearly in the manuscript that since the formation of small clusters is the limiting step for nucleation, improving nucleation thermodynamics by applying QC data is critically important. While interpolation or extrapolation may lead to possible uncertainties which has been clearly acknowledged in the original manuscript, this approach provides nucleation thermochemistry of much better quality than conventional bulk liquid/capillarity approximation, which fails to predict free energies and formation rates of small molecular clusters, and is innovative in terms of connecting thermochemical properties of QC data for small binary and ternary clusters that cannot be adequately described by the capillarity approximation with those for large clusters that can be adequately described by the very same capillarity approximation. In order to address the Reviewer's concern, additional discussion on uncertainties associated with the interpolation has been added to the revised manuscript.

As for the comparison with CLOUD data, Figures 6 & 7 show clearly that we have compared our model predictions with 48 data points from CLOUD measurement in the original manuscript. The comparisons include the dependences of nucleation rates on all the key parameters controlling nucleation rates: $[\text{NH}_3]$, ion production rate, $[\text{H}_2\text{SO}_4]$, temperature, and RH. In order to address the Reviewer's concern, we have made additional comparisons with CLOUD data and included them in the revised manuscript.

Thermodynamic data

The thermodynamic input data includes quantum chemical (QC) data for the very smallest clusters of a few molecules. Particles containing more than at least ten sulfuric acid molecules are assumed to behave according to the electrically neutral macroscopic liquid droplet model. For the intermediate sizes below ten H_2SO_4 molecules, QC data and liquid data are connected together by a type of exponential function.

(1) In general, it would be extremely helpful to explain the thermodynamic data in the form of a table which lists the different cluster / particle compositions and sizes, and the approaches used for their Gibbs free energies. It's much easier and faster for the reader than finding the information in the text.

Agreed. QC data are already in the form of a table (see Tables A1-A4).

Quantum chemical (QC) data for small molecular clusters

The QC data has been obtained using the PW91PW91/6-311++G(3df,3pd) density functional theory (DFT) method. PW91 is a commonly used DFT method in atmospheric cluster calculations, and it has been shown to yield mean errors similar to (although somewhat higher than) other common DFT methods in QC benchmarking studies (e.g. Elm and Kristensen, 2017).

In terms of the number of sulfuric acid molecules, which is the principal building block of the clusters and particles in the presented kinetic model, the used QC data covers cluster sizes up to (a) 1 sulfuric acid molecule for positively charged, (b) 4 for

negatively charged (5 if the bisulfate ion is counted in), and (c) 4 for electrically neutral clusters.

(2) Page 5, line 152: "The thermodynamic data sets used for binary clusters were also updated." For which clusters were the data updated: All or just some of them? What kind of differences are there compared to the previously published data for these clusters?

We have meant that the scheme to calculate the evaporation rates of binary clusters has been updated. In the previous IMN model (Yu, ACP, 2006), the evaporation rates of binary clusters were calculated with an equation considering the Thomson effect and dipole-charge interaction (Eq. 14 in Yu (2006)). The present TIMN uses quite different approach to calculate the evaporation rates, as detailed in the text. In order to avoid confusion, this sentence has been deleted.

(3) Page 9, line 250: "We have extended the earlier QC studies of binary and ternary clusters to larger sizes."

Which sizes? Please indicate clearly which clusters are new, and which have been studied in previous publications. Also, list clearly the clusters for which QC data is applied (instead of other type of thermodynamic data). Are these the clusters listed in Tables 2-4?

Yes, these are clusters listed in Tables A2-A4. The data from earlier studies and experimental data are properly marked, and notes describing their origin are given below the tables.

(4) Page 9, lines 254-255: The authors have used also a "locally developed sampling code, which creates a 'mesh' around the cluster, in which molecules being attached to the cluster are the mesh nodes", but this sentence is all that is said about the code. Please elaborate what this code exactly does, and give a reference, if possible.

The code is based on the following principle: mesh, with molecule to be added to the cluster placed in the mesh nodes, is created around the cluster, and blind search algorithm is used to generate the guess geometries. The mesh density and orientation of molecules are variable, as well as the minimum distance between molecules and cluster. We have added this elaboration to the revised manuscript.

(5) Page 10, lines 289-292: "Both the absolute values and trends in ΔG_{0+w} derived from calculations are in agreement with the laboratory measurements within the uncertainty range of $\pm 1-2$ kcal mol⁻¹ for both QC calculations and measurements. This confirms the efficiency and precision of QC methods in calculating thermodynamic data needed for the development of nucleation models."

$\pm 1-2$ kcal mol⁻¹ can be expected to be the general uncertainty of quantum chemical methods. However, as the Gibbs free energies are incorporated in the exponential factor of the evaporation rate (Eq. (7)), this uncertainty may propagate to an uncertainty of up to orders of magnitude in the particle formation rates and concentrations. This is discussed and demonstrated e.g. by Kürten et al. (2016), who estimated the uncertainties in the modeled particle formation rates by increasing or decreasing all Gibbs free energies by 1 kcal mol⁻¹. Depending on the conditions, this changes the formation rate by less than an order of magnitude, or even by up to several orders of magnitude. Please discuss also the sensitivity of the particle kinetics to the evaporation rates, and the impact of the uncertainties in ΔG on the formation rate.

We agree with the referee that the uncertainties in computed free energies of $1-2$ kcal mol⁻¹ may lead to large uncertainties in particle formation rates under some conditions. However, uncertainties estimated by Kürten et al. (2016) represent the upper limit because estimates of Kürten et al. (2016) do not consider the error cancellation. In reality there probably does not exist such a thing as a systematic error of plus or minus 1 kcal mol⁻¹ assigned to each step of the

cluster formation, because computed free energies may be overestimated for some clusters and underpredicted for others that leads to partial or, in some case, full error cancelation. In order to make it clear, we have added discussion on these matters in the revised manuscript.

(6) Page 11, lines 321-322: "Since positively charged H₂SO₄ dimers are expected to contain large number of water molecules, no quantum chemical data for these clusters are available."

What does this mean? Does it mean that the data cannot be computed at all, or that the authors haven't computed such data in these studies?

This means that neither the authors nor other groups have computed these clusters. While it is hypothetically possible to compute them, no one has it done so far. Here the most difficult part is the adequate configurational sampling because the number of conformers is growing quickly with increasing hydration number and cluster size. We have modified the sentence to make it clear.

(7) Page 12, lines 348-351: "Table 3 shows that the presence of NH₃ in H₂SO₄ clusters suppress hydration and that ΔG_{0+W} for S₂A₂ falls below -2.0 kcal mol⁻¹. This is consistent with earlier studies by our group and others showing that large S_nA_n clusters (n>2) are not hydrated under typical atmospheric conditions."

Please give references for these studies, especially for those conducted by other groups. Does this mean that all clusters and nanoparticles larger than (H₂SO₄)₂(NH₃)₂ are generally not hydrated, or do the particles become hydrated again at some larger size? At which size? What is assumed about the hydration of electrically neutral H₂SO₄-NH₃ clusters beyond the quantum chemistry data set, i.e. larger than (H₂SO₄)₄(NH₃)₅?

Generally, the hydration of a specific cluster (S₂A₂) tells nothing about the hydration of other clusters with different numbers of acid and base molecules. Therefore, it should be stated here that neglecting water in the larger clusters is just an assumption that has to be made due to the lack of thermodynamic data (as the authors have actually done later on line 454).

We have added references to the relevant studies in the revised manuscript:

Henschel, H., Navarro, J. C. A., Yli-Juuti, T., Kupiainen-Määttä, O., Olenius, T., Ortega, I. K., ... & Vehkamäki, H. (2014). Hydration of atmospherically relevant molecular clusters: Computational chemistry and classical thermodynamics. *The Journal of Physical Chemistry A*, 118(14), 2599-2611.

Henschel, H., Kurtén, T., & Vehkamäki, H. (2016). Computational study on the effect of hydration on new particle formation in the sulfuric acid/ammonia and sulfuric acid/dimethylamine systems. *The Journal of Physical Chemistry A*, 120(11), 1886-1896.

Herb, J., Nadykto, A. B., & Yu, F. (2011). Large ternary hydrogen-bonded pre-nucleation clusters in the Earth's atmosphere. *Chemical Physics Letters*, 518, 7-14.

We agree with the Referee that the hydration of a specific cluster (S₂A₂) tells nothing about the hydration of other clusters with different numbers of acid and base molecules, and that neglecting water in the larger clusters is just an assumption that has to be made due to the lack of thermodynamic data. We have pointed this out in the revised manuscript. However, it is also important to note that the recent study by Henschel et al. (2016) confirms our conclusion. In particular, Fig. 3 in their study shows clearly that in the case of fairly large cluster consisting of 3 H₂SO₄ and 3 NH₃ molecules, the average hydration number is less than 0.7 even if RH=100%.

(8) Page 12, lines 365-367: “This finding is fully consistent with the laboratory measurements showing that growth of neutral S_sA_a clusters follows $s = a$ pathway (Schobesberger et al., 2015).”

The study by Schobesberger et al. (2015) does not present any measurement data for neutral clusters. (Instead, they are modeled by the ACDC program in that study.) Please correct the sentence.

Corrected.

(9) Page 13, lines 389-393: “ $_G0$

+s values for $S-S_3-4W_w$ are consistently $_1.5-3$

kcal mol⁻¹ less negative than the corresponding semi-experimental estimates (Table 4). The possible reasons behind the observed systematic difference are yet to be identified and include the use of low-level ab initio HF method to compute reaction enthalpies and uncertainties in experimental enthalpies in studies by Froyd and Lovejoy (2003).”

The computed values for $_G0+W$ (as well as for $_G0+W$ for some positive clusters), on the other hand, are more negative than those determined by Froyd and Lovejoy (2003). Why doesn't the discussed systematic difference apply to these values?

Yes, it's applicable to all the relevant comparisons. Another important issue is that there exist multiple sources of uncertainties in the data sets of Froyd and Lovejoy (2003). First of all, the data sets for both positively and negatively charged clusters are not strictly experimental. While in the case of negative clusters, the low level ab initio is used to get the final semi-experimental energy values, in the case of positive ions, a theoretical thermochemical cycle is applied. The accuracy of these “experimental” data are pretty much unknown; however, these data sets are currently the only ones that report some sort of experimental values for negative and positive clusters of sulfuric acid with water and, thus, we had no choice other than to compare computed data with these particular data sets.

(10) Page 15, lines 471-472: “In the TIMN model, the equilibrium distributions are used to calculate number concentrations weighted stepwise Gibbs free energy change”

Where is this averaged $_G$ used in the model? Doesn't the model use averaged evaporation frequencies (Eq. (10)), which are calculated over the individual evaporation rates and thus do not correspond to the averaged $_G$?

The mode actually uses the averaged $\overline{\Delta G_{s-1,s}}$ to calculate averaged evaporation rates. To avoid confusion, we have modified Eq. (10) (Eq. 12 in the revised manuscript).

(11) Page 15, lines 477-479: “In the atmosphere, where substantial nucleation is observed, the sizes of critical clusters are generally small ($s < 5-10$) and nucleation rates are largely controlled by the stability (or) of small clusters with $s < 5 - 10$.” Please give references for this.

The number of H_2SO_4 molecules in critical clusters has been estimated from $d(\ln J)/d(\ln[H_2SO_4])$. A reference (Sipilä et al., Science, 2010) is now added.

(12) Table 2 and discussion on pages 17-19: For positively charged clusters, there is QC data only up to clusters containing one H_2SO_4 molecule and two NH_3 molecules. That is, not even the first growth step with respect to H_2SO_4 clustering (i.e. the formation of a H_2SO_4 dimer) is covered, and in practice all the data for positive clusters is guessed by using Eq. (11) (except for clusters containing more than 10 acid molecules, starting from which data for electrically neutral bulk solutions is used also for the positive clusters).

This is an extremely crude approximation. Please bring up this fact, and explain what new “insights” we can learn about the thermodynamics of these clusters by using these type of data.

We agree with the referee that the QC data for positively charged clusters are very limited and the interpolation approximation is subject to large uncertainty. In order for the nucleation on positive ions to occur, the first step is for H₂SO₄ to attach to a positive ion that does not contain H₂SO₄. Unlike negative ions, the effect of charge on the bonding of H₂SO₄ with positive ions is much weaker and thus the stepwise Gibbs free energy change for the addition of one H₂SO₄ molecule to form a positively charged cluster is likely to be similar to that of neutral clusters, i.e., decreasing with cluster size. Therefore, the QC data for positively charged clusters containing one H₂SO₄ molecule provides a critical constrain. The success of the model in predicting the [NH₃] needed for nucleation on positive ions to occur (Fig. 6) show the usefulness of the first step data and approximation. Nevertheless, we agree with the referee about the uncertainty and bring up the fact of the lack of thermodynamic data for positive ions in the revised manuscript.

(13) Page 17, lines 536-538: Similarly to positive clusters, the results for the thermodynamics of negative clusters raise some questions: “The effect of NH₃ on negative ions becomes important at $s \geq 4$, when bonding between the clusters and NH₃ becomes strong enough to contaminate a large fraction of binary clusters with ammonia (Fig.3).” No QC data or experimental bulk data is used for the clusters around sizes $s = 4 - 9$. Considering that this behavior is deduced by interpolating between QC data for small clusters that take up ammonia rather weakly, and macroscopic solution data for an electrically neutral H₂SO₄-H₂O-NH₃ liquid, it is difficult to see this result as very reliable. Please state that the thermodynamics of these clusters are highly uncertain (or explain why they would not be).

This is a good point. We feel that the interpolation is more than likely a reasonable approximation for negatively charged clusters with $s=4-9$, as indirectly confirmed by the success of our model in predicting the observed dependence of nucleation rates on [H₂SO₄] and [NH₃] (Figs. 6 and 7). Please note that in many conditions where nucleation is significant, $s \leq 5$ and the uncertainty associated with the interpolation is small. We agree that further experimental or QC study will be helpful to reduce the uncertainty and have empathized this in the revised manuscript.

(14) Table 4: The hydrate data for the negatively charged clusters is quite sparse for some clusters. Why are not hydrates with more water molecules considered for, for example, S-S₁ or S-S₂?

The hydration of these clusters is weak and, thus, does not impact the cluster formation because none of them are hydrated under typical atmospheric conditions (see refs. below).

Herb, J., Xu, Y., Yu, F., & Nadykto, A. B. (2012). Large hydrogen-bonded pre-nucleation (HSO₄⁻)(H₂SO₄)_m(H₂O)_k and (HSO₄⁻)(NH₃)(H₂SO₄)_m(H₂O)_k clusters in the Earth’s atmosphere. *The Journal of Physical Chemistry A*, 117(1), 133-152.

Nadykto, A. B., Yu, F., & Herb, J. (2008). Towards understanding the sign preference in binary atmospheric nucleation. *Physical Chemistry Chemical Physics*, 10(47), 7073-7078.

(15) Tables 2-4: Why isn’t all QC data that is used in the model given in the tables? For example, binary electrically neutral clusters are not included in Table 3. Please indicate clearly where these data can be found.

To keep the manuscript concise, we choose not to repeat results already published unless really necessary. We have provided references for the binary neutral clusters.

Nadykto, A. B., Al Natsheh, A., Yu, F., Mikkelsen, K. V., & Herb, J. (2008). Computational quantum chemistry: A new approach to atmospheric nucleation. *Advances in quantum chemistry*, 55, 449-478.

Herb, Jason, Alexey B. Nadykto, and Fangqun Yu. "Large ternary hydrogen-bonded pre-nucleation clusters in the Earth's atmosphere." *Chemical Physics Letters* 518 (2011): 7-14.

(16) Figure 3: Why are some hydrates with different numbers of water molecules grouped together? For instance, $(\text{H}_2\text{SO}_4)_2(\text{H}_2\text{O})_{1-7}$ is presented as one bar; this doesn't tell much about the hydration as 1 and 7 are quite different numbers. Also, in panel (d), please clarify that there is no hydrate data for these clusters; otherwise the figure panel might be understood so that the clusters don't take up water at all.

We group together some clusters with different numbers of water molecules to make the figure more clear and neat. We have clarified it in the figure caption for panel (d) as suggested by the Reviewer.

(17) Figure 4: Why is the cumulative Gibbs free energy zero for the first growth steps of the negative clusters in panel (b)? In panel (a), it does not look like these values add up to zero, but should be negative instead.

$\overline{\Delta G}_{s-1,s}$ for small negatively charged clusters are strongly negative, implying that their formation is barrierless. However, these small clusters cannot be considered as nucleated particles because $\overline{\Delta G}_{s-1,s}$ can become positive for larger clusters due to the charge effect decreasing quickly as the clusters are growing. The negative $\overline{\Delta G}_{s-1,s}$ for small clusters is not able to cancel the positive $\overline{\Delta G}_{s-1,s}$ for larger clusters and thus $\overline{\Delta G}_{s-1,s}$ for small clusters are set to zero when they are negative in the cumulative Gibbs free energy calculation. This has been pointed out in the revised manuscript.

(18) Caption of Figure 4: "Calculations were carried out at T=292 K, RH=38%, $[\text{H}_2\text{SO}_4]=3 \times 10^8 \text{ cm}^{-3}$ and $[\text{NH}_3]= 0.3 \text{ ppb}$." How were the vapor concentrations, e.g. $[\text{H}_2\text{SO}_4]$, used in the calculations?

P in Eq. (12) (Eq. 11 in the revised manuscript).

Experimental bulk data for larger nanoparticles

Bulk thermodynamic data is assumed for particles of all charging states containing at least ten H_2SO_4 molecules. While this is in practice the only available option due to the lack of other type of data, the approximation calls for some discussion about the related uncertainties.

(19) At which conditions (temperature, partial pressures of the H_2SO_4 , NH_3 , H_2O vapors) were the measurements (Marti et al., 1997; Hyvärinen et al., 2005) performed? How reliably can it be extrapolated to different conditions outside the measurement range?

The conditions of the measurements are given and possible uncertainties are discussed in the revised manuscript.

(20) Page 16, lines 487-491: "Based on experimental data (Kebarle et al., 1967;

Davidson et al., 1977; Wlodek et al., 1980; Holland and Castleman, 1982; Froyd and Lovejoy, 2003), the stepwise ΔG values for clusters decreases exponentially as the cluster sizes increase and approaches to the bulk values when clusters containing more than 8-10 molecules (Yu, 2005)."

Is possible size-dependent chemical composition, i.e. acid:base molar ratio, considered here (e.g. Chen et al., 2018)? How does it affect the model results?

This is a general statement about the decrease of stepwise ΔG with the size of charged clusters. The possible size-dependent chemical position may be taken into account implicitly through the interpolation as the compositions of small clusters are different from those of large ($s > 10$) clusters. Please see reply to comment #13 for the discussion concerning impacts of on our model results.

(21) Page 16, lines 491-494: "Cluster compositions measured with an atmospheric pressure interface time-of-flight (API-TOF) mass spectrometer during CLOUD experiments also show that the chemical effect of charge-carrying becomes unimportant when the cluster contains more than 9 H₂SO₄ molecules (Schobesberger et al., 2015)." In the study by Schobesberger et al. (2015), it looks like the different charges approach similar composition somewhere in the size range where the H₂SO₄ content is 20-100 molecules (Figure 9 in the study). At 10 H₂SO₄ molecules, the composition of negative and positive particles is still different. Please comment.

Figure 9 of Schobesberger et al. (2015) shows that the difference in the composition of positively and negatively charged clusters quickly decreases as number of H₂SO₄ molecules increases from 1 to ~ 10 and exhibits little further changes. It is true that at 10 H₂SO₄ molecules, the composition of negative and positive particles is still different but the difference is much smaller than that in the case of small clusters. We have pointed this out in the revised manuscript.

(22) Page 17, line 524: "consistent with the laboratory measurements (Marti et al., 1997)" Isn't the discussed ΔG data derived from these measurements (i.e. naturally, it is consistent)? Please clarify.

Yes. The sentence has been modified to make it clear.

Page 24, lines 774-776: Is this the correct reference?

This is a wrong reference. Thank you for pointing this out. The correct one is: Hyvärinen, A., T. Raatikainen, A. Laaksonen, Y. Viisanen, and H. Lihavainen, Surface tensions and densities of H₂SO₄ + NH₃ + water solutions, *Geophys. Res. Lett.*, 32, L16806, doi:10.1029/2005GL023268, 2005.

Approximated values for intermediate sizes with < 10 H₂SO₄ molecules

(23) Eq. (11): What is this "extrapolation" formula based on? It is not clear why this functional form would be suitable for connecting QC and bulk measurements. Please explain clearly how the formula is derived, and discuss the related uncertainties.

Linear and exponential extrapolations are two common methods for this type of application. We choose exponential extrapolation as it fits better the stepwise ΔG change of neutral clusters that QC data are available. The related uncertainties are discussed in the revised manuscript.

(24) Page 16, lines 503-506: "c in Eq. (11) is the exponential coefficient that determines how fast $\Delta G_{s-1,s}$ approaches to bulk values as s increases. In the present study, c is estimated from $\Delta G_{s-1,s}$ at s=2 and s=3 for neutral binary and ternary

cluster for which experimental (Hanson and Lovejoy, 2006; Kazil et al., 2007) or quantum-chemical data (Table 3) are available.”

What can the data for clusters that contain 2 or 3 H₂SO₄ molecules possibly tell about how fast β approaches bulk values?

Is β estimated based on QC data, experimental data, or both? How is this done exactly? Is it only for neutral clusters, or also for charged clusters?

It's an approximation. See our reply to comment 23 above. In the present model, we estimated β based on QC data of neutral clusters. We acknowledge that the extrapolation approximation is subject to uncertainty but this is the best approach we can come up with at this point in order to develop a model that can be applied to all conditions. Further QC and experimental studies of the thermodynamics of larger clusters can help to reduce the uncertainty.

(25) Finally, the most important issue regarding the thermodynamics is the fact that the “critical sizes”, i.e. the barriers for nucleation, are located around cluster sizes for which there is no reliable thermodynamic data (Figure 4). For all different types of clusters (binary, ternary, all charging states), the maximum of the free energy curve is beyond the QC data (or just at the upper limit of the QC data in the case of negative ternary clusters). That is, the critical stage of nucleation is based on Eq. (11), which in turn does not seem to be based on an actual physical model.

Considering this, can the model really give important new information on H₂SO₄-H₂O-NH₃ particle formation mechanisms?

The maximum of the free energy curve shown in Fig. 4b is the accumulative free energy change and the maximum value (or nucleation barrier) is dominated by smaller clusters (Fig. 4a). In other words, the formation of small clusters are limiting steps and the uncertainty of stepwise ΔG for larger clusters where QC data are not available has limited impact on the predicted nucleation rate. As demonstrated in the paper, the model reveals the general favor of nucleation of negative ions, followed by nucleation on positive ions and neutral nucleation, for which higher NH₃ concentrations are needed, in excellent agreement with CLOUD measurements. The usefulness of the model can be seen from its success in reproducing the observed dependence of nucleation rates on various parameters and its ability to calculate nucleation rates under conditions for which measurements are not available.

Kinetic model

(26) In the kinetic model, the clusters are assumed to be in equilibrium with respect to both water and ammonia. Such equilibration assumption can be made if the time scales of the attachment and evaporation processes of some compound are substantially shorter than those of other compounds. This is the case for water, as (a) its concentration (to which the attachment, i.e. molecular collision, frequency is directly proportional) is around ~ 10 orders of magnitude higher than that of H₂SO₄ or NH₃, and (b) its binding to the clusters is so much weaker that its evaporation rate is \sim several orders of magnitude higher than that of other compounds (except for some charged clusters in e.g. Table 2).

This is, however, generally not the case for ammonia. The binding of NH₃ depends strongly on the cluster composition: Depending on the acid:base ratio, either NH₃ or H₂SO₄ evaporates much faster than the other. Within the set of small clusters, the weakest and strongest bindings of NH₃ are of the same order as those of H₂SO₄ (e.g. Table 3). The collision rates of NH₃ are not necessarily multiple times higher than those of H₂SO₄, either: While ammonia is generally more abundant than H₂SO₄ in the atmosphere, there are environments where [H₂SO₄] and [NH₃] are around the same order (such as some of those simulated in this study).

Due to these reasons, the explanation for assuming equilibrium with respect to NH₃ is not justifiable (pages 13-14, lines 414-418): "In the lower troposphere, where most of

the nucleation events were observed, [H₂SO₄] is typically at sub-ppt to ppt level, while [NH₃] is in the range of sub-ppb to ppb levels. This means that small ternary clusters can be considered to be in equilibrium with H₂O and NH₃ vapors."

(a) Doesn't ammonia need to also evaporate much faster from the clusters for the equilibrium assumption to be justified? (b) At the simulated conditions, [H₂SO₄] and [NH₃] are in many cases of the same order. For instance, in Figure 6 at the lower end of the [NH₃] axis, [NH₃] is of the same order or even lower than [H₂SO₄]. In Figure 7a, [NH₃] is around 10 ppt, i.e. $\sim 10^8 \text{ cm}^{-3}$, and [H₂SO₄] is around $10^7 \dots 10^9 \text{ cm}^{-3}$.

Please show that the equilibrium with respect to NH₃ really is a valid assumption for these simulation systems.

For the equilibrium assumption to be justified, the collision rate of clusters with NH₃ should be substantially higher than that with H₂SO₄. The evaporation rate of NH₃ depends on the composition of the cluster and can be very fast when NH₃:H₂SO₄ ratio are above one for small clusters. In many atmospheric conditions, especially in lower troposphere, [NH₃] is generally a few orders of magnitude higher than [H₂SO₄] and equilibrium assumption should be reasonable. For practical applications, nucleation rates are generally predicted based on the assumption that the clusters are in equilibrium and nucleation rates reach the steady state. Please note that the nucleation rates measured in CLOUD are also steady state values.

We agree with the Referee that the system may deviate from equilibrium if [NH₃] is less than or close to [H₂SO₄]. Under such cases, the equilibrium assumption may overestimate nucleation rates. We have added discussion on these matters in the revised manuscript. It should be noted that all previous ternary nucleation models discussed in Section 2.1 assume the equilibrium with respect to NH₃.

(27) Some other aspects of the model also need clarification. The kinetic equations (Eqs.(1-6)) seem to include also collisions between charged clusters / particles of the same polarity. How high are the rate constants for such processes? Doesn't electrostatic repulsion prevent these attachments?

Further, if multiply charged particles can form in these collisions, how are these different charge numbers treated in the model? Shouldn't there be separate equations for particles that contain a single charge, two charges, three, and so on?

Yes, the electrostatic repulsion is too strong for small clusters to gain more than one charge. However, small charged clusters can be scavenged by large pre-existing particles of same polarity. Large pre-existing particles serve as the sink for small clusters in the model and the effect of multiple charge is small and thus is not tracked.

(28) Page 5, lines 162-166: "The initial negative ions, which are normally assumed to be NO₃⁻, are converted into HSO₄⁻ core ions (i.e., S⁻) and, then, to larger H₂SO₄ clusters in the presence of gaseous H₂SO₄. The initial positive ions H₊W_w are converted into H₊A₁₋₂W_w in the presence of NH₃, H₊S_sW_w in the presence of H₂SO₄, or H₊A_aS_sW_w in the case, when both NH₃ and H₂SO₄ are present in the nucleating vapors." What are the rate constants for the conversions of NO₃⁻ and H₊W_w?

This is a general statement of ion clustering process in the atmosphere when nucleation occurs. The rate constant for the conversion of initial negative and positive ions to the one containing H₂SO₄ is the typical ion reaction rate of $\sim 2 \times 10^{-9} \text{ cm}^3 \text{ s}^{-1}$.

What does H₊A₁₋₂W_w (or H₊S_sW_w and H₊A_aS_sW_w) mean, i.e. how many ammonia and water molecules does it contain?

It's a general expression of cluster formula. As given in the Figure 1 caption, S, W, and A represent sulfuric acid (H₂SO₄), water (H₂O), and ammonia (NH₃) respectively, while *s*, *w*, and *a* refer to the number of S, W, and A molecules in the clusters/droplets, respectively.

In the equations (page 7, lines 192-193), "N₊, -₀ and Q are the concentration of initial ions not containing H₂SO₄ and the ionization rate, respectively"

What do the "initial ions" refer to, e.g. H₊W_w or H₊A₁₋₂W_w? NO₃⁻ or HSO₄⁻?

Initial positive ions include both H⁺W_w and H⁺A₁₋₂W_w (in equilibrium). Negative initial ion is NO₃⁻.

(29) Eq. (3): Why does the evaporation term for creating H₂SO₄ monomers from a dimer includes a factor of two ($\gamma_{j,2}$), but the corresponding collision term, removing monomers in the collision creating a dimer, does not?

Evaporation of one dimer generates two monomers. For the corresponding collision term (monomer with monomer), a factor of two (in loss) cancels the double count of collisions among monomers.

(30) Page 8, lines 212-213: "The methods for calculating $\gamma_{j,1}$, $\gamma_{j,2}$, and $\gamma_{j,3}$ for binary H₂SO₄-H₂O clusters have been described in detail in Yu (2006b)."

I was not able to find the descriptions for $\gamma_{j,1}$, $\gamma_{j,2}$, and $\gamma_{j,3}$ in the given reference; the paper only seems to re-direct the reader to discussion in 3 other papers. Please briefly summarize how these parameters are obtained.

We have added additional references and a brief description.

(31) Page 8, lines 221-222: "N₀ is the number concentration of H₂SO₄ at a given T under the reference vapor pressure P of 1 atm."

Isn't N₀ simply the number concentration corresponding to the reference pressure P of the QC calculations? What does it have to do with any [H₂SO₄]? In general, the evaporation rate should not be related to the concentration of any compound, as it does not depend on the composition of surrounding vapor (only on the temperature, i.e. the inert gas).

The referee is correct that the evaporation rate should not be related to the concentration of any compound. N₀ in the equation will be cancelled out with the N₀ in $\Delta G_{i-1,i}$. Details of the derivation and relationship can be found in the reference given (i.e., Yu, 2007). Please note that we have corrected a missed term in Eq. (8).

(32) Page 8, lines 223-225: "The temperature dependence of γ_{H_0} and γ_{S_0} , which is generally small and typically negligible over the temperature range of interest, was not considered." Can you give a reference for the negligible temperature dependence?

The conclusion is based on typical calculated ΔC_p , which largely controls the temperature dependence of ΔH and ΔS (see A.B. Nadykto et al. / Chemical Physics 360 (2009) 67–73 and references therein) and does not exceed a few tens of cal/mol/K in most cases studied here. The reference is added to the revised text.

(33) Page 19, lines 572-573: "mean evaporation rate ($\bar{\gamma}$) of an H₂SO₄ molecule"

Is it assumed that only a single H₂SO₄ molecule evaporates, i.e. no water ligands, for instance, are attached to it? If so, please discuss the validity of this assumption, or even better, average the evaporation rates over all evaporation pathways with different

numbers of other compounds attached to the acid molecule.

Yes, the present model assumes only a single H_2SO_4 molecule evaporates. This is likely the dominant evaporation pathway. We have pointed this out in the revised manuscript.

(34) Page 19, lines 573-574: “The shapes of \bar{J} curves are similar to those of $\bar{J}_{s-1,s}$ (Fig. 4a) as \bar{J} values are largely controlled by $\bar{J}_{s-1,s}$.”
How is \bar{J} related to the averaged values $\bar{J}_{s-1,s}$? Isn't \bar{J} calculated based on individual values $\bar{J}_{s-1,s}$ (Eq. (10)), i.e. not exactly equivalent to $\bar{J}_{s-1,s}$?

Please see our reply to comment #10 above.

(35) The discussion on page 19, lines 575-584, feels somewhat confusing: First it's said that the effect of ammonia is significant for larger clusters and of less importance for small clusters (e.g. “the binding of NH_3 to small neutral and charged clusters are weaker compared to that for larger clusters”), but after this it's concluded that “The nucleation rates, limited by formation of small clusters ($s < 5$), depend strongly on the stability or evaporation rate of these small clusters and, thus, on $[\text{NH}_3]$.”
So is or is not NH_3 important for the small clusters and nucleation? Please clarify.

While the binding of NH_3 to small neutral and charged clusters is weaker compared to that to larger clusters, small clusters containing NH_3 are much more stable than those without (Fig. 4) and thus ammonia is important for nucleation. We have clarified this in the revised manuscript.

(36) Page 19, line 588: “the concentrations of clusters of all sizes are explicitly predicted”
A quasi-unary model cannot be called “explicit”; please re-formulate.

Please see our reply to the general comments in the beginning. To address the Reviewer's concern, we have deleted the word “explicitly” from the sentence.

(37) Eq. (13): Is it so that only growth through H_2SO_4 vapor is taken into account in the calculation of the particle formation rate? What about the effects of coagulation and recombination?

The quantity J that can be deduced from measurements -and that also is the relevant quantity for atmospheric modeling- includes all processes through which particles form, not only monomer condensation and evaporation. Therefore, these should be included also in the model-based formation rate.

For the chemical system considered in the present study, generally $N_1 \gg N_2 \gg N_3 \dots$. As a result, H_2SO_4 vapor growth dominates the steady state flux crossing 1.7 nm.

(38) Figure 1: The figure is confusing, and using patterns to fill the lines or spheres makes it somewhat difficult to read. For instance, it looks like “Condensation” means that electrically neutral clusters are ionized into charged particles (the arrows lead only to the charged blocks), and that “Coagulation / Scavenging” means that positively charged particles attached to each other or neutral particles. What is the difference between “Coagulation / Scavenging” and “Coagulation”?

We were trying to use “Scavenging” to represent the removal of small clusters by large pre-existing particles, also through coagulation. Condensation is actually implied in the green arrows. To avoid the confusion, we have deleted words “Condensation” and “Scavenging”.

Results and discussion

(39) As a general comment, the description of the model should be a bit less ambitious. As one-compound discrete-sectional kinetic models have existed at least since the 1970s, the model cannot be considered “first”, nor is it exactly “comprehensive” or “accurate” due to the quasi-unary assumption.

The addition of NH₃ to the previous BIMN model does not make the model very new, either, as it means simply using different thermodynamic data in an existing model - and the main author has also previously published a modeling study entitled “Effect of ammonia on new particle formation: A kinetic H₂SO₄-H₂O-NH₃ nucleation model constrained by laboratory measurements” (Yu, 2006a). Besides, as the authors themselves also bring up, the kinetics of H₂SO₄-H₂O-NH₃ molecular clusters including the different charging states have been previously modeled e.g. by the ACDC program (which the authors quite extensively criticize).

To address the Reviewer’s concern, we have removed “first” and “accurate”. For the reasons we gave in our reply to the general comments in the beginning, we think the present model is quite comprehensive.

(40) As previously (e.g. Nadykto et al., 2011; Nadykto et al., 2014), the main criticism is targeted at the modeling work by University of Helsinki (and this time also at the particle formation rate parameterization CLOUDpara based on the experimental data from the CLOUD chamber). In general, the authors criticize the ACDC model; however, the output of a clustering model is determined by the input parameters, namely the thermodynamic data. The ACDC program does not use any specific QC data, but the data is instead given by the user.

The ACDC data presented by Kürten et al. (2016) results from QC thermochemistry calculated with the RI-CC2/aug-cc-pV(T+d)Z//B3LYP/CBSB7 method. Therefore, the authors should call this rather e.g. “RI-CC2//B3LYP” data than “ACDC” data. The RI-CC2//B3LYP method is known to have a tendency to over-predict cluster stability, as has been discussed for example by the Helsinki group (e.g. Kupiainen-Määttä et al., 2015; Myllys et al., 2016), and thus it is not much used anymore in QC calculations.

We meant to point out the limitation of previous results which we aim to address in the present study. The over-predictions of the thermochemical stability of nucleating clusters by RI-CC2//B3LYP used in ACDC code was actually first pointed out by Nadykto et al. (2014) and discussed by Nadykto et al. (2015) and Kupiainen-Määttä et al. (2015). We agree with the Reviewer that ACDC program can use other types of QC data, however, the data obtained using ACDC we were referring to in the paper are based on RI-CC2//B3LYP thermochemistry. In order to address the Reviewer’s concern, we have replace “ACDC data” with “ACDC predictions based on nucleation thermochemistry obtained using RI-CC2//B3LYP method”.

(41) Page 4, lines 122-123: “ACDC is also an acid–base reaction model, with the largest clusters containing 4-5 acid and 4-5 base molecules (no water molecules)”: This is not the case, as ACDC is simply a program that solves the kinetic equations (similar to Eqs. (1-6)) for a given set of molecular clusters using given thermodynamic input data, which does not need to involve acids or bases. It is not limited to some fixed specific largest cluster sizes; in the cited studies, the largest sizes were determined by the availability of QC data for the systems of interest.

We have deleted this sentence.

(42) Page 4, lines 127-130: “In ACDC, the nucleation rate is calculated as the rate of clusters growing larger than the upper bounds of the simulated system (i.e., clusters containing 4 or 5 H₂SO₄ molecules) (Kurten et al., 2016) and thus may over-predict nucleation rates when critical clusters contain more than 5 H₂SO₄ molecules.” It is of course not reasonable to model a system where the critical size region is outside the system boundaries. Thus, this region should be examined before simulating given

conditions, as also discussed in the study by Olenius et al. (2013).

The second half of the sentence has been deleted.

(43) Page 4, lines 130-132: "All clusters simulated by the ACDC model do not contain H₂O molecules and the effect of relative humidity (RH) on nucleation thermochemistry is neglected." Page 21, lines 645-646: "an important influence of RH on nucleation rates (which is neglected in both the CLOUDpara and ACDC models)"

The authors of the present manuscript are well aware of the fact that water can be included in the ACDC model: in fact, the effect of cluster hydration was recently the topic of a rather heated discussion between these authors and the researchers at University of Helsinki (Nadykto et al., 2014; Kupiainen-Määttä et al., 2015; Nadykto et al., 2015; in this case, the question was about H₂SO₄-dimethylamine clusters), including i.a. ACDC simulations conducted as a function of RH.

Hydration can naturally be included in a kinetic model, such as ACDC, given that there is thermodynamic input data for clusters containing water. Please correct your claims about this. The effect of water in the H₂SO₄-H₂O-NH₃ system has been studied by ACDC e.g. by Henschel et al. (2016).

In view of the information the Reviewer provided us with, we have deleted this sentence.

(44) Also the particle formation rate parameterization by Dunne et al. (2016) is criticized. It would be fair to note that the deviations of the parameterization from the CLOUD data are not a new finding, as the uncertainties and weaknesses of the parameterization are discussed rather extensively in the work by Dunne et al. (e.g. supplementary Figures S3-S6).

We don't feel it is a criticism. We meant to point out the limitation of previous results which we aim to address in the present study.

(45) Page 11, line 333-334: "most of these studies, except for Nadykto and Yu (2007), did not consider the impact of H₂O on cluster thermodynamics"

The effect of H₂O on H₂SO₄-NH₃ clusters containing up to three H₂SO₄ and three NH₃ molecules has been considered by Henschel et al. (2014; 2016).

Thanks for the information. We have updated the discussion on this.

(46) Page 13, lines 396-397: The sentence "The binding of the second NH₃ to S-S₃A to form S-S₃A₂ is much weaker than that of the first NH₃ molecule. This indicates that most of S-A_a can only contain one NH₃ molecule" isn't clear: How does the binding of NH₃ to a cluster containing 3 H₂SO₄ molecules indicate something about the attachment of NH₃ to a bisulfate ion S-?

It's a typo. Should be S·S₃A_a. Corrected.

(47) Comparisons to CLOUD data (Figures 6 and 7): Many of the comparisons look quite nice indeed. However, **more experimental data over a wider range of conditions should be shown to support the claim that the model is "in excellent agreement with CLOUD measurements"**.

For instance, in the work by Kürten et al. (2016) on CLOUD-based J1.7, the model used in the study (ACDC with input thermodynamics computed with the RICC2//B3LYP method) is at some conditions in excellent agreement with CLOUD data, and at some conditions there are significant differences.

Therefore, comparisons with CLOUD data should be shown for **a large set of data**, for example the figures of the study by Kürten et al. (2016), including also electrically neutral cases and a wider range of ammonia concentrations.

We have extended the comparison with CLOUD data, including the neutral cases.

(48) Figure 6: The original CLOUD data includes also $J_{1.7}$ for experiments with no ions. Please add these electrically neutral experimental and model data to the figure. It looks like the slope of the modeled $J_{1.7}$ is quite steep when neutral nucleation takes over; it is interesting to see how this compares with the measurements.

Neutral cases without ions are now included and discussed.

(49) Figure 7, top panel: For most lines, there are only 3 experimental data points, which doesn't make the comparison of these data to the model lines very strong. As there is so much CLOUD data available, please pick more representative data from e.g. the work by Kürten et al. (2016). Especially low but still non-negligible ammonia mixing ratios are not shown in the current comparisons. If the model is said to cover "a wide range of atmospheric conditions", these should be included.

To be comparable, $[\text{NH}_3]$ and T should be the same for each line, which limits the number of experimental points. We have extended the comparison with CLOUD data in separate figures.

Technical comments:

(50) Change all occurrences of "physio-chemical" to "physico-chemical"; presumably "physio" refers to physiology, not physics.

Done. Thanks for pointing these out.

(51) Page 2, line 35: Change "specie" to "species".

Done.

(52) Page 9, lines 240-245: The sentence "In earlier studies, this method has been applied to a large variety of atmospherically-relevant clusters and has been shown to be well suited to study the ones, (...)" is clumsy (i.e. what does "the ones" refer to?); please re-formulate.

Changed "the ones" to "the $\text{H}_2\text{SO}_4\text{-H}_2\text{O}$ and $\text{H}_2\text{SO}_4\text{-H}_2\text{O-NH}_3$ clusters".

(53) Page 9, line 253: Change "basin hoping" to "basin hopping".

Done.

(54) Page 11, line 332: It is misleading to list Kürten et al. (2015) as a computational study, as it doesn't present any computationally obtained thermodynamics.

We have changed Kürten et al. (2015) to Kürten et al. (2007) and added it in the reference list.

(55) Page 16, line 505: Change "cluster" to "clusters".

Done.

(56) Table 1: Please give units for the energy quantities. Please also clarify that "H" and "S" may refer to either the energetics, or the cluster composition (the first column), or use different symbols for some of the abbreviations / quantities. Also change "based" in the footnote to "based on".

That's a good point. Instead of using abbreviations, we keep the original words in the table. Units are now given in the table.

“based” in the footnote of Table A2 has been changed to “based on”.

(57) The resolution and/or clarity of some figures, mainly 1 and 3, is rather poor. Please fix this.

Fixed.

Anonymous Referee #3

The kind of model introduced in this paper is definitely needed in atmospheric new particle formation research, so I am in principle in favor of publishing this work. I have, however, a few concerns that should be addressed before accepting the paper for publication.

I am not fully comfortable with the current structure of the paper. Sections 1 and 2.1 provide a nice introduction and background for this work. Section 2.2 is a compact description of the model and fine as well. Section 2.3 is, however, a mixture of technical details, model evaluations and scientific results/findings. I would prefer separating these issues to the extend possible. For example, the technical details related to the used thermodynamic and other data as well as QC calculations could be put into a separate Appendix/Appendicies. Such details are a very important part of this paper, but not of major interest to most of the readers.

This is a good point. Following the referee's suggestion, we have moved some of the technical details related to the used thermodynamic and other data as well as QC calculations to Appendix.

The authors state that a detailed description of QC calculations will be reported in separate papers. The authors should be very careful in this regard: this paper needs to have enough material to justify the obtained results.

This paper contains the adequate materials (as provided in the tables now in the supplementary material) to justify the obtained results. To address the reviewer's concern, we have deleted this sentence.

Minor issues:

Please add to the text (line 197) that PH_2SO_4 refers to gas-phase production of sulfuric acid (in the atmosphere, sulfuric acid/sulfate can also be produced in liquid/aerosol phase).

Modified as suggested.

The given ammonia concentration levels (beginning of section 2.4.1) should be backed up with suitable references. The authors should better justify the statement that small ternary clusters can be considered to be in equilibrium with ammonia. Mentioning solely the typical ammonia concentrations is not enough.

We have added several references about the ammonia concentration levels. We have also added discussions about the validity of the equilibrium assumption.

CLOUD should be defined also in the abstract.

Done.

There are a small number of grammatical issues that should be corrected, e.g. indicating (line 64), a nucleation model (line 67), did not (line 107), a similar pattern (line 296), the $s=a$ pathway (line 367), even when they (line 384), under the condition??? (line 559).

Thanks for the careful reading. We have fixed these grammatical issues.

1 **H₂SO₄-H₂O-NH₃ ternary ion-mediated nucleation (TIMN): Kinetic-based model and**
2 **comparison with CLOUD measurements**

3
4 Fangqun Yu¹, Alexey B. Nadykto^{1,2}, Jason Herb¹, Gan Luo¹, Kirill M. Nazarenko², and
5 Lyudmila A. Uvarova²

6 Correspondence to: F. Yu (fyu@albany.edu)

7
8 ¹ Atmospheric Sciences Research Center, University at Albany, Albany, New York, US

9 ² Department of Applied Mathematics, Moscow State Univ. of Technology “Stankin”, Russia

10
11
12 **Abstract.** New particle formation (NPF) is known to be an important source of atmospheric
13 particles that impacts air quality, hydrological cycle, and climate. Although laboratory
14 measurements indicate that ammonia enhances NPF, the physico-chemical processes underlying
15 the observed effect of ammonia on NPF are yet to be understood. Here we present ~~at the first~~
16 comprehensive kinetically-based H₂SO₄-H₂O-NH₃ ternary ion-mediated nucleation (TIMN)
17 model that is based on the thermodynamic data derived from both quantum-chemical calculations
18 and laboratory measurements. NH₃ was found to reduce nucleation barriers for neutral, positively
19 charged, and negatively charged clusters differently, due to large differences in the binding
20 strength of NH₃, H₂O, and H₂SO₄ to small clusters of different charging states. The model reveals
21 the general favor of nucleation of negative ions, followed by nucleation on positive ions and neutral
22 nucleation, for which higher NH₃ concentrations are needed, in excellent agreement with Cosmics
23 Leaving Outdoor Droplets (CLOUD) measurements. The TIMN model explicitly resolves
24 dependences of nucleation rates on all the key controlling parameters, and captures well the
25 absolute values of nucleation rates as well as the dependence of TIMN rates on concentrations of
26 NH₃ and H₂SO₄, ionization rates, temperature, and relative humidity observed in the well-
27 controlled CLOUD measurements. The kinetic model offers physico-chemical insights into the
28 ternary nucleation process and provides a physics-based ~~n-accurate~~ approach to calculate TIMN
29 rates under a wide range of atmospheric conditions.

30

31 **1. Introduction**

32 New particle formation (NPF), an important source of particles in the atmosphere, is a dynamic
33 process involving interactions among precursor gas molecules, small clusters, and pre-existing
34 particles (Yu and Turco, 2001; Zhang et al., 2012). H_2SO_4 and H_2O are known to play an important
35 role in atmospheric particle formation (e.g., Doyle, 1961). In typical atmospheric conditions, the
36 species dominating the formation and growth of small clusters is H_2SO_4 . The contribution of H_2O
37 to the nucleation is related to the hydration of H_2SO_4 clusters (or, in the other words, modification
38 of the composition of nucleating clusters) that reduces the H_2SO_4 vapor pressure and hence
39 diminishes the evaporation of H_2SO_4 from the pre-nucleation clusters. NH_3 , the most abundant
40 gas-phase base molecule in the atmosphere and a very efficient neutralizer of sulfuric acid
41 solutions, has long been proposed to enhance nucleation in the lower troposphere (Coffman and
42 Hegg, 1995) although it has been well recognized that earlier versions of classical ternary
43 nucleation model (Coffman and Hegg, 1995; Korhonen et al., 1999; Napari et al., 2002)
44 significantly over-predict the effect of ammonia (Yu, 2006a; Merikanto et al., 2007; Zhang et al.,
45 2010).

46 The impacts of NH_3 on NPF have been investigated in a number of laboratory studies (Kim et
47 al., 1998; Ball et al., 1999; Hanson and Eisele, 2002; Benson et al., 2009; Kirkby et al., 2011;
48 Zollner et al., 2012; Froyd and Lovejoy, 2012; Glasoe et al., 2015; Schobesberger et al., 2015;
49 Kurten et al., 2016) including those recently conducted at the European Organization for Nuclear
50 Research (CERN) in the framework of the CLOUD (Cosmics Leaving Outdoor Droplets)
51 experiment that has provided a unique dataset for quantitatively examining the dependences of
52 ternary H_2SO_4 - H_2O - NH_3 nucleation rates on concentrations of NH_3 ($[\text{NH}_3]$) and H_2SO_4
53 ($[\text{H}_2\text{SO}_4]$), ionization rate (Q), temperature (T), and relative humidity (RH) (Kirkby et al., 2011;
54 Kurten et al., 2016). The experimental conditions in the CLOUD chamber, a 26.1 m³ stainless steel
55 cylinder, were well controlled, while impacts of potential contaminants were minimized
56 (Schnitzhofer et al., 2014; Duplissy et al., 2016). Based on CLOUD measurements in H_2SO_4 - H_2O -
57 NH_3 vapor mixtures, Kirkby et al. (2011) reported that an increase of $[\text{NH}_3]$ from ~ 0.03 ppb (parts
58 per billion, by volume) to ~ 0.2 ppb can enhance ion-mediated (or induced) nucleation rate by 2-3
59 orders of magnitude and that the ion-mediated nucleation rate is a factor of 2 to >10 higher than
60 that of neutral nucleation under typical level of contamination by amines. In the presence of
61 ionization, highly polar common atmospheric nucleation precursors such as H_2SO_4 , H_2O , and NH_3
62 molecules tend to cluster around ions; and charged clusters are generally much more stable than
63 their neutral counterparts with enhanced growth rates as a result of dipole-charge interactions (Yu
64 and Turco, 2001).

65 Despite of various laboratory measurements indicatinge that ammonia enhances NPF, the
66 physico-chemical processes underlying the observed different effects of ammonia on the formation
67 of neutral, positively charged and negatively charged clusters (Schobesberger et al., 2015) are yet
68 to be understood. To achieve such an understanding, a nucleation model based on the first
69 principles is needed. Such a model is also necessary to extrapolate data obtained in a limited
70 number of experimental conditions to a wide range of atmospheric conditions, where $[\text{NH}_3]$,
71 $[\text{H}_2\text{SO}_4]$, ionization rates, T, RH and surface areas of preexisting particles vary widely depending
72 on the region, pollution level and season. The present work aims to address these issues by
73 developing a kinetically-based $\text{H}_2\text{SO}_4\text{-H}_2\text{O-NH}_3$ ternary ion-mediated nucleation (TIMN) model
74 that is based on the molecular clustering thermodynamic data. The model predictions are compared
75 with relevant CLOUD measurements and previous studies.

77 **2. Kinetic-based $\text{H}_2\text{SO}_4\text{-H}_2\text{O-NH}_3$ ternary ion-mediated nucleation (TIMN) model**

78 2.1. Background

79 Most nucleation models developed in the past for $\text{H}_2\text{SO}_4\text{-H}_2\text{O}$ binary homogeneous nucleation
80 (e.g., Vehkamäki et al., 2002), $\text{H}_2\text{SO}_4\text{-H}_2\text{O}$ ion-induced nucleation (e.g., Hamill et al., 1982; Raes
81 et al., 1986; Laakso et al., 2003), and $\text{H}_2\text{SO}_4\text{-H}_2\text{O-NH}_3$ ternary homogeneous nucleation (Coffman
82 and Hegg, 1995; Korhonen et al., 1999; Napari et al., 2002) have been based on the classical
83 approach, which employs capillarity approximation (i.e., assuming that small clusters have same
84 properties as bulk) and calculate nucleation rates according to the free energy change associated
85 with the formation of a “critical embryo”. Yu and Turco (1997, 2000, 2001) developed a neutral
86 and charged binary $\text{H}_2\text{SO}_4\text{-H}_2\text{O}$ nucleation model using a kinetic approach that explicitly treats
87 the complex interactions among small air ions, neutral and charged clusters of various sizes,
88 precursor vapor molecules, and pre-existing aerosols. The formation and evolution of cluster size
89 distributions for positively and negatively charged cluster ions and neutral clusters affected by
90 ionization, recombination, neutralization, condensation, evaporation, coagulation, and scavenging,
91 has been named as ion-mediated nucleation (IMN) (Yu and Turco, 2000). The IMN theory
92 significantly differs from classical ion-induced nucleation (IIN) theory (e.g., Hamill et al., 1982;
93 Raes et al., 1986; Laakso et al., 2003) which is based on a simple modification of the free energy
94 for the formation of a “critical embryo” by including the electrostatic potential energy induced by
95 the embedded charge (i.e., Thomson effect (Thomson, 1888)). The classical approach does not
96 properly account for the kinetic limitation to embryo development, enhanced stability and growth
97 of charged clusters associated with dipole-charge interaction (Nadykto and Yu, 2003; Yu, 2005),
98 and the important contribution of neutral clusters resulting from ion-ion recombination to
99 nucleation (Yu and Turco, 2011). In contrast, these important physical processes are explicitly
100 considered in the kinetic-based IMN model (Yu, 2006b).

101 Since the beginning of the century, nucleation models based on kinetic approach have also
102 been developed in a number of research groups (Lovejoy et al., 2004; Sorokin et al., 2006; Chen
103 et al., 2012; Dawson et al., 2012; McGrath et al., 2012). Lovejoy et al. (2004) developed a kinetic
104 ion nucleation model, which explicitly treats the evaporation of small neutral and negatively
105 charged H₂SO₄-H₂O clusters. The thermodynamic data used in their model were obtained from
106 measurements of small ion clusters, ab initio calculations, thermodynamic cycle, and some
107 approximations (adjustment of Gibbs free energy for neutral clusters calculated based on liquid
108 droplet model, interpolation, etc.). Lovejoy et al. (2004) did ~~not~~ consider the nucleation on
109 positive ions. Sorokin et al. (2006) developed an ion-cluster-aerosol kinetic (ICAK) model which
110 uses the thermodynamic data reported in Froyd and Lovejoy (2003a, b) and empirical correction
111 terms proposed by Lovejoy et al. (2004). Sorokin et al. (2006) used the ICAK model to simulate
112 dynamics of neutral and charged H₂SO₄-H₂O cluster formation and compared the modeling results
113 with their laboratory measurements. Chen et al. (2012) developed an approach for modeling new
114 particle formation based on a sequence of acid-base reactions, with sulfuric acid evaporation rates
115 (from clusters) estimated empirically based on measurements of neutral molecular clusters taken
116 in Mexico City and Atlanta. Dawson et al. (2012) presented a semi-empirical kinetics model for
117 nucleation of methanesulfonic acid (MSA), amines, and water that explicitly accounted for the
118 sequence of reactions leading to formation of stable particles. The kinetic models of Chen et al.
119 (2012) and Dawson et al. (2012) consider only neutral clusters.

120 McGrath et al. (2012) developed the Atmospheric Cluster Dynamics Code (ACDC) to model
121 the cluster kinetics by solving the birth–death equations explicitly, with evaporation rate
122 coefficients derived from formation free energies calculated by quantum chemical methods. ~~ACDC is also an acid–base reaction model, with the largest clusters containing 4–5 acid and 4–5
123 base molecules (no water molecules)~~ (Almeida et al., 2013; Olenius et al., 2013). The ACDC
124 model applied to the H₂SO₄-dimethylamine (DMA) system considers 0–4 base molecules and 0–
125 4 sulfuric acid molecules (Almeida et al., 2013). Olenius et al. (2013) applied the ACDC model to
126 simulate the steady-state concentrations and kinetics of neutral, and negatively and positively
127 charged clusters containing up to 5 H₂SO₄ and 5 NH₃ molecules. In ACDC, the nucleation rate is
128 calculated as the rate of clusters growing larger than the upper bounds of the simulated system
129 (i.e., clusters containing 4 or 5 H₂SO₄ molecules) (Kurten et al., 2016) ~~and thus may over-predict
130 nucleation rates when critical clusters contain more than 5 H₂SO₄ molecules. All clusters simulated
131 by the ACDC model do not contain H₂O molecules and the effect of relative humidity (RH) on
132 nucleation thermochemistry is neglected.~~

134 The kinetic IMN model developed by Yu and Turco (1997, 2001) explicitly simulates the
135 dynamics of neutral, positively charged, and negatively charged clusters, based on a discrete-
136 sectional bin structure that covers the clusters containing 0, 1, 2, ..., 15, ... H₂SO₄ molecules to

137 particles containing thousands of H₂SO₄ (and H₂O) molecules. In the first version of the kinetic
138 IMN model (Yu and Turco, 1997, 2001), due to the lack of thermodynamic data for the small
139 clusters, the compositions of neutral and charged clusters were assumed to be the same and the
140 evaporation of small clusters was accounted for using a simple adjustment to the condensation
141 accommodation coefficients. Yu (2006b) developed a second-generation IMN model which
142 incorporated newer thermodynamic data (Froyd, 2002; Wilhelm et al., 2004) and physical
143 algorithms (Froyd, 2002; Wilhelm et al., 2004) and explicitly treated the evaporation of neutral
144 and charged clusters. Yu (2007) further improved the IMN model by using two independent
145 measurements (Marti et al., 1997; Hanson and Eisele, 2000) to constrain monomer hydration in
146 the H₂SO₄-H₂O system and by incorporating experimentally determined energetics of small
147 neutral H₂SO₄-H₂O clusters that became available then (Hanson and Lovejoy, 2006; Kazil et al.,
148 2007). The first and second generations of the IMN model were developed for the H₂SO₄-H₂O
149 binary system, although the possible effects of ternary species such as the impact of NH₃ on the
150 stability of both neutral and charged pre-nucleation clusters have been pointed out in these
151 previous studies (Yu and Turco, 2001; Yu, 2006b). The present work extends the previous versions
152 of the IMN model in binary H₂SO₄-H₂O system to ternary H₂SO₄-H₂O-NH₃ system, as described
153 below. ~~The thermodynamic data sets used for binary clusters were also updated.~~

154

155 2.2. Model representation of kinetic ternary nucleation processes

156 Figure 1 schematically illustrates the evolution of charged and neutral clusters/droplets
157 explicitly simulated in the kinetic H₂SO₄-H₂O-NH₃ TIMN model. Here, H₂SO₄ (S) is the key
158 atmospheric nucleation precursor driving the TIMN process while ions, H₂O (W), and NH₃ (A)
159 stabilize the H₂SO₄ clusters and enhance in this way H₂SO₄ nucleation rates. Ions also enhance
160 cluster formation rates due to the interaction with polar nucleating species leading to enhanced
161 collision cross sections (Nadykto and Yu, 2003). The airborne ions are generated by galactic
162 cosmic rays (GCRs) or produced by radioactive emanations, lightning, corona discharge,
163 combustion and other ionization sources. The initial negative ions, which are normally assumed to
164 be NO₃⁻, are converted into HSO₄⁻ core ions (i.e., S⁻) and, then, to larger H₂SO₄ clusters in the
165 presence of gaseous H₂SO₄. The initial positive ions H⁺W_w are converted into H⁺A₁₋₂W_w in the
166 presence of NH₃, H⁺S_sW_w in the presence of H₂SO₄, or H⁺A_aS_sW_w in the case, when both NH₃
167 and H₂SO₄ are present in the nucleating vapors. Some of the binary H₂SO₄-H₂O clusters, both
168 neutral and charged, transform into ternary ones by taking up NH₃ vapors. The molar fraction of

169 ternary clusters in nucleating vapors depends on $[\text{NH}_3]$, the binding strength of NH_3 to binary and
 170 ternary pre-nucleation clusters, cluster composition, and ambient conditions such as T and RH.

171 Similar to the kinetic binary IMN (BIMN) model (Yu, 2006b), the kinetic TIMN model
 172 employs a discrete-sectional bin structure to represent clusters/particles. The bin index i represent
 173 the amount of core component (i.e., H_2SO_4). For small clusters ($i \leq i_d = 30$ in this study), i is the
 174 number of H_2SO_4 molecules in the cluster (i.e., $i = s$) and the core volume of i^{th} bin $v_i = i \times v_l$, where
 175 v_l is the volume of one H_2SO_4 molecule. When $i > i_d$, $v_i = VRAT_i \times v_{i-1}$, where $VRAT_i$ is the volume
 176 ratio of i^{th} bin to $(i-1)^{\text{th}}$ bin. The discrete-sectional bin structure enables the model to cover a wide
 177 range of sizes of nucleating clusters/particles with the highest possible size resolution for small
 178 clusters (Yu, 2006b). For clusters with a given bin i , the associated amounts of water and NH_3 and
 179 thus the effective radius of each ternary cluster are calculated based on the equilibrium of
 180 clusters/particles with the water vapor and/or ammonia, as described in later sections.

181 The evolution of positive, negative, and neutral clusters due to the simultaneous condensation,
 182 evaporation, recombination, coagulation, and other loss processes, is described by the following
 183 differential equations obtained by the modification of those describing for the evolution of binary
 184 $\text{H}_2\text{SO}_4\text{-H}_2\text{O}$ system (Yu, 2006b):

$$185 \quad \frac{\partial N_0^+}{\partial t} = Q + \gamma_1^+ N_1^+ - N_0^+ \left(\sum_{j=1}^{i_{\max}} \beta_{i,j}^+ N_j^0 + \sum_{j=0}^{i_{\max}} \eta_{i,j}^+ N_j^+ + \sum_{j=0}^{i_{\max}} \alpha_{0,j}^{+,-} N_j^- \right) - N_0^+ L_0^+ \quad (1)$$

$$186 \quad \frac{\partial N_0^-}{\partial t} = Q + \gamma_1^- N_1^- - N_0^- \left(\sum_{j=1}^{i_{\max}} \beta_{i,j}^- N_j^0 + \sum_{j=0}^{i_{\max}} \eta_{i,j}^- N_j^- + \sum_{j=0}^{i_{\max}} \alpha_{0,j}^{-,+} N_j^+ \right) - N_0^- L_0^- \quad (2)$$

$$187 \quad \frac{\partial N_1^0}{\partial t} = P_{\text{H}_2\text{SO}_4} + \sum_{j=2}^{i_{\max}} \delta_{j,2} \gamma_j^0 N_j^0 + \sum_{j=1}^{i_{\max}} (\gamma_j^+ N_j^+ + \gamma_j^- N_j^-) \\ - N_1^0 \left(\sum_{j=1}^{i_{\max}} (1 - f_{1,j,1}) \beta_{1,j}^0 N_j^0 + \sum_{j=0}^{i_{\max}} (\beta_{j,1}^+ N_j^+ + \beta_{j,1}^- N_j^-) \right) - N_1^0 L_1^0 \quad (3)$$

$$188 \quad \frac{\partial N_i^+(i \geq 1)}{\partial t} = g_{i+1,i} \gamma_{i+1}^+ N_{i+1}^+ - g_{i,i-1} \gamma_i^+ N_i^+ + \sum_{j=0}^{i-1} \sum_{k=1}^i \frac{v_j}{v_i} f_{j,k,i} \beta_{j,k}^+ N_j^+ N_k^0 + \sum_{j=0}^{i-1} \sum_{k=0}^i \frac{v_j}{v_i} f_{j,k,i} \eta_{j,k}^+ N_j^+ N_k^+ \\ + \sum_{j=0}^i \sum_{k=1}^i \frac{v_k}{v_i} f_{j,k,i} \beta_{j,k}^+ N_j^+ N_k^0 - N_i^+ \left(\sum_{j=1}^{i_{\max}} (1 - f_{i,j,i}) \beta_{i,j}^+ N_j^0 + \sum_{j=0}^{i_{\max}} (1 - f_{i,j,i}) \eta_{i,j}^+ N_j^+ + \sum_{j=0}^{i_{\max}} \alpha_{i,j}^{+,-} N_j^- \right) - N_i^+ L_i^+ \quad (4)$$

$$189 \quad \frac{\partial N_i^-(i \geq 1)}{\partial t} = g_{i+1,i} \gamma_{i+1}^- N_{i+1}^- - g_{i,i-1} \gamma_i^- N_i^- + \sum_{j=0}^{i-1} \sum_{k=1}^i \frac{v_j}{v_i} f_{j,k,i} \beta_{j,k}^- N_j^- N_k^0 + \sum_{j=0}^{i-1} \sum_{k=0}^i \frac{v_j}{v_i} f_{j,k,i} \eta_{j,k}^- N_j^- N_k^- \\ + \sum_{j=0}^i \sum_{k=1}^i \frac{v_k}{v_i} f_{j,k,i} \beta_{j,k}^- N_j^- N_k^0 - N_i^- \left(\sum_{j=1}^{i_{\max}} (1 - f_{i,j,i}) \beta_{i,j}^- N_j^0 + \sum_{j=0}^{i_{\max}} (1 - f_{i,j,i}) \eta_{i,j}^- N_j^- + \sum_{j=0}^{i_{\max}} \alpha_{i,j}^{-,+} N_j^+ \right) - N_i^- L_i^- \quad (5)$$

$$\begin{aligned}
190 \quad \frac{\partial N_i^0(i \geq 2)}{\partial t} &= g_{i+1,i} \gamma_{i+1}^0 N_{i+1}^0 - g_{i,i-1} \gamma_i^0 N_i^0 + \sum_{j=1}^i \sum_{k=1}^{i-1} \frac{v_k}{v_i} f_{j,k,i} \beta_{j,k}^0 N_j^0 N_k^0 \\
&+ \sum_{j=0}^i \sum_{k=0}^i f_{j,k,i} \alpha_{j,k}^{+,-} \left(\frac{v_k}{v_i} N_j^+ N_k^- + \frac{v_j}{v_i} N_j^- N_k^+ \right) - N_i^0 \left(\sum_{j=1}^{i_{\max}} (1 - f_{i,j,i}) \beta_{i,j}^0 N_j^0 + \sum_{j=0}^{i_{\max}} (\beta_{j,i}^+ N_j^+ + \beta_{j,i}^- N_j^-) \right) - N_i^0 L_i^0
\end{aligned} \tag{6}$$

191
192 In Eqs. (1-6), the superscripts “+”, “-”, and “0” refer to positive, negative, and neutral clusters,
193 respectively, while subscripts i, j, k represent the bin indexes. $N_0^{+,-}$ and Q are the concentration of
194 initial ions not containing H₂SO₄ (i.e., H⁺A_aW_w and NO₃⁻) and the ionization rate, respectively. N_i
195 is the total number concentration (cm⁻³) of all cluster/particles (binary + ternary) in the bin i . For
196 small clusters ($i \leq i_d$), N_i is the number concentration (cm⁻³) of all clusters containing i H₂SO₄
197 molecules. For example, N_1^0 is the total concentration of binary and ternary neutral clusters
198 containing one H₂SO₄ molecules. $P_{\text{H}_2\text{SO}_4}$ is the gas-phase production rate of neutral H₂SO₄
199 molecules. $L_i^{+,-,0}$ is the loss rate due to scavenging by pre-existing particles, and wall and dilution
200 losses in the laboratory chamber studies (Kirkby et al., 2011; Olenius et al., 2013; Kurten et al.,
201 2016). $f_{j,k,i}$ is the volume fraction of intermediate particles (volume = $v_j + v_k$) partitioned into bin
202 i with respect to the core component – H₂SO₄, as defined in Jacobson et al. (1994).
203 $g_{i+1,i} = v_1 / (v_{i+1} - v_i)$ is the volume fraction of intermediate particles of volume ($v_{i+1} - v_i$)
204 partitioned into bin i . $\delta_{j,2} = 2$ at $j=2$ and $\delta_{j,2} = 1$ at $j \neq 2$. γ_i^+ , γ_i^- , and γ_i^0 are the mean (or effective)
205 cluster evaporation coefficients for positive, negative and neutral clusters in bin i , respectively.
206 $\beta_{i,j}^+$, $\beta_{i,j}^-$, $\beta_{i,j}^0$ are the coagulation kernels for the neutral clusters/particles in bin j interacting
207 with positive, negative, and neutral clusters/particles in bin i , respectively, which reduce to the
208 condensation coefficients for H₂SO₄ monomers at $j=1$. $\eta_{j,k}^+$ and $\eta_{j,k}^-$ are coagulation kernels for
209 clusters/particles of like sign from bin j and clusters/particles from bin k . $\alpha_{i,j}^{+,-}$ is the
210 recombination coefficient for positive clusters/particles in bin i interacting with negative
211 clusters/particles in bin j , while $\alpha_{i,j}^{-,+}$ is the recombination coefficient negative clusters/particles
212 from bin i interacting with positively charged clusters/particles from bin j .

213 The methods for calculating β , γ , η , and α for binary H₂SO₄-H₂O clusters have been described
 214 in ~~detail our previous publications (Yu and Turco, 2001; Nadykto and Yu, 2003; in Yu, (2006b).~~
 215 ~~Dipole-charge interaction (Nadykto and Yu, 2003), image capture and three-body trapping effects~~
 216 ~~(Hoppel and Frick, 1986) are considered in the calculation of these coefficients.~~ Since β , η , and α
 217 depend on the cluster mass (or size) rather than on the cluster composition, schemes for calculating
 218 these properties in binary and ternary clusters are identical ~~(Yu, 2006b)~~. In contrast, γ is quite
 219 sensitive to cluster composition. The evaporation rate coefficient of H₂SO₄ molecules from
 220 clusters containing i H₂SO₄ molecules (γ_i) is largely controlled by the stepwise Gibbs free energy
 221 change $\Delta G_{i-1,i}$ of formation of an i -mer from an $(i-1)$ -mer (Yu, 2007)

$$222 \quad \gamma_i = \beta_{i-1} N^\circ \exp\left(\frac{\Delta G_{i-1,i}}{RT}\right) \quad (7)$$

$$223 \quad \Delta G_{k-1,k} = -RT \ln\left(\frac{N_1^\circ}{N^\circ}\right) \pm \Delta H_{k-1,k}^\circ - T \Delta S_{k-1,k}^\circ \quad (8)$$

224 where R is the molar gas constant, N° is the number concentration of H₂SO₄ at a given T under the
 225 reference vapor pressure P of 1 atm. ΔH° and ΔS° are enthalpy and entropy changes under the
 226 standard conditions (T=298 K, P=1 atm), respectively. The temperature dependence of ΔH° and
 227 ΔS° , which is generally small and typically negligible over the temperature range of interest
 228 ~~(Nadykto et al., 2009)~~, was not considered.

230 2.3. Thermochemical data of neutral and charged binary and ternary clusters

231 ΔH , ΔS and ΔG values needed to calculate cluster evaporation rates (Eq. 7) for the TIMN
 232 model can be derived from laboratory measurements and computational quantum chemistry (QC)
 233 calculation. Thermochemical properties of neutral and charged binary and ternary clusters
 234 obtained using the computational chemical methods and comparisons of computed energies with
 235 available experimental data and semi-experimental estimates are given in Tables A1-A4 and
 236 discussed in Appendix below. As an example,

238 ~~2.3. Quantum chemical studies of neutral and charged binary and ternary clusters~~

239 ~~Thermochemical data for small neutral and charged binary H₂SO₄-H₂O and ternary H₂SO₄-H₂O-~~
 240 ~~NH₃ clusters has been reported in a number of earlier publications (Bandy and Ianni, 1998; Ianni~~

241 and Bandy, 1999; Torpo et al., 2007; Nadykto et al., 2008; Herb et al., 2011, 2013; Temelso et al.,
242 2012a, b; DePalma et al., 2012; Ortega et al., 2012; Chon et al., 2014; Husar et al., 2014; Henschel
243 et al., 2014, 2016; Kurten et al., 2015). The PW91PW91/6-311++G(3df,3pd) method, which is a
244 combination of the Perdue Wang PW91PW91 density functional with the largest Pople 6-
245 311++G(3df,3pd) basis set, has thoroughly been validated and agrees well with existing
246 experimental data. In earlier studies, this method has been applied to a large variety of
247 atmospherically relevant clusters (Nadykto et al. 2006, 2007a, b, 2008, 2014, 2015; Torpo et al.
248 2007; Zhang et al., 2009; Elm et al. 2012; Leverentz et al. 2013; Xu and Zhang, 2012; Xu and
249 Zhang, 2013; Elm et al., 2013; Zhu et al. 2014; Bork et al. 2014; Elm and Mikkelsen, 2014; Peng
250 et al. 2015; Miao et al 2015; Chen et al., 2015; Ma et al., 2016) and has been shown to be well
251 suited to study the ones, as evidenced by a very good agreement of the computed values with
252 measured cluster geometries, vibrational fundamentals, dipole properties and formation Gibbs free
253 energies (Nadykto et al., 2007a, b, 2008, 2014, 2015; Herb et al., 2013; Elm et al., 2012, 2013;
254 Leverentz et al., 2013; Bork et al., 2014) and with high level ab initio results (Temelso et al., 2012a,
255 b; Husar et al., 2012; Bustos et al., 2014).

256 We have extended the earlier QC studies of binary and ternary clusters to larger sizes. The
257 computations have been carried out using Gaussian 09 suite of programs (Frisch et al., 2009). In
258 order to ensure the quality of the conformational search we have carried out a thorough sampling
259 of conformers. We have used both basin hopping algorithm, as implemented in Biovia Materials
260 Studio 8.0, and locally developed sampling code, which creates a “mesh” around the cluster, in
261 which molecules being attached to the cluster are the mesh nodes. Typically, for each cluster of a
262 given chemical composition a thousand to several thousands of isomers have been sampled. We
263 used a three step optimization procedure, which includes (i) pre-optimization of initial/guess
264 geometries by semi-empirical PM6 method, separation of the most stable isomers located within
265 15 kcal mol⁻¹ of the intermediate global minimum and duplicate removal, followed by (ii)
266 optimization of the selected isomers meeting the aforementioned stability criterion by
267 PW91PW91/CBSB7 method and (iii) the final optimization of the most stable at
268 PW91PW91/CBSB7 level isomers within 5 kcal mol⁻¹ of the current global minimum using
269 PW91PW91/6-311++G(3df,3pd) method. Typically, only ~4-30% of initially sampled isomers
270 reach the second (PW91PW91/CBSB7) level, where ~10-40% of isomers optimized with
271 PW91PW91/CBSB7 are selected for the final run. Typically, the number of equilibrium isomers
272 of hydrated clusters is larger than that of unhydrated ones of similar chemical composition. Table
273 1 shows the numbers of isomers converged at the final PW91PW91/6-311++G(3df,3pd)
274 optimization step for selected clusters and HSG values of the most stable isomers used in the
275 present study. The number of isomers optimized at the PW91PW91/6-311++G(3df,3pd) level of
276 theory varies from case to case, typically being in the range of ~10-200.

277 ~~The computed stepwise enthalpy, entropy, and Gibbs free energies of cluster formation have been~~
278 ~~thoroughly evaluated and used to calculate the evaporation rates of H₂SO₄ from neutral, positive~~
279 ~~and negative charged clusters. A detailed description of QC calculations and the full range of~~
280 ~~computed properties of binary and ternary clusters will be reported in separate papers.~~

282 2.3.1 Positively charged clusters

283 ~~Table 2 presents the computed stepwise Gibbs free energy changes under standard conditions~~
284 ~~(ΔG°) for positive binary and ternary clusters, along with the corresponding experimental data or~~
285 ~~semi-experimental estimates.~~ Figure 2 shows ΔG associated with the addition of water (ΔG_{+W}°),
286 ammonia (ΔG_{+A}°), and sulfuric acid (ΔG_{+S}°) to binary and ternary clusters as a function of the cluster
287 hydration number w .

288 H₂O has high proton affinity and, thus, H₂O is strongly bonded to all positive ions with low w .
289 ΔG_{+W}° expectedly becomes less negative and binding of H₂O to binary and ternary clusters
290 weakens due to the screening effect as the hydration number w is growing (Fig. 2a). The presence
291 of NH₃ in the clusters weakens binding of H₂O to positive ions. For example, ΔG_{+W}° for
292 H⁺A₁W_wS₁ is ~3-4 kcal mol⁻¹ less negative than that for H⁺W_wS₁ at $w=3-6$. The addition of one
293 more NH₃ to the clusters to form H⁺A₂W_w and H⁺A₂W_wS₁ further weakens H₂O binding by ~1.5-
294 6 kcal mol⁻¹ at $w=1-3$, while exhibiting much smaller impact on hydration free energies at $w>3$.
295 Both the absolute values and trends in ΔG_{+W}° derived from calculations are in agreement with the
296 laboratory measurements within the uncertainty range of ~1-2 kcal mol⁻¹ for both QC calculations
297 and measurements. This confirms the efficiency and precision of QC methods in calculating
298 thermodynamic data needed for the development of nucleation models.

299 The proton affinity of NH₃ is 204.1 kcal mol⁻¹, which is 37.5 kcal mol⁻¹ higher than that of
300 H₂O (166.6 kcal mol⁻¹) (Jolly, 1991). The hydrated hydronium ions (H⁺W_w) are easily converted
301 to H⁺A₁W_w in the presence of NH₃. The binding of NH₃ and H₂O molecule to H⁺W_w exhibits a
302 similar pattern. In particular, binding of NH₃ to H⁺W_w decreases as w is growing, with ΔG_{+A}° for
303 H⁺A₁W_w ranging from -52.08 kcal mol⁻¹ at $w=1$ to -8.32 kcal mol⁻¹ at $w=9$. The binding of NH₃
304 to H⁺W_wS₁ ions is also quite strong, with ΔG_{+A}° for H⁺A₁W_wS₁ ranging from -33.14 kcal mol⁻¹ at
305 $w=1$ and to -10.57 kcal mol⁻¹ at $w=6$. The addition of the NH₃ molecule to H⁺A₁W_w (to form
306 H⁺A₂W_w) is much less favorable thermodynamically than that to H⁺W_w, with the corresponding
307 ΔG_{+A}° being -22 kcal mol⁻¹ and -6 kcal mol⁻¹ at $w=2$ and $w=6$, respectively. The ΔG_{+A}° values for
308 H⁺A₂W_w are 3-5 kcal mol⁻¹ more negative than the experimental values at $w=0-1$; however, they
309 are pretty close to experimental data at $w=2-3$ (Fig. 2b and Table A2). While it is possible that the
310 QC method overestimates the charge effect on the formation free energies of smallest clusters, the
311 possible overestimation at $w=0-1$ will not affect nucleation calculations because most of H⁺A₂W_w

312 in the atmosphere contain more than 2 water molecules (i.e., $w>2$) due to the strong hydration (see
313 Table [A2](#) and Fig. 2a).

314 A comparison of QC and semi-experimental estimates of ΔG_{+S}^0 values associated with the
315 attachment of H_2SO_4 to positive ions shown in Fig. 2c indicates that computed ΔG_{+S}^0 values agree
316 well with observations for $\text{H}^+\text{W}_w\text{S}_1$ and $\text{H}^+\text{A}_1\text{W}_w\text{S}_1$ but differ by $\sim 2\text{--}4$ kcal mol⁻¹ from semi-
317 experimental values for $\text{H}^+\text{A}_2\text{W}_w\text{S}_1$. As seen from Figs. 2a and 2c, the attachment of NH_3 to
318 $\text{H}^+\text{W}_w\text{S}_1$ weakens the binding of both H_2O and H_2SO_4 to the clusters. This suggests that the
319 attachment of NH_3 leads to the evaporation of H_2SO_4 and H_2O molecules from the clusters. In
320 other words, H_2SO_4 is less stable in $\text{H}^+\text{A}_1\text{W}_w\text{S}_1$ than in $\text{H}^+\text{W}_w\text{S}_1$ (Fig. 2c). While this may be taken
321 for the indication that NH_3 inhibits nucleation on positive ions at the first look, further calculations
322 show that binding of NH_3 to $\text{H}^+\text{A}_1\text{W}_w\text{S}_1$ is quite strong (Fig. 2b) and that H_2SO_4 in $\text{H}^+\text{A}_2\text{W}_w\text{S}_1$
323 cluster is much more stable than that in $\text{H}^+\text{A}_1\text{W}_w\text{S}_1$, with ΔG_{+S}^0 being by ~ 7 kcal mol⁻¹ more
324 negative at $w>2$. The $\text{H}^+\text{A}_2\text{W}_w\text{S}_1$ cluster can also be formed via the attachment of H_2SO_4 to
325 $\text{H}^+\text{A}_2\text{W}_w$. In the presence of sufficient concentrations of NH_3 , a large fraction of positively charged
326 H_2SO_4 monomers exist in the form of $\text{H}^+\text{A}_2\text{W}_w\text{S}_1$ and, hence, NH_3 enhances nucleation of positive
327 ions. Since positively charged H_2SO_4 dimers are expected to contain large number of water
328 molecules, we have not yet computed ~~no and derived~~ quantum chemical data for these clusters ~~are~~
329 available. The CLOUD measurements do indicate that once $\text{H}^+\text{A}_2\text{W}_w\text{S}_1$ are formed, they can
330 continue to grow to larger $\text{H}^+\text{A}_a\text{W}_w\text{S}_s$ clusters along $a=s+1$ pathway (Schobesberger et al., 2015).

331 ~~Table 2 and~~ Figure 2 shows clearly that the calculated values in most cases agree with
332 measurements within the uncertainty range that justifies the application of QC values in the case,
333 when no reliable experimental data are available.

334

335 2.3.2 Neutral clusters

336 ~~Table 3 presents the computed stepwise Gibbs free energy changes for the formation of ternary~~
337 ~~$\text{S}_s\text{A}_a\text{W}_w$ clusters under standard conditions. The thermodynamic properties of the S_1A_1 have been~~
338 ~~reported in a number of computational studies (e.g., Herb et al., 2011; Kurten et al., 2015; Nadykto~~
339 ~~and Yu, 2007). However, as pointed out by Kurten et al. (2015), most of these studies, except for~~
340 ~~Nadykto and Yu (2007), did not consider the impact of H_2O on cluster thermodynamics. We have~~
341 ~~extended the earlier studies of Nadykto and Yu (2007) and Herb et al. (2011) to larger clusters up~~
342 ~~to S_4A_5 (no hydration) and up to S_2A_2 (hydration included). The free energy of binding of NH_3 to~~
343 ~~H_2SO_4 (or H_2SO_4 to NH_3) obtained using our method is -7.77 kcal mol⁻¹ that is slightly more~~
344 ~~negative than values reported by other groups (-6.6 – -7.61 kcal mol⁻¹) and within less than 0.5 kcal~~
345 ~~mol⁻¹ of the experimental value of -8.2 kcal mol⁻¹ derived from CLOUD measurements (Kurten et~~
346 ~~al., 2015).~~

As it may be seen from Table 3, the NH_3 -binding to S_{1-2}W_w weakens as w increases. The average $\Delta G_{\text{TW}}^\circ$ for S_1W_w formation derived from a combination of laboratory measurements and quantum chemical studies are -3.02, -2.37, and -1.40 kcal mol⁻¹ for the first, second, and third hydration, respectively (Yu, 2007). This indicates that a large fraction of H_2SO_4 monomers in the Earth's atmosphere is likely hydrated. Therefore, the decreasing NH_3 -binding strength to hydrated H_2SO_4 monomers implies that RH (and T) will affect the relative abundance of H_2SO_4 monomers containing NH_3 . Currently, no experimental data or observations are available to evaluate the impact of hydration (or RH) on $\Delta G_{\text{TA}}^\circ$. Table 3 shows that the presence of NH_3 in H_2SO_4 clusters suppress hydration and that $\Delta G_{\text{TW}}^\circ$ for S_2A_2 falls below -2.0 kcal mol⁻¹. This is consistent with earlier studies by our group and others showing that large S_nA_n clusters ($n > 2$) are not hydrated under typical atmospheric conditions. In the present study, the hydration of neutral S_nA_n clusters at $n > 2$ is neglected.

The number of NH_3 molecules in the cluster (or H_2SO_4 to NH_3 ratio) significantly affects $\Delta G_{\text{TS}}^\circ$ and $\Delta G_{\text{TA}}^\circ$ values. For example, $\Delta G_{\text{TS}}^\circ$ for S_3A_a clusters increases from -7.08 kcal mol⁻¹ to -16.92 kcal mol⁻¹ and $\Delta G_{\text{TA}}^\circ$ decreases from -16.14 kcal mol⁻¹ to -8.93 kcal mol⁻¹ as a is growing from 1 to 3. For S_4A_a clusters, $\Delta G_{\text{TS}}^\circ$ is increasing from -7.48 kcal mol⁻¹ to -16.26 kcal mol⁻¹ and $\Delta G_{\text{TA}}^\circ$ decreases from -17.16 kcal mol⁻¹ to -11.34 kcal mol⁻¹ as a increases from 2 to 4. $\Delta G_{\text{TA}}^\circ$ for S_4A_1 cluster is by 1.38 kcal mol⁻¹ less negative than that for S_4A_2 . $\Delta G_{\text{TS}}^\circ$ for the S_4A_1 cluster is also quite low (-4.16 kcal mol⁻¹) that might indicate the possible existence of a more stable S_4A_1 isomer, which is yet to be identified. In the presence of NH_3 , the uncertainty in the thermochemistry data for S_4A_1 will not significantly affect ternary nucleation rates because most of S_4 clusters contain 3 or 4 NH_3 molecules.

For the S_sA_a clusters with $s=a$, $\Delta G_{\text{TA}}^\circ$ increases as cluster is growing while $\Delta G_{\text{TS}}^\circ$ first increases significantly as S_1A_1 is converting into S_2A_2 and then levels off as S_2A_2 is converting into S_4A_4 . We also observe a significant drop in $\Delta G_{\text{TA}}^\circ$ in the case when $\text{NH}_3/\text{H}_2\text{SO}_4$ ratio exceeds 1. This finding is fully consistent with the laboratory measurements showing that growth of neutral S_sA_a clusters follows $s=a$ pathway (Schobesberger et al., 2015).

2.3.3 Negative ionic clusters

Table 4 shows $\Delta G_{\text{TW}}^\circ$, $\Delta G_{\text{TA}}^\circ$, and $\Delta G_{\text{TS}}^\circ$ needed to form negatively charged clusters under standard conditions, along with available semi-experimental values (Froyd and Lovejoy, 2003). H_2O binding to negatively charged S^-S_s clusters significantly strengths with increasing s , from $\Delta G_{\text{TW}}^\circ = -0.61 - 1.83$ kcal mol⁻¹ at $s=1-2$ to $\Delta G_{\text{TW}}^\circ = -3.5$ kcal mol⁻¹ at $w=1$ and -2.25 kcal mol⁻¹ at $w=4$ at $s=4$. $\Delta G_{\text{TW}}^\circ$ values at $s=3$ and 4 are slightly more negative (by $\sim 0.1 - 0.9$ kcal mol⁻¹) than those reported by Froyd and Lovejoy (2003). Just like H_2O binding, NH_3 -binding to S^-S_s at $s < 3$ is very weak, with $\Delta G_{\text{TA}}^\circ$ ranging from +2.81 kcal mol⁻¹ at $s=0$ to -4.85 kcal mol⁻¹ at $s=2$. However,

383 it significantly increases as s is growing. In particular, at $s \geq 3$ $\Delta G_{\pm A}^{\circ}$ is ranging from -11.89 kcal
384 mol^{-1} for $S^-S_3A_1$ to -15.37 kcal mol^{-1} for $S^-S_4A_1$. NH_3 clearly cannot get into small negative ions.
385 However, it can easily attach to larger negative ions with $s \geq 3$ that is consistent with CLOUD
386 measurements (Schobesberger et al., 2015). Since hydration weakens NH_3 binding in $S^-S_3A_1W_w$
387 and $S^-S_4A_1W_w$ clusters, its impacts on the cluster formation and nucleation rates may potentially
388 be important.

389 In contrast to H_2O and NH_3 , binding of H_2SO_4 to small negative ions ($s < 3$) is very strong.
390 These ions are very stable even they contain no NH_3 or H_2O molecules. High electron affinity of
391 H_2SO_4 molecules results in the high stability of S^-S_s at $s=1-2$. However, the charge effect reduces
392 as s is growing. In particular, $\Delta G_{\pm S}^{\circ}$ of S^-S_s drops from -32.74 kcal mol^{-1} at $s=1$ to -10.58 kcal mol^{-1}
393 $^+$ and -8.28 kcal mol^{-1} at $s=3$ and 4, respectively. At the same time, $\Delta G_{\pm A}^{\circ}$ increases from 0.08 kcal
394 mol^{-1} ($s=1$) to -11.89 kcal mol^{-1} ($s=3$) and -15.37 kcal mol^{-1} ($s=4$). The hydration of S^-S_s at $s=3, 4$
395 enhances the strength of H_2SO_4 binding, especially at $s=4$. $\Delta G_{\pm S}^{\circ}$ values for $S^-S_{3-4}W_w$ are
396 consistently $\sim 1.5-3$ kcal mol^{-1} less negative than the corresponding semi-experimental estimates
397 (Table 4). The possible reasons behind the observed systematic difference are yet to be identified
398 and include the use of low-level *ab initio* HF method to compute reaction enthalpies and
399 uncertainties in experimental enthalpies in studies by Froyd and Lovejoy (2003).

400 NH_3 binding to S^-S_3 significantly enhances the stability of H_2SO_4 in the cluster by ~ 7 kcal mol^{-1}
401 $^+$ compared to $\Delta G_{\pm S}^{\circ}$ for the corresponding binary counterpart. The binding of the second NH_3 to
402 S^-S_3A to form $S^-S_3A_2$ is much weaker ($\Delta G_{\pm A}^{\circ} = -7.27$ kcal mol^{-1}) than that of the first NH_3 molecule
403 ($\Delta G_{\pm A}^{\circ} = -11.89$ kcal mol^{-1}). This indicates that most of S^-A_n can only contain one NH_3 molecule,
404 in a perfect agreement with the laboratory study of Schobesberger et al. (2015). In the case of S^-
405 S_4 , binding of the first ($\Delta G_{\pm A}^{\circ} = -15.37$ kcal mol^{-1}) and second (and -12.23 kcal mol^{-1}) NH_3
406 molecules to the cluster is quite strong, while the attachment of NH_3 leads to substantial
407 stabilization of H_2SO_4 in the cluster, as evidenced by $\Delta G_{\pm S}^{\circ}$ growing from -8.28 kcal mol^{-1} at $a=0$
408 to -11.76 kcal mol^{-1} and -16.71 kcal mol^{-1} at $a=1$ and $a=2$, respectively. The NH_3 binding free
409 energy to $S^-S_4A_2$ (to form $S^-S_4A_3$) drops to -7.59 kcal mol^{-1} , indicating, in agreement with the
410 CLOUD measurements (Schobesberger et al., 2015) that most of S^-S_4 clusters contain 1 or 2 NH_3
411 molecules.

412 2.4. Nucleation barriers for neutral/charged clusters and size-dependent evaporation rates

413 Nucleation barriers and cluster evaporation rates are critically important for calculations of
414 nucleation rates. This section describes the methods employed to calculate the evaporation rates
415 of nucleating clusters of variable sizes and compositions (i.e., γ in Eqs. 1-6) in the TIMN model.
416
417

418 2.4.1 Equilibrium distributions of small binary and ternary clusters

419 In the atmosphere, $[\text{H}_2\text{O}]$ is much higher than $[\text{H}_2\text{SO}_4]$ and, thus, H_2SO_4 clusters/particles are
 420 always in equilibrium with water vapor (Yu, 2007). In the lower troposphere, where most of the
 421 nucleation events were observed, $[\text{H}_2\text{SO}_4]$ is typically at sub-ppt to ppt level, while $[\text{NH}_3]$ is in the
 422 range of sub-ppb to ppb levels (Butler et al., 2016; Warner et al., 2016) (note that, in what follows,
 423 all references to vapor mixing ratios – parts per billion and parts per trillion – are by volume). This
 424 means that small ternary clusters can be considered to be in equilibrium with H_2O and NH_3 vapors.
 425 Like the previous BIMN model derived assuming equilibrium of binary clusters with water vapor,
 426 the present TIMN model treats small clusters containing a given number of H_2SO_4 molecules as
 427 being in equilibrium with both H_2O and NH_3 . Their relative concentrations are calculated using
 428 the thermodynamic data shown in Tables A1-A4. It should be noted that the system may deviate
 429 from equilibrium if $[\text{NH}_3]$ is less than or close to $[\text{H}_2\text{SO}_4]$. Under such cases, the equilibrium
 430 assumption may overestimate nucleation rates.

431 Figure 3 shows the relative abundance (or molar fractions) of small positive, negative, and
 432 neutral clusters ($f_{s,a,w}^{+,-,0}$) containing a given number of H_2SO_4 molecules at the ambient temperature
 433 of 292 K and three different combinations of RH and $[\text{NH}_3]$ values. As a result of relative
 434 instability of H_2SO_4 in $\text{H}^+\text{A}_1\text{W}_w\text{S}_1$ compared to $\text{H}^+\text{W}_w\text{S}_1$ or $\text{H}^+\text{A}_2\text{W}_w\text{S}_1$ (Fig. 2c), most of positive
 435 ions with one H_2SO_4 molecule exist in the form of either as $\text{H}^+\text{W}_w\text{S}_1$ or $\text{H}^+\text{A}_2\text{W}_w\text{S}_1$ (i.e., containing
 436 either zero or two NH_3 molecules, Fig. 3a). When $[\text{NH}_3]=0.3$ ppb (with $T=292$ K), most of the
 437 positive ions containing one H_2SO_4 molecule do not contain NH_3 and their composition is
 438 dominated by $\text{H}^+\text{W}_w\text{S}_1$ ($\bar{w} \approx 7$). At the given T and $[\text{NH}_3]=0.3$ ppb, around 17% of positive ions
 439 with one H_2SO_4 molecule contain two NH_3 molecules at RH=38%. The fraction of positive ions
 440 containing one H_2SO_4 and two NH_3 molecules decreases to 0.9%, when RH = 90%. At $T=292$ K
 441 and RH=38%, the increase in $[\text{NH}_3]$ by a factor of 10 to 3 ppb leads to the domination of
 442 $\text{H}^+\text{A}_2\text{W}_w\text{S}_1$ (~95%) in the composition of positively charged H_2SO_4 monomers. As expected, the
 443 composition of positive ions and their contribution to nucleation depends on T, RH, and $[\text{NH}_3]$.
 444 The incorporation of the quantum chemical and experimental clustering thermodynamics in the
 445 framework of the kinetic nucleation model enables us to study all these dependencies.

446 As a result of very weak binding of H_2O and NH_3 to small negative ions (Table A4), nearly all
 447 negatively charged clusters with $s=0-1$ do not contain water and ammonia (not shown). In the case,
 448 when s is growing to 2, all $\text{S}^-\text{S}_2\text{A}_a\text{W}_w$ clusters still do not contain NH_3 (i.e., $a=0$), while only 20-
 449 40% of them contain one water molecule ($w=1$) (Fig. 3b). As s further increases to 3, NH_3 begins
 450 to get into some of the negatively charged ions. The fraction of $\text{S}^-\text{S}_3\text{A}_a\text{W}_w$ clusters containing one
 451 NH_3 molecule is 9% at RH=38% and $[\text{NH}_3]=0.3$ ppb, 3% at RH=90% and $[\text{NH}_3]=0.3$ ppb, and
 452 50% at RH=38% and $[\text{NH}_3]=3$ ppb. Most of $\text{S}^-\text{S}_3\text{W}_w$ clusters are hydrated while the fraction of S^-
 453 $\text{S}_3\text{A}_a\text{W}_w$ clusters containing two NH_3 molecules at these ambient conditions is negligible. The
 454 fraction of negative cluster ions containing two NH_3 molecules becomes significant at $s=4$ (Fig.

455 3b) and increases from 28% at $[\text{NH}_3]=0.3$ ppb to 80% at $[\text{NH}_3]=3$ ppb at $\text{RH}=38\%$. At $[\text{NH}_3]=0.3$
 456 ppb, the increase in RH from 38% to 90% reduces the fraction of NH_3 containing $\text{S}^s\text{S}_3\text{A}_a\text{W}_w$
 457 clusters (i.e., $a \geq 1$) from 95% to 70%, demonstrating a significant impact of RH on cluster
 458 compositions and emphasizing the importance of accounting for the RH in calculations of ternary
 459 nucleation rates.

460 The equilibrium distributions of neutral clusters are presented in Fig. 3c (H_2SO_4 monomers
 461 and dimers) and Fig. 3d (H_2SO_4 trimers and tetramers). Hydration is accounted for in the case of
 462 monomers and dimers and not included, due to lack of thermodynamic data, in calculations for
 463 trimers and tetramers. Based on the thermodynamic data shown in Table A3, the dominant fraction
 464 of neutral monomers is hydrated (79% at $\text{RH}=38\%$ and 94% at $\text{RH}=90\%$) while the fraction of
 465 monomers containing NH_3 is negligible (0.02% at $[\text{NH}_3]=0.3$ ppb and 0.2% at $[\text{NH}_3]=3$ ppb,
 466 $\text{RH}=38\%$). As a result of the growing binding strength of NH_3 with the cluster size (Table A3),
 467 the fraction of neutral sulfuric acid dimers containing one NH_3 molecule reaches 18% at
 468 $[\text{NH}_3]=0.3$ ppb and 69% at $[\text{NH}_3]=3$ ppb when $T=292$ K and $\text{RH}=38\%$. In the case of H_2SO_4
 469 trimers and tetramers, data shown in Figure 3d are limited to the relative abundance of unhydrated
 470 clusters only. Under the given conditions, most of trimers contain two NH_3 molecules while most
 471 tetramers contain three NH_3 molecules. At $[\text{NH}_3]=3$ ppb, $\sim 2\%$ of trimers contain three NH_3 molecules
 472 (i.e., $s=a=3$) and 55% of tetramers contain four NH_3 molecules (i.e., $s=a=4$). As a result of a
 473 significant drop of ΔG_{+A}^0 in the case, when a/s ratio exceeds one (Table A3), the fraction of neutral
 474 clusters with $a=s+1$ are negligible. The cluster distributions clearly indicate that small sulfuric acid
 475 clusters are still not fully neutralized by NH_3 even if $[\text{NH}_3]$ is at ppb level; and that the degree of
 476 neutralization (i.e., $a:s$ ratio) increases with the cluster size.

477

478 2.4.2 Mean stepwise and accumulative Gibbs free energy change and impact of ammonia

479 In the TIMN model, the equilibrium distributions are used to calculate number concentrations
 480 weighted stepwise Gibbs free energy change for adding one H_2SO_4 molecule to form a neutral,
 481 positively charged, and negatively charged cluster containing s H_2SO_4 molecules ($\overline{\Delta G}_{s-1,s}$):

$$482 \quad \overline{\Delta G}_{s-1,s}^{+,-,0} = \sum_{a,w} f_{s,a,w}^{+,-,0} \Delta G_{s-1,s,a,w}^{+,-,0} \quad (9)$$

483 where $f_{s,a,w}^{+,-,0}$ is the equilibrium fraction of a particular cluster within a cluster type as shown in
 484 Fig. 3.

485 In the atmosphere, where substantial nucleation is observed, the sizes of critical clusters are
 486 generally small ($s < \sim 5-10$) (e.g., Sipilä et al., 2010) and nucleation rates are largely controlled by
 487 the stability (or γ) of small clusters with $s < \sim 5-10$. QC calculations and experimental data on
 488 clustering thermodynamics available for clusters of small sizes (Tables A2–A4), are critically
 489 important as the formation of these small clusters is generally the limiting step for nucleation.

490 Nevertheless, thermodynamics data for larger clusters are also needed to develop a robust
 491 nucleation model that can calculate nucleation rates under various conditions. Both measurements
 492 and QC calculations (Tables [A2–A4](#)) show significant effects of charge and charge signs (i.e.,
 493 positive or negative) on the stability and composition of small clusters. These charge effects
 494 decrease quickly as the clusters grow, due to the short-ranged nature of dipole-charge interaction
 495 and the quick decrease of electrical field strength around charged clusters as cluster sizes increase
 496 (Yu, 2005). Based on experimental data (Kearle et al., 1967; Davidson et al., 1977; Wlodek et
 497 al., 1980; Holland and Castleman, 1982; Froyd and Lovejoy, 2003), the stepwise ΔG values for
 498 clusters decreases exponentially as the cluster sizes increase and approaches to the bulk values
 499 when clusters containing more than ~ 8 -10 molecules (Yu, 2005). Cluster compositions measured
 500 with an atmospheric pressure interface time-of-flight (APi-TOF) mass spectrometer during
 501 CLOUD experiments also show that the difference in the composition of positively and negatively
 502 charged clusters quickly decreases as the number of H₂SO₄ molecules increases from 1 to ~ 10 and
 503 exhibits little further changes the chemical effect of charge-carrying becomes unimportant when
 504 the cluster contains more than 9 H₂SO₄ molecules (Schobesberger et al., 2015).

505 In the present TIMN model, we assume that both neutral and charged clusters have the same
 506 composition when $s \geq 10$ and the following extrapolation scheme is used to calculate $\Delta G_{s-1,s}$ for
 507 clusters up to $s=10$:

$$508 \quad \Delta G_{s-1,s} = \Delta G_{s_1-1,s_1} + \frac{\left(\Delta G_{s_2-1,s_2} - \Delta G_{s_1-1,s_1}\right)\left(e^{-sc} - e^{-s_1c}\right)}{\left(e^{-s_2c} - e^{-s_1c}\right)} \quad (10\pm)$$

509 where $\Delta G_{s_1-1,s_1}$ is the stepwise mean Gibbs free energy change for H₂SO₄ addition for a specific
 510 type (neutral, positive, or negative) of clusters at $s=s_1$ that can be derived from QC calculation
 511 and/or experimental measurements, and $\Delta G_{s_2-1,s_2}$ is the corresponding value for clusters at $s=s_2$
 512 ($=10$ in the present study) that is calculated in the capillarity approximation accounting for the
 513 Kelvin effect. c in Eq. [10±](#) is the exponential coefficient that determines how fast $\Delta G_{s-1,s}$
 514 approaches to bulk values as s increases. In the present study, c is estimated from $\Delta G_{s-1,s}$ at $s=2$
 515 and $s=3$ for neutral binary and ternary clusters for which experimental (Hanson and Lovejoy, 2006;
 516 Kazil et al., 2007) or quantum-chemical data (Table [A3](#)) are available. Apparently the interpolation
 517 approximation Eq. (10) is subject to uncertainty. Nevertheless, it is a reasonable approach to
 518 connect thermochemical properties of QC data for small binary and ternary clusters that cannot be

adequately described by the capillarity approximation with those for large clusters that can be adequately described the very same capillarity approximation, and is the best approach we can come up with at this point in order to develop a model that can be applied to all conditions. Further QC and experimental studies of the thermodynamics of relatively larger clusters can help to reduce the uncertainty.

For clusters with $s \geq 2$, the capillarity approximation is used to calculate $\Delta G_{s-1,s}$ as

$$\Delta G_{s-1,s} = -RT \ln(P/P_s) + \frac{2\sigma v_1 N_A}{r_s} \quad (112)$$

where P is the H_2SO_4 vapor pressure and P_s is the H_2SO_4 saturation vapor pressure over a flat surface with the same composition as the cluster. σ is the surface tension and v_1 is the volume of one H_2SO_4 molecule. r_s is the radius of the cluster and N_A is the Avogadro's number.

The scheme to calculate bulk $\Delta G_{s-1,s}$ ($s \geq 10$) for H_2SO_4 - H_2O binary clusters has been described in Yu (2007). For ternary nucleation, both experiments (Schobesberger et al., 2015) and QC calculations (Table A4) indicate that the growth of relatively large clusters follows the $s=a$ line (i.e, in the composition of ammonia bisulfate). In the present TIMN model, the bulk $\Delta G_{s-1,s}$ values for ternary clusters are calculated based on ~~parameterized measured~~ H_2SO_4 saturation vapor pressure over ammonia bisulfate as a function of temperature, derived from by Martin et al. (1997) from vapor pressures measured at temperature between 27 °C and 60 C, and surface tension measured at 298 K from Hyvarinen et al. (2005).- The uncertainty in saturation vapor pressures and surface tension used in the calculation of the bulk $\Delta G_{s-1,s}$ values is another source of uncertainty in the TIMN model, although it is likely to be small compared to other uncertainties as the nucleation is generally limited by the formation of small clusters.

Figure 4 presents stepwise ($\overline{\Delta G}_{s-1,s}$) and cumulative (total) $\overline{\Delta G}_s$ Gibbs free energy changes associated with the formation of neutral, positively charged, and negatively charged binary and ternary clusters containing s H_2SO_4 molecules under the conditions specified in the figure caption. The clusters are assumed to be in equilibrium with water (Yu, 2007) and ammonia (Fig. 3). As seen from Fig. 4, the presence of NH_3 reduces the mean $\overline{\Delta G}_{s-1,s}$ for larger clusters, which can be treated as the bulk binary H_2SO_4 - H_2O solution (Schobesberger et al., 2015), by $\sim 3 \text{ kcal mol}^{-1}$, ~~consistent with the laboratory measurements (Marti et al., 1997)~~ indicating a substantial reduction in the H_2SO_4 vapor pressure over ternary solutions (Marti et al., 1997). The comparison also shows

548 that the influence of NH_3 on $\overline{\Delta G}_{s-1,s}$ of small clusters ($s \leq \sim 4$) is much lower than that on larger
549 ones and bulk solutions. For example, at $[\text{NH}_3]=0.3$ ppb, the differences in $\overline{\Delta G}_{s-1,s}$ between
550 binary and ternary positive ions with $s=1$ and neutral clusters with $s=2$ are only $0.45 \text{ kcal mol}^{-1}$
551 and $\sim 1 \text{ kcal mol}^{-1}$, respectively. In the case of negative ions, zero and $0.27\text{--}0.45 \text{ kcal mol}^{-1}$
552 differences at $s \leq 2$ and $s=3\text{--}4$, respectively, were observed. The reduced effect of ammonia on
553 smaller clusters is explained (Tables [A2](#)–[A5](#)) by ammonia's weaker bonding to smaller clusters
554 than to larger ones, which in turn yields lower average NH_3 to H_2SO_4 ratios (Fig. 3). It should be
555 noted that QC data for positively charged clusters are very limited and the interpolation
556 approximation is subject to large uncertainty. In order for the nucleation on positive ions to occur,
557 the first step is for H_2SO_4 to attach to a positive ion that does not contain H_2SO_4 . Unlike negative
558 ions, the effect of charge on the bonding of H_2SO_4 with positive ions is much weaker and thus the
559 stepwise Gibbs free energy change for the addition of one H_2SO_4 molecule to form a positively
560 charged cluster is likely to be similar to that of neutral clusters, i.e., decreasing with cluster size.
561 Therefore, the QC data for positively charged clusters containing one H_2SO_4 molecule provides a
562 critical constrain. The success of the model in predicting the $[\text{NH}_3]$ needed for nucleation on
563 positive ions to occur (see Section 3) show the usefulness of the first step data and approximation.

564 As seen from Fig. 4, bonding of H_2SO_4 to small negatively charged clusters ($s < 3$) is much
565 stronger than that to neutrals and positive ions. As a result, at $s < 3$ the formation of negatively
566 charged clusters is barrierless ($\overline{\Delta G}_{s-1,s} < 0$). These small clusters cannot be considered as nucleated
567 particles because $-\overline{\Delta G}_{s-1,s}$ (Fig. 4a), and with growing s first increases and then decreases with
568 growing s , reaching the maximum barrier values at $s = \sim 3 - 6$. $\overline{\Delta G}_{s-1,s}$ can become positive for
569 larger clusters due to the charge effect decreasing quickly as the clusters are growing. The negative
570 $\overline{\Delta G}_{s-1,s}$ for small clusters is not able to cancel the positive $\overline{\Delta G}_{s-1,s}$ for larger clusters and thus,
571 to show properly the overall nucleation barrier, $\overline{\Delta G}_{s-1,s}$ for small clusters are set to zero when
572 they are negative in the cumulative Gibbs free energy calculation. The effect of NH_3 on negative
573 ions becomes important at $s \geq \sim 4$, when bonding between the clusters and NH_3 becomes strong
574 enough to contaminate a large fraction of binary clusters with ammonia (Fig. 3). In contrast, the
575 impact of NH_3 on neutral dimers and positively charged monomers of H_2SO_4 , as well as on

576 $\overline{\Delta G}_{s-1,s}$ for both positively charged and neutral clusters, monotonically decreases for all s ,
577 including $s \leq 5$.

578 $\overline{\Delta G}_{s-1,s}$ for charged and neutral clusters converge into the bulk values at $s \sim 10$, when impact
579 of the chemical identity of the core ion on the cluster composition becomes diffuse (Schobesberger
580 et al., 2015) and when the contribution of the electrostatic effect to $\overline{\Delta G}_{s-1,s}$ becomes less than \sim
581 $0.5 \text{ kcal mol}^{-1}$. The comparison of cumulative (total) $\overline{\Delta G}_s$ (Fig. 4b) indicates the lowest nucleation
582 barrier for the case of negative ions, followed by positive ions and neutrals. The barrierless
583 formation of clusters with s ranging from 1 to 3 substantially reduces the nucleation barrier for
584 negatively charged ions and facilitates their nucleation. The presence of 0.3 ppb of NH_3 lowers the
585 nucleation barrier for negative, positive and neutral clusters from $\sim 17, 24$ and 38 kcal mol^{-1} to 2,
586 7 and 16 kcal mol^{-1} , respectively. A relatively low nucleation barrier for charged ternary clusters
587 is explained by the simultaneous effect of ionization and NH_3 which also reduces the size of the
588 critical cluster (s^*).

589 It is important to note that the size of the critical cluster, commonly used to “measure” the
590 activity of nucleation agents in the classical nucleation theory (Coffman and Hegg, 1995;
591 Korhonen et al., 1999; Vehkamäki et al., 2002; Napari et al., 2002; Hamill et al., 1982) is no longer
592 a valid indicator, when charged molecular clusters and small nanoparticles are considered. As seen
593 from Fig. 4, positively charged ternary critical clusters ($s^*=3-4$) are smaller than the corresponding
594 negatively charged ones ($s^*=4-5$); however, the nucleation barrier for ternary positive clusters
595 under the condition specified in the figure caption is more than three times higher than that for
596 ternary negatives ones.

597
598

599 2.4.3 Size- and composition- dependent H_2SO_4 evaporation rates

600 As we mentioned earlier, H_2SO_4 is the key atmospheric nucleation precursor driving the
601 formation and growth of clusters in the ternary $\text{H}_2\text{SO}_4\text{-H}_2\text{O-NH}_3$ system while ions, H_2O , and
602 NH_3 act to stabilize the H_2SO_4 clusters. The clustering thermodynamic data derived from QC
603 calculations and measurements (Section 2.3) are used to constrain size- and composition-
604 dependent Gibbs free energy changes and evaporation rates of H_2SO_4 which are critically
605 important. ~~Similar to $\overline{\Delta G}_{s-1,s}$, Average~~ or effective rates of H_2SO_4 molecule evaporation from

606 positively charged, negatively charged, and neutral clusters containing s H₂SO₄ molecules
 607 ($\bar{\gamma}_s^{+,-,0}$) are calculated from $\overline{\Delta G}_{s-1,s}$ as:

$$608 \quad \bar{\gamma}_s^{+,-,0} = \beta_{s-1}^{+,-,0} N^0 \exp\left(\frac{\overline{\Delta G}_{s-1,s}}{RT}\right) \quad (120)$$

609 where ~~$\gamma_{s,a,w}^{+,-,0}$ is the H₂SO₄ evaporation coefficient from a particular cluster within a cluster type as~~
 610 ~~shown in Fig. 3, which can be calculated based on Eq. (7) with $\Delta G_{\mp s}^0$ from Tables 2-4 N^0 is as~~
 611 ~~defined in Eq. (7). The present model assumes only a single H₂SO₄ molecule evaporates, i.e. no~~
 612 ~~water ligands, for instance, are attached to it. This is likely the dominant evaporation pathway as~~
 613 ~~hydrated H₂SO₄ molecules are generally more stable.~~

614 Figure 5 gives the ~~number concentration weighted~~ mean evaporation rate ($\bar{\gamma}$) of an H₂SO₄
 615 molecule from these clusters under the conditions corresponding to Fig. 4. The shapes of $\bar{\gamma}$ curves
 616 are similar to those of $\overline{\Delta G}_{s-1,s}$ (Fig. 4a) as $\bar{\gamma}$ values are largely controlled by $\overline{\Delta G}_{s-1,s}$ (Eq. 127).

617 The presence of ammonia, as expected, significantly reduces the vapor pressure of H₂SO₄ over
 618 bulk aerosol (Marti et al., 1997), and, hence, the H₂SO₄ evaporation rate. The evaporation rates of
 619 both neutral and positive clusters decrease as s increases, and the positive clusters are uniformly
 620 more stable than corresponding neutral clusters. $\bar{\gamma}$ for negative ions first increases and then
 621 decreases as s increases, peaking around $s = \sim 3 - 6$. The presence of NH₃ reduces the evaporation
 622 rates of larger clusters by more than two orders of magnitude and the effect decreases for smaller
 623 clusters, as the binding of NH₃ to small neutral and charged clusters are weaker compared to that
 624 for larger clusters (Fig. 4). [NH₃] influences the average NH₃:H₂SO₄ ratio (Fig. 3) and the
 625 evaporation rates of these small clusters. The nucleation rates, limited by formation of small
 626 clusters ($s < \sim 5$), depend strongly on the stability or evaporation rate of these small clusters ~~and,~~
 627 ~~thus, on [NH₃].~~ While the binding of NH₃ to small neutral and charged clusters is weaker compared
 628 to that to larger clusters, small clusters containing NH₃ are much more stable than those without
 629 (Fig. 4) and thus ammonia is important for nucleation.

630

631 3. TIMN rates and comparisons with CLOUD measurements

632 The evolution of cluster/particle size distributions can be obtained by solving the dynamic
 633 equations 1-6. Since the concentrations of clusters of all sizes are ~~explicitly~~ predicted, the
 634 nucleation rates in the kinetic model can be calculated for any cluster size larger than the critical
 635 size of neutral clusters ($i > i^*$) (Yu, 2006b),

$$636 \quad J_i = J_i^+ + J_i^- + J_i^0 = \beta_{i,1}^+ N_1^0 N_i^+ - \gamma_i^+ N_{i+1}^+ + \beta_{i,1}^- N_1^0 N_i^- - \gamma_i^- N_{i+1}^- + \beta_{i,1}^0 N_1^0 N_i^0 - \gamma_i^0 N_{i+1}^0 \quad (13)$$

637 where J_i^+ , J_i^- , and J_i^0 are nucleation rates associated with positive, negative, and neutral clusters
638 containing i H₂SO₄ molecules. As a result of scavenging by pre-existing particles or wall loss, the
639 steady state J_i decreases as i increases. To compare with CLOUD measurements, we calculate
640 nucleation at cluster mobility diameter of 1.7 nm ($J_{1.7}$).

641 Many practical applications require information on the steady state nucleation rates. For each
642 nucleation case presented in this paper, constant values of [H₂SO₄] (i.e., N_1^0), [NH₃], T, RH, Q,
643 and $L_i^{+,-,0}$ are assumed. The pre-existing particles with fixed surface area or wall loss serve as a
644 sink for all clusters. Under a given condition, cluster distribution and nucleation rate reach steady
645 state after a certain amount of time. We calculate size-dependent coefficients for a given case, and
646 then solve equations (1-6) to obtain the steady state cluster distribution and nucleation rate, with
647 the approach described in Yu (2006b).

648 Figure 6 shows a comparison of the model TIMN rates $J_{1.7}$ with CLOUD measurements, as a
649 function of [NH₃] under two ionization rates. It should be noted that Dunne et al. (2016) developed
650 a simple empirical parameterization (denoted thereafter as “CLOUDpara”) of binary, ternary and
651 ion-induced nucleation rates in CLOUD measurements as a function of [NH₃], [H₂SO₄], T, and
652 negative ion concentration. The predictions ~~based on of~~ CLOUDpara (Dunne et al., 2016) and
653 ACDC based on nucleation thermochemistry obtained using RI-CC2//B3LYP method (McGrath
654 et al., 2012; Kurten et al., 2016) are also presented in Fig. 6 for comparisons.

655 Like the CLOUD measurements, the TIMN predictions reveal a complex dependence of $J_{1.7}$
656 on [NH₃], and an analysis of the TIMN results shows this behavior can be explained by the
657 differing responses of negative, positive and neutral clusters to the presence of ammonia (Fig. 4).
658 Under the conditions specified in Fig. 6, nucleation is dominated by negative ions for [NH₃] <~0.5
659 ppb, by both negative and positive ions for [NH₃] from ~0.5 ppb to ~10 ppb (with background
660 ionization), or ~20 ppb (with pion-enhanced ionization), and by neutrals at higher [NH₃].
661 According to TIMN, [NH₃] of at least 0.6–1 ppb are needed before positive ions contribute
662 significantly to nucleation rates – in good agreement with the threshold found in the CLOUD
663 experiments (Kirkby et al., 2011; Schobesberger et al., 2015). TIMN simulations also extend
664 CLOUD data at [NH₃] of ~1 ppb to include a “zero-sensitivity zone” in the region of 1-10 ppb,
665 followed by a region of strong sensitivity of $J_{1.7}$ to [NH₃] commencing at [NH₃] > ~10-20 ppb. The
666 latter zone may have important implications for NPF in heavily polluted regions, including much
667 of India and China, where [NH₃] may exceed 10-20 ppb (Behera and Sharma, 2010; Meng et al.,
668 2017). It is noteworthy in Fig. 6 that the dependence of $J_{1.7}$ on [NH₃] and Q predicted by the ACDC
669 model (McGrath et al., 2012) and the CLOUD data parameterization (Dunne et al., 2016) deviate

670 substantially from the experimental data as well as the TIMN simulations. The CLOUDpara does
671 not consider impacts of positive ions and such key controlling parameters as RH and surface area
672 of pre-existing particles. Dunne et al. (2016) reported that CLOUDpara is also very sensitive to
673 the approach to parameterize T dependence, showing that the contribution of ternary ion-induced
674 nucleation to NPF below 15 km altitude has grown from 9.6% to 37.5%, after the initial empirical
675 temperature function was replaced with a simpler one.

676 Figure 7 presents a more detailed comparison of TIMN simulations with CLOUD
677 measurements of $J_{1.7}$ as a function of $[\text{H}_2\text{SO}_4]$, T, and RH. The TIMN model **accurately** reproduces
678 both the absolute values of $J_{1.7}$ and its dependencies on $[\text{H}_2\text{SO}_4]$, T, and RH, in a wide range of
679 temperatures ($T=208 - 292$ K) and $[\text{H}_2\text{SO}_4]$ ($5 \times 10^5 - 5 \times 10^8 \text{ cm}^{-3}$). As expected, nucleation rates
680 are very sensitive to $[\text{H}_2\text{SO}_4]$ and T. For example, $J_{1.7}$ increases by three to five orders of magnitude
681 with an increase in $[\text{H}_2\text{SO}_4]$ of a factor of 10, and by roughly one order of magnitude for a
682 temperature decrease of 10 degree, except in cases where the nucleation rate is limited by Q (for
683 example, $[\text{H}_2\text{SO}_4] = \sim 10^8 - 10^9 \text{ cm}^{-3}$ at $T=278$ K and 292 K, shown in Fig. 7a). The key difference
684 between CLOUDpara and TIMN predictions is that $\text{dln}J_{1.7}/\text{dln}[\text{H}_2\text{SO}_4]$ ratio predicted by
685 CLOUDpara is nearly constant while TIMN shows that this ratio depends on both $[\text{H}_2\text{SO}_4]$ and T.
686 The CLOUD measurements taken at $T=278$ K clearly show (in agreement with the TIMN) that
687 $\text{dln}J_{1.7}/\text{dln}[\text{H}_2\text{SO}_4]$ is not constant. CLOUDpara overestimates $J_{1.7}$ compared to both
688 measurements and TIMN simulations, except for the case, when $T=278$ K and $[\text{H}_2\text{SO}_4]$ ranges
689 from $\sim 7 \times 10^6$ to $5 \times 10^7 \text{ cm}^{-3}$, with deviation of CLOUDpara from experimental data and TIMN
690 growing with the lower temperature.

691 Both CLOUD measurements and TIMN simulations (Fig. 7b) show an important influence of
692 RH on nucleation rates (which is neglected in both the CLOUDpara and ACDC models). In
693 particular, CLOUD measurements indicate 1-5 order of magnitude rise in $J_{1.7}$ after RH increases
694 from 10% to 70-80% and a stronger effect of RH on nucleation rates at higher temperatures under
695 the conditions shown in Fig. 7b. The RH dependence of $J_{1.7}$ predicted by the TIMN model is
696 consistent with measurements, being slightly weaker than the measured at high RH.

697 Figure 8 compares TIMN model predictions with all 377 data points of CLOUD measurements
698 reported in data Table S1 of Dunne et al. (2016). The vertical error bars show the range of J_{model}
699 associated with the uncertainty in the $[\text{H}_2\text{SO}_4]$ measured (-50%, +100%). The effect of uncertainty
700 in measured $[\text{NH}_3]$ (-50%, +100%) is not included. At the presence of ionization (Fig. 8a), J_{model}
701 agrees with CLOUD measurements within the uncertainties under mainly all conditions, although
702 J_{model} tends to be slightly lower than J_{obs} when $T=292 - 300$ K and J_{obs} is relatively small ($< \sim 1 \text{ cm}^{-3} \text{ s}^{-1}$).
703 For the neutral nucleation (Fig. 8b), the model agrees well with observations at low T ($T=205$
704 - 223 K) but deviates from observations as T increases. The under-prediction of the model for
705 neutral nucleation at $T=278 - 300$ K cannot be explained by the uncertainties in measured $[\text{H}_2\text{SO}_4]$

706 and [NH₃]. Apparently for neutral nucleation the model predicts much stronger temperature
707 dependence than the CLOUD measurements. The possible reasons for the difference include the
708 uncertainties in both the model (especially the thermodynamics data and approximation) and
709 measurements. The contamination (by amines) in the CLOUD measurements (Kirkby et al., 2011)
710 can be another possible reason. The level of contamination in the cloud chamber appears to
711 increase with temperature (Kurten et al., 2016), which may explain the good agreement at low T
712 and increased deviation at higher T. Further research is needed to identify the source of the
713 difference for neutral ternary nucleation at high T.

714

715 **4. Summary**

716 A comprehensive kinetically-based H₂SO₄-H₂O-NH₃ ternary ion-mediated nucleation (TIMN)
717 model, constrained with thermodynamic data from quantum-chemical calculations and laboratory
718 measurements, has been developed and used to shed a new light on physico-chemical processes
719 underlying the effect of ammonia on NPF. We show that the stabilizing effect of NH₃ grows with
720 the cluster size, and that the reduced effect of ammonia on smaller clusters is caused by weaker
721 bonding that in turn yields lower average NH₃ to H₂SO₄ ratios. NH₃ was found to impact nucleation
722 barriers for neutral, positively charged, and negatively charged clusters differently due to the large
723 difference in the binding energies of NH₃, H₂O, and H₂SO₄ to small clusters of different charging
724 states. The lowest and highest nucleation barriers are observed in the case of negative ions and
725 neutrals, respectively. Therefore, nucleation of negative ions is favorable, followed by nucleation
726 of positive ions and neutrals. Different responses of negative, positive and neutral clusters to
727 ammonia result in a complex dependence of ternary nucleation rates on [NH₃]. The TIMN model
728 reproduces both the absolute values of nucleation rates and their dependencies on the key
729 controlling parameters and agrees with the CLOUD measurements for all the cases at the presence
730 of ionization. For the neutral ternary nucleation, the model agrees well with observations at low
731 temperature but deviates from observations as temperature increases. ~~much better than other~~
732 ~~models being tested here over a wide range of ambient conditions encompassing those encountered~~
733 ~~in the global atmosphere.~~

734 The TIMN model developed in the present study may be subject to uncertainties associated with
735 the use of uncertainties in experimental and thermodynamic data and interpolation approximation
736 for pre-nucleation clusters. Further measurements and quantum calculations, especially for
737 relatively larger clusters, -are needed to reduce the uncertainties. While the TIMN model predicts
738 nucleation rates in a good overall agreement with the CLOUD measurements, its ability to explain
739 the NPF events observed in the real atmosphere is yet to be quantified and will be investigated in
740 further studies.

742 Appendix

743 2.3A1. Quantum-chemical studies of neutral and charged binary and ternary clusters

744 Thermochemical data for small neutral and charged binary H₂SO₄-H₂O and ternary H₂SO₄-
745 H₂O-NH₃ clusters has been reported in a number of earlier publications (Bandy and Ianni, 1998;
746 Ianni and Bandy, 1999; Torpo et al., 2007; Nadykto et al., 2008; Herb et al., 2011, 2013; Temelso
747 et al., 2012a, b; DePalma et al., 2012; Ortega et al., 2012; Chon et al., 2014; Husar et al., 2014;
748 Henschel et al., 2014, 2016; Kurten et al., 2015). The PW91PW91/6-311++G(3df,3pd) method,
749 which is a combination of the Perdue-Wang PW91PW91 density functional with the largest Pople
750 6-311++G(3df,3pd) basis set, has thoroughly been validated and agrees well with existing
751 experimental data. In earlier studies, this method has been applied to a large variety of
752 atmospherically-relevant clusters (Nadykto et al. 2006, 2007a, b, 2008, 2014, 2015; Torpo et al.
753 2007; Zhang et al., 2009; Elm et al. 2012; Leverentz et al. 2013; Xu and Zhang, 2012; Xu and
754 Zhang, 2013; Elm et al., 2013; Zhu et al. 2014; Bork et al. 2014; Elm and Mikkelsen, 2014; Peng
755 et al. 2015; Miao et al 2015; Chen et al., 2015; Ma et al., 2016) and has been shown to be well
756 suited to study the ~~ones~~H₂SO₄-H₂O and H₂SO₄-H₂O-NH₃ clusters, as evidenced by a very good
757 agreement of the computed values with measured cluster geometries, vibrational fundamentals,
758 dipole properties and formation Gibbs free energies (Nadykto et al., 2007a, b, 2008, 2014, 2015;
759 Herb et al., 2013; Elm et al., 2012, 2013; Leverentz et al., 2013; Bork et al., 2014) and with high
760 level ab initio results (Temelso et al., 2012a, b; Husar et al., 2012; Bustos et al., 2014).

761 We have extended the earlier QC studies of binary and ternary clusters to larger sizes. The
762 computations have been carried out using Gaussian 09 suite of programs (Frisch et al., 2009). In
763 order to ensure the quality of the conformational search we have carried out a thorough sampling
764 of conformers. We have used both basin hopping algorithm, as implemented in Biovia Materials
765 Studio 8.0, and locally developed sampling code, ~~which creates a “mesh” around the cluster, in~~
766 ~~which molecules being attached to the cluster are the mesh nodes. The sampling code is based on~~
767 ~~the following principle: mesh, with molecule to be added to the cluster placed in the mesh nodes,~~
768 ~~is created around the cluster, and blind search algorithm is used to generate the guess geometries.~~
769 ~~The mesh density and orientation of molecules are variable, as well as the minimum distance~~
770 ~~between molecules and cluster.~~ Typically, for each cluster of a given chemical composition a
771 thousand to several thousands of isomers have been sampled. We used a three-step optimization
772 procedure, which includes (i) pre-optimization of initial/guess geometries by semi-empirical PM6
773 method, separation of the most stable isomers located within 15 kcal mol⁻¹ of the intermediate
774 global minimum and duplicate removal, followed by (ii) optimization of the selected isomers
775 meeting the aforementioned stability criterion by PW91PW91/CBSB7 method and (iii) the final
776 optimization of the most stable at PW91PW91/CBSB7 level isomers within 5 kcal mol⁻¹ of the
777 current global minimum using PW91PW91/6-311++G(3df,3pd) method. Typically, only ~4-30%

778 of initially sampled isomers reach the second (PW91PW91/CBSB7) level, where ~10-40% of
779 isomers optimized with PW91PW91/CBSB7 are selected for the final run. Typically, the number
780 of equilibrium isomers of hydrated clusters is larger than that of unhydrated ones of similar
781 chemical composition. Table [A1](#) shows the numbers of isomers converged at the final
782 PW91PW91/6-311++G(3df,3pd) optimization step for selected clusters and HSG values of the
783 most stable isomers used in the present study. The number of isomers optimized at the
784 PW91PW91/6-311++G(3df,3pd) level of theory varies from case to case, typically being in the
785 range of ~10-200.

786 The computed stepwise enthalpy, entropy, and Gibbs free energies of cluster formation have
787 been thoroughly evaluated and used to calculate the evaporation rates of H₂SO₄ from neutral,
788 positive and negative charged clusters. ~~A detailed description of QC calculations and the full range
789 of computed properties of binary and ternary clusters will be reported in separate papers.~~

790

791 [2.3A1.1](#) Positively charged clusters

792 Table [A2](#) presents the computed stepwise Gibbs free energy changes under standard conditions
793 (ΔG°) for positive binary and ternary clusters, along with the corresponding experimental data or
794 semi-experimental estimates. Figure 2 [in the main text](#) shows ΔG associated with the addition of
795 water (ΔG_{+W}°), ammonia (ΔG_{+A}°), and sulfuric acid (ΔG_{+S}°) to binary and ternary clusters as a
796 function of the cluster hydration number w .

797 Both the absolute values and trends in ΔG_{+W}° derived from calculations are in agreement with
798 the laboratory measurements within the uncertainty range of ~1-2 kcal mol⁻¹ for both QC
799 calculations and measurements. This confirms the efficiency and precision of QC methods in
800 calculating thermodynamic data needed for the development of nucleation models. ~~Nevertheless,
801 it should be noted that the uncertainties in computed free energies of 1-2 kcal mol⁻¹ may lead to
802 large uncertainty in predicted particle formation rates. By increasing or decreasing all Gibbs free
803 energies by 1 kcal mol⁻¹, Kürten et al. (2016) showed that, depending on the conditions, the
804 modeled particle formation rate can change from less than an order of magnitude to several orders
805 of magnitude. Uncertainties estimated by Kürten et al. (2016) represent the upper limit because
806 computed free energies may be overestimated for some clusters and underpredicted for others that
807 leads to partial or, in some case, full error cancellation.~~

808

809 [2.3A1.2](#) Neutral clusters

810 Table [A3](#) presents the computed stepwise Gibbs free energy changes for the formation of
811 ternary S_sA_aW_w clusters under standard conditions. ~~The corresponding binary electrically neutral
812 clusters can be found in previous publications (e.g., Nadykto et al., 2008; Herb et al., 2011).~~ The
813 thermodynamic properties of the S₁A₁ have been reported in a number of computational studies

814 (e.g., Herb et al., 2011; Kurten et al., 2007~~15~~; Nadykto and Yu, 2007). However, ~~as pointed out~~
815 ~~by Kurten et al. (2015)~~, most of these studies, except for Nadykto and Yu (2007) ~~and Henschel et~~
816 ~~al. (2014; 2016)~~, did not consider the impact of H₂O on cluster thermodynamics. We have extended
817 the earlier studies of Nadykto and Yu (2007) and Herb et al. (2011) to larger clusters up to S₄A₅
818 (no hydration) and up to S₂A₂ (hydration included). The free energy of binding of NH₃ to H₂SO₄
819 (or H₂SO₄ to NH₃) obtained using our method is -7.77 kcal mol⁻¹ that is slightly more negative
820 than values reported by other groups (-6.6 --7.61 kcal mol⁻¹) and within less than 0.5 kcal mol⁻¹
821 of the experimental value of -8.2 kcal mol⁻¹ derived from CLOUD measurements (Kurten et al.,
822 2015).

823 As it may be seen from Table [A3](#), the NH₃ binding to S₁₋₂W_w weakens as *w* increases. The
824 average ΔG_{+W}^0 for S₁W_w formation derived from a combination of laboratory measurements and
825 quantum chemical studies are -3.02, -2.37, and -1.40 kcal mol⁻¹ for the first, second, and third
826 hydration, respectively (Yu, 2007). This indicates that a large fraction of H₂SO₄ monomers in the
827 Earth's atmosphere is likely hydrated. Therefore, the decreasing NH₃ binding strength to hydrated
828 H₂SO₄ monomers implies that RH (and T) will affect the relative abundance of H₂SO₄ monomers
829 containing NH₃. Currently, no experimental data or observations are available to evaluate the
830 impact of hydration (or RH) on ΔG_{+A}^0 . Table [A3](#) shows that the presence of NH₃ in H₂SO₄ clusters
831 suppress hydration and that ΔG_{+W}^0 for S₂A₂ falls below -2.0 kcal mol⁻¹. This is consistent with
832 earlier studies by our group ([Herb et al., 2011](#)) and others ([Henschel et al., 2014, 2016](#)) showing
833 that large S_nA_n clusters (*n*>2) are not hydrated under typical atmospheric conditions. In the present
834 study, the hydration of neutral S_nA_n clusters at *n*>2 is neglected, due to the lack of thermodynamic
835 data.

836 The number of NH₃ molecules in the cluster (or H₂SO₄ to NH₃ ratio) significantly affects ΔG_{+S}^0
837 and ΔG_{+A}^0 values. For example, ΔG_{+S}^0 for S₃A_a clusters increases from -7.08 kcal mol⁻¹ to -16.92
838 kcal mol⁻¹ and ΔG_{+A}^0 decreases from -16.14 kcal mol⁻¹ to -8.93 kcal mol⁻¹ as *a* is growing from 1
839 to 3. For S₄A_a clusters, ΔG_{+S}^0 is increasing from -7.48 kcal mol⁻¹ to -16.26 kcal mol⁻¹ and ΔG_{+A}^0
840 decreases from -17.16 kcal mol⁻¹ to -11.34 kcal mol⁻¹ as *a* increases from 2 to 4. ΔG_{+A}^0 for S₄A₁
841 cluster is by 1.38 kcal mol⁻¹ less negative than that for S₄A₂. ΔG_{+S}^0 for the S₄A₁ cluster is also quite
842 low (-4.16 kcal mol⁻¹) that might indicate the possible existence of a more stable S₄A₁ isomer,
843 which is yet to be identified. In the presence of NH₃, the uncertainty in the thermochemistry data
844 for S₄A₁ will not significantly affect ternary nucleation rates because most of S₄-clusters contain
845 3 or 4 NH₃ molecules.

846 For the S_sA_a clusters with *s*=*a*, ΔG_{+A}^0 increases as cluster is growing while ΔG_{+S}^0 first increases
847 significantly as S₁A₁ is converting into S₂A₂ and then levels off as S₂A₂ is converting into S₄A₄.
848 We also observe a significant drop in ΔG_{+A}^0 in the case when NH₃/H₂SO₄ ratio exceeds 1. This

849 finding is **fully** consistent with the **laboratory measurements** **ACDC model calculation** showing that
850 growth of neutral S_sA_a clusters follows **the** $s=a$ pathway (Schobesberger et al., 2015).

851 **2.3A1.3** Negative ionic clusters

852 Table **A4** shows ΔG_{+W} , ΔG_{+A} , and ΔG_{+S} needed to form negatively charged clusters under
853 standard conditions, along with available semi-experimental values (Froyd and Lovejoy, 2003).
854 H_2O binding to negatively charged S^-S_s clusters significantly strengthens with increasing s , from
855 $\Delta G_{+W}^0 = -0.61$ to -1.83 kcal mol⁻¹ at $s=1-2$ to $\Delta G_{+W}^0 = -3.5$ kcal mol⁻¹ at $w=1$ and -2.25 kcal mol⁻¹ at
856 $w=4$ at $s=4$. ΔG_{+W}^0 values at $s=3$ and 4 are slightly more negative (by $\sim 0.1 - 0.9$ kcal mol⁻¹) than
857 those reported by Froyd and Lovejoy (2003). Just like H_2O binding, NH_3 binding to S^-S_s at $s < 3$ is
858 very weak, with ΔG_{+A}^0 ranging from $+2.81$ kcal mol⁻¹ at $s=0$ to -4.85 kcal mol⁻¹ at $s=2$. However,
859 it significantly increases as s is growing. In particular, at $s \geq 3$ ΔG_{+A}^0 is ranging from -11.89 kcal
860 mol⁻¹ for $S^-S_3A_1$ to -15.37 kcal mol⁻¹ for $S^-S_4A_1$. NH_3 clearly cannot get into small negative ions.
861 However, it can easily attach to larger negative ions with $s \geq 3$ that is consistent with CLOUD
862 measurements (Schobesberger et al., 2015). Since hydration weakens NH_3 binding in $S^-S_3A_1W_w$
863 and $S^-S_4A_1W_w$ clusters, its impacts on the cluster formation and nucleation rates may potentially
864 be important.

865 In contrast to H_2O and NH_3 , binding of H_2SO_4 to small negative ions ($s < 3$) is very strong.
866 These ions are very stable even **when** they contain no NH_3 or H_2O molecules. High electron
867 affinity of H_2SO_4 molecules results in the high stability of S^-S_s at $s=1-2$. However, the charge
868 effect reduces as s is growing. In particular, ΔG_{+S}^0 of S^-S_s drops from -32.74 kcal mol⁻¹ at $s=1$ to
869 -10.58 kcal mol⁻¹ and -8.28 kcal mol⁻¹ at $s=3$ and 4 , respectively. At the same time, ΔG_{+A}^0 increases
870 from 0.08 kcal mol⁻¹ ($s=1$) to -11.89 kcal mol⁻¹ ($s=3$) and -15.37 kcal mol⁻¹ ($s=4$). The hydration
871 of S^-S_s at $s=3, 4$ enhances the strength of H_2SO_4 binding, especially at $s=4$. ΔG_{+S}^0 values for S^-S_3-
872 $4W_w$ are consistently $\sim 1.5 - 3$ kcal mol⁻¹ less negative than the corresponding semi-experimental
873 estimates (Table **A4**). The possible reasons behind the observed systematic difference are yet to
874 be identified and include the use of low-level *ab initio* HF method to compute reaction enthalpies
875 and uncertainties in experimental enthalpies in studies by Froyd and Lovejoy (2003).

876 NH_3 binding to S^-S_3 significantly enhances the stability of H_2SO_4 in the cluster by ~ 7 kcal mol⁻¹
877 compared to ΔG_{+S}^0 for the corresponding binary counterpart. The binding of the second NH_3 to
878 S^-S_3A to form $S^-S_3A_2$ is much weaker ($\Delta G_{+A}^0 = -7.27$ kcal mol⁻¹) than that of the first NH_3 molecule
879 ($\Delta G_{+A}^0 = -11.89$ kcal mol⁻¹). This indicates that most of $S^-S_3A_a$ can only contain one NH_3 molecule,
880 in a perfect agreement with the laboratory study of Schobesberger et al. (2015). In the case of S^-
881 S_4 , binding of the first ($\Delta G_{+A}^0 = -15.37$ kcal mol⁻¹) and second (and -12.23 kcal mol⁻¹) NH_3
882 molecules to the cluster is quite strong, while the attachment of NH_3 leads to substantial
883 stabilization of H_2SO_4 in the cluster, as evidenced by ΔG_{+S}^0 growing from -8.28 kcal mol⁻¹ at $a=0$
884

885 to $-11.76 \text{ kcal mol}^{-1}$ and $-16.71 \text{ kcal mol}^{-1}$ at $a=1$ and $a=2$, respectively. The NH_3 binding free
886 energy to $\text{S}^-\text{S}_4\text{A}_2$ (to form $\text{S}^-\text{S}_4\text{A}_3$) drops to $-7.59 \text{ kcal mol}^{-1}$, indicating, in agreement with the
887 CLOUD measurements (Schobesberger et al., 2015) that most of S^-S_4 clusters contain 1 or 2 NH_3
888 molecules.

889
890 **Acknowledgments.** The authors thank Richard Turco (Distinguished Professor Emeritus, UCLA)
891 for comments that helped to improve the manuscript. This study was supported by NSF under
892 grant 1550816, NASA under grant NNX13AK20G, and NYSERDA under contract 100416. ABN
893 would like to thank the Russian [Science Foundation and the Ministry of Education and Science](#)
894 [for its support and Education of Russia \(under grants 1.6198.2017/6.7 and 1.7706.2017/8.9\) for](#)
895 [support and the Center of Collective Use of MSTU Stankin for providing resources.](#)

896
897 **Data availability.** All relevant data are available in the article, or from the corresponding authors
898 upon request.

899 **References**

- 901 Almeida, J., et al., Molecular understanding of sulphuric acid–amine particle nucleation in the
902 atmosphere, *Nature*, 502, 359-363, 2013.
- 903 Ball, S. M., Hanson, D. R., Eisele, F. L., and McMurry, P. H., Laboratory studies of particle
904 nucleation: Initial results for H_2SO_4 , H_2O , and NH_3 vapors, *J. Geophys. Res.*, 104, 23709-23718,
905 10.1029/1999JD900411, 1999.
- 906 Bandy, A.R. and Ianni, J.C., Study of the hydrates of H_2SO_4 using density functional theory. *The*
907 *Journal of Physical Chemistry A*, 102(32), pp.6533-6539, 1998.
- 908 Behera, S. N., and M. Sharma, Investigating the potential role of ammonia in ion chemistry of fine
909 particulate matter formation for an urban environment, *The Science of the Total Environment*,
910 408(17), 3569-3575, 2010.
- 911 Benson, D. R., M. E. Erupe, and S.-H. Lee, Laboratory-measured H_2SO_4 - H_2O - NH_3 ternary
912 homogeneous nucleation rates: Initial observations, *Geophys. Res. Lett.*, 36, L15818,
913 doi:10.1029/2009GL038728, 2009.
- 914 Bork, N., Du, L., Reiman, H., Kurtén, T. and Kjaergaard, H.G., Benchmarking ab initio binding
915 energies of hydrogen-bonded molecular clusters based on FTIR spectroscopy, *Journal of*
916 *Physical Chemistry A*, 118(28), 5316-5322, 2014.
- 917 Bustos, D.J., Temelso, B. and Shields, G.C., Hydration of the Sulfuric Acid–Methylamine
918 Complex and Implications for Aerosol Formation. *The Journal of Physical Chemistry A*,
919 118(35), pp.7430-7441, 2014.

920 [Butler, T., Vermeulen, F., Lehmann, C. M., Likens, G. E., & Puchalski, M.. Increasing ammonia](#)
921 [concentration trends in large regions of the USA derived from the NADP/AMoN network.](#)
922 [Atmospheric Environment, 146, 132–140. 2016.](#)

923 Chen, M., M. Titcombe, J. Jiang, C. Kuang, M. L. Fischer, E. Edgerton, F. L. Eisele, J. I. Siepmann,
924 D. H. Hanson, J. Zhao, and P. H. McMurry, Acid-base chemical reaction model for nucleation
925 rates in the polluted boundary layer. *Proc. Nat. Acad. Sci.*, 109, 18713–18718, 2012.

926 Chon, N.L., Lee, S.H. and Lin, H., A theoretical study of temperature dependence of cluster
927 formation from sulfuric acid and ammonia. *Chemical Physics*, 433, pp.60-66, 2014.

928 Coffman, D. J., and Hegg, D. A., A preliminary study of the effect of ammonia on particle
929 nucleation in the marine boundary layer, *J. Geophys. Res.*, 100, 7147-7160, 1995.

930 Davidson, J. A., Fehsenfeld, F.C., Howard, C.J.: The heats of formation of NO_3^- and NO_3^-
931 association complexes with HNO_3 and HBr , *Int. J. Chem. Kinet.*, 9, 17, 1977.

932 Dawson M.L., et al., Simplified mechanism for new particle formation from methanesulfonic acid,
933 amines and water via experiments and ab initio calculations, *Proc Natl Acad Sci USA*
934 109:18719–18724, 2012.

935 DePalma, J.W., Bzdek, B.R., Doren, D.J. and Johnston, M.V., Structure and energetics of
936 nanometer size clusters of sulfuric acid with ammonia and dimethylamine, *Journal of Physical*
937 *Chemistry A*, 116(3), pp.1030-1040, 2012.

938 Doyle, G. J., Self-nucleation in the sulfuric acid-water system, *J. Chem. Phys.*, 35, 795–799, 1961.

939 Dunne, E. M., et al., Global particle formation from CERN CLOUD measurements, *Science*,
940 doi:10.1126/science.aaf2649, 2016.

941 Duplissy J., et al., Effect of ions on sulfuric acid-water binary particle formation: 2. Experimental
942 data and comparison with QC-normalized classical nucleation theory, *J. Geophys. Res. Atmos.*,
943 121, 1752–1775, doi:10.1002/2015JD023539, 2016.

944 Elm, J. and Mikkelsen, K.V., Computational approaches for efficiently modelling of small
945 atmospheric clusters, *Chemical Physics Letters*, 615, 26-29, 2014.

946 Elm, J., Bilde, M. and Mikkelsen, K.V., Assessment of binding energies of atmospherically
947 relevant clusters, *Physical Chemistry Chemical Physics*, 15(39), 16442-16445, 2013.

948 Elm, J., Bilde, M. and Mikkelsen, K.V., Assessment of density functional theory in predicting
949 structures and free energies of reaction of atmospheric prenucleation clusters, *Journal of*
950 *chemical theory and computation*, 8(6), 2071-2077, 2012.

951 Frisch, M. J., Trucks, G. W., Schlegel, H. B., Scuseria, G. E., Robb, M. A., Cheeseman, J. R.,
952 Scalmani, G., Barone, V., Mennucci, B., et al., *Gaussian 09*, Gaussian, Inc., Wallingford CT,
953 2009.

954 Froyd K. D., and Lovejoy E. R., Bond energies and structures of ammonia-sulfuric acid positive
 955 cluster ions, *J. Phys. Chem. A*, 116(24), 5886–5899, doi:10.1021/jp209908f, 2012.

956 Froyd, K. D., and Lovejoy, E. R., Experimental thermodynamics of cluster ions composed of
 957 H₂SO₄ and H₂O. 1. Positive ions, *J. Phys. Chem. A*, 107, 9800–9811, 2003.

958 Froyd, K. D., and Lovejoy, E. R., Experimental thermodynamics of cluster ions composed of
 959 H₂SO₄ and H₂O. 2. Measurements and ab initio structures of negative ions, *J. Phys. Chem. A*,
 960 107, 9812–9824, 2003.

961 Froyd, K. D., and Lovejoy, E. R., Experimental thermodynamics of cluster ions composed of
 962 H₂SO₄ and H₂O. 1. Positive ions, *J. Phys. Chem. A*, 107, 9800–9811, 2003.

963 Froyd, K. D., Ion induced nucleation in the atmosphere: Studies of NH₃, H₂SO₄, and H₂O cluster
 964 ions, Ph.D. thesis, Univ. of Colo., Boulder, 2002.

965 Glasoe, W. A., Volz, K., Panta, B., Freshour, N., Bachman, R., Hanson, D. R., McMurry, P. H.,
 966 and Jen, C.. Sulfuric acid nucleation: An experimental study of the effect of seven bases. *Journal*
 967 *of Geophysical Research: Atmospheres*, 120(5), 1933-1950, 2015.

968 Hamill, P., Turco, R. P., Kiang, C. S., Toon, O. B., & Whitten, R. C., An analysis of various
 969 nucleation mechanisms for sulfate particles in the stratosphere. *Journal of Aerosol Science*, 13,
 970 561–585, 1982.

971 Hanson, D. R., and F. Eisele, Diffusion of H₂SO₄ in humidified nitrogen: Hydrated H₂SO₄, *J. Phys.*
 972 *Chem. A*, 104, 1715 – 1719, 2000.

973 Hanson, D. R., and F. L. Eisele, Measurement of prenucleation molecular clusters in the NH₃,
 974 H₂SO₄, H₂O system, *J. Geophys. Res.*, 107(D12), 4158, doi:10.1029/2001JD001100, 2002.

975 Hanson, DR., Lovejoy, ER, Measurement of the thermodynamics of the hydrated dimer and
 976 trimers, *J. Phys. Chem. A* 110: 9525-9538 DOI: 10.1021/jp062844w, 2006.

977 Henschel, H., J. C. A. Navarro, T. Yli-Juuti, O. Kupiainen-Määttä, T. Olenius, I. K. Ortega, S. L.
 978 Clegg, T. Kurtén, I. Riipinen, and H. Vehkamäki, Hydration of atmospherically relevant
 979 molecular clusters: Computational chemistry and classical thermodynamics, *J. Phys. Chem. A*,
 980 118, 2599–2611, 2014.

981 Henschel, H., T. Kurtén, and H. Vehkamäki, Computational study on the effect of hydration on
 982 new particle formation in the sulfuric acid/ammonia and sulfuric acid/dimethylamine systems,
 983 *J. Phys. Chem. A*, 120, 1886–1896, doi:10.1021/acs.jpca.5b11366, 2016.

984 Herb, J., Y. Xu, F. Yu, and A. B. Nadykto, Large Hydrogen-Bonded Pre-Nucleation (HSO₄⁻
 985)(H₂SO₄)_m(H₂O)_k and (HSO₄⁻)(NH₃)(H₂SO₄)_m(H₂O)_k Clusters in the Earth's Atmosphere, *J.*
 986 *Phys. Chem., A*, 117, 133-152, DOI: 10.1021/jp3088435, 2013.

987 Herb., J., A. Nadykto, and F. Yu, Large Ternary Hydrogen-Bonded Pre-Nucleation Clusters in the
 988 Earth's Atmosphere, *Chemical Physics Letters*, 518, 7-14, 10.1016/j.cplett.2011.10.035, 2011.

989 Holland, P. M., and Castleman, A. W., Jr.: Thomson equation revisited in light of ion-clustering
990 experiments, *J. Phys. Chem.*; 86, 4181-4188, 1982.

991 Hoppel, W.A., and G. M. Frick, Ion-aerosol attachment coefficients and the steady-state charge
992 distribution on aerosols in a bipolar ion environment, *Aerosol Sci. Tech.*, 1-21, 1986.

993 Husar, D.E., Temelso, B., Ashworth, A.L. and Shields, G.C., Hydration of the bisulfate ion:
994 atmospheric implications. *The Journal of Physical Chemistry A*, 116(21), pp.5151-5163, 2012.

995

996 Hyvärinen, A., T. Raatikainen, A. Laaksonen, Y. Viisanen, and H. Lihavainen, Surface tensions
997 and densities of H₂SO₄ + NH₃ + water solutions, *Geophys. Res. Lett.*, 32, L16806,
998 doi:10.1029/2005GL023268, 2005~~Hyvärinen A., Heikki Lihavainen, Yrjö Viisanen, and~~
999 ~~Markku Kulmala, Homogeneous nucleation rates of higher n-alcohols measured in a laminar~~
1000 ~~flow diffusion chamber, *The Journal of Chemical Physics* 2004 120:24, 11621-11633, 2005.~~

1001 Ianni, J.C. and Bandy, A.R., A Density Functional Theory Study of the Hydrates of NH₃-H₂SO₄
1002 and Its Implications for the Formation of New Atmospheric Particles. *The Journal of Physical*
1003 *Chemistry A*, 103(15), pp.2801-2811, 1999.

1004 Jacobson, M., Turco, R., Jensen, E. and Toon O.: Modeling coagulation among particles of
1005 different composition and size, *Atmos. Environ.*, 28, 1327-1338, 1994.

1006 Jolly, William L., *Modern Inorganic Chemistry (2nd Edn.)*. New York: McGraw-Hill. ISBN 0-07-
1007 112651-1, 1991.

1008 Kazil, J., Lovejoy, E. R., Jensen, E. J., and Hanson, D. R.: Is aerosol formation in cirrus clouds
1009 possible?, *Atmos. Chem. Phys.*, 7, 1407-1413, <https://doi.org/10.5194/acp-7-1407-2007>, 2007.

1010 Kebarle, P., S. K. Searles, A. Zolla, J. Scarborough, and M. Arshadi, *J. Am. Chem. Soc.*, 89, 6393,
1011 1967.

1012 Kim, T. O., T. Ishida, M. Adachi, K. Okuyama, and J. H. Seinfeld, Nanometer-Sized Particle
1013 Formation from NH₃/SO₂/H₂O/Air Mixtures by Ionizing Irradiation, *Aerosol Science and*
1014 *Technology*, 29, 112-125, 1998.

1015 Kirkby, J., Curtius, J., Almeida, J., Dunne, E., Duplissy, J., et al., The role of sulfuric acid,
1016 ammonia and galactic cosmic rays in atmospheric aerosol nucleation, *Nature*, 476, 429-433,
1017 2011.

1018 Korhonen, P., Kulmala, M., Laaksonen, A., Viisanen, Y., McGraw, R., and Seinfeld, J. H., Ternary
1019 nucleation of H₂SO₄, NH₃, and H₂O in the atmosphere, *J. Geophys. Res.*, 104, 26,349-26,353,
1020 1999.

1021 Kurtén, T., Torpo, L., Ding, C.-G., Vehkamäki, H., Sundberg, M. R., Laasonen, K., and Kulmala,
1022 M.: A density functional study on water-sulfuric acid-ammonia clusters and implications for at-

- 1023 [atmospheric cluster formation, J. Geophys. Res., 112, D04210, doi:10.1029/2006JD007391,](#)
1024 [2007.](#)
- 1025 Kürten, A., et al., Experimental particle formation rates spanning tropospheric sulfuric acid and
1026 ammonia abundances, ion production rates, and temperatures, J. Geophys. Res. Atmos., 121,
1027 12,377–12,400, doi:10.1002/2015JD023908, 2016.
- 1028 Kürten, A., Münch, S., Rondo, L., Bianchi, F., Duplissy, J., Jokinen, T., Junninen, H., Sarnela, N.,
1029 Schobesberger, S., Simon, M. and Sipilä, M., Thermodynamics of the formation of sulfuric acid
1030 dimers in the binary (H₂SO₄–H₂O) and ternary (H₂SO₄–H₂O–NH₃) system. Atmospheric
1031 Chemistry and Physics, 15(18), pp.10701-10721, 2015.
- 1032 Laakso, L., Mäkelä, J. M., Pirjola, L., and Kulmala, M., Model studies of ion-induced nucleation
1033 in the atmosphere, J. Geophys. Res., 107, 4427, doi:10.1029/2002JD002140, 2003.
- 1034 Leverentz, H.R., Siepmann, J.I., Truhlar, D.G., Loukonen, V. and Vehkamäki, H., Energetics of
1035 atmospherically implicated clusters made of sulfuric acid, ammonia, and dimethyl amine,
1036 Journal of Physical Chemistry A, 117(18), 3819-3825, 2013.
- 1037 Lovejoy, E. R., Curtius, J., and Froyd, K. D., Atmospheric ion-induced nucleation of sulfuric acid
1038 and water, J. Geophys. Res., 109, D08204, doi:10.1029/2003JD004460, 2004.
- 1039 Ma, Y., Chen, J., Jiang, S., Liu, Y.R., Huang, T., Miao, S.K., Wang, C.Y. and Huang, W.,
1040 Characterization of the nucleation precursor (H₂SO₄–(CH₃)₂NH) complex: intra-cluster
1041 interactions and atmospheric relevance. RSC Advances, 6(7), pp.5824-5836, 2016.
- 1042 Marti, J. J., A. Jefferson, X. Ping Cai, C. Richert, P. H. McMurry, and F. Eisele, H₂SO₄ vapor
1043 pressure of sulfuric acid and ammonium sulfate solutions, J. Geophys. Res., 102(D3), 3725–3736,
1044 1997.
- 1045 McGrath, M. J., Olenius, T., Ortega, I. K., Loukonen, V., Paasonen, P., Kurtén, T., Kulmala, M.,
1046 and Vehkamäki, H.: Atmospheric Cluster Dynamics Code: a flexible method for solution of the
1047 birth-death equations, Atmos. Chem. Phys., 12, 2345-2355, doi:10.5194/acp-12-2345-2012,
1048 2012.
- 1049 Meng, Z., Xu, X., Lin, W., Xie, Y., Song, B., Jia, S., Zhang, R., Peng, W., Wang, Y., Cheng, H.,
1050 Yang, W., and Zhao, H., Role of ambient ammonia in particulate ammonium formation at a rural
1051 site in the North China Plain, Atmos. Chem. Phys. Discuss., [https://doi.org/10.5194/acp-2017-](https://doi.org/10.5194/acp-2017-174)
1052 174, in review, 2017.
- 1053 Meot-Ner (Mautner), M., The Ionic Hydrogen Bond and Ion Solvation. 2. Hydration of Onium
1054 Ions by 1 - 7 H₂O Molecules. Relations Between Monomolecular, Specific and Bulk Hydration,
1055 J. Am. Chem. Soc., 106, 5, 1265, 1984.

1056 Merikanto J., I. Napari, H. Vehkamäki, T. Anttila, M. Kulmala, New parameterization of sulfuric
1057 acid-ammonia-water ternary nucleation rates at tropospheric conditions, *J. Geophys. Res.*, 112,
1058 D15207, doi:10.1029/2006JD007977, 2007.

1059 Miao, S.K., Jiang, S., Chen, J., Ma, Y., Zhu, Y.P., Wen, Y., Zhang, M.M. and Huang, W.,
1060 Hydration of a sulfuric acid–oxalic acid complex: acid dissociation and its atmospheric
1061 implication, *RSC Advances*, 5(60), 48638-48646, 2015.

1062 Nadykto, A. B., A. Al Natsheh, F. Yu, K.V. Mikkelsen, and J. Herb, *Computational Quantum*
1063 *Chemistry: A New Approach to Atmospheric Nucleation*, *Advances in Quantum Chemistry*, 55,
1064 449-478, 2008.

1065 Nadykto, A. B., Al Natsheh, A., Yu, F., Mikkelsen, K. V., and Ruuskanen, J., Quantum nature of
1066 the sign preference in the ion-induced nucleation, *Physical Review Letters*, 96, 125701, 2006.

1067 Nadykto, A., and Yu, F., Uptake of neutral polar vapour molecules by charged particles:
1068 Enhancement due to dipole-charge interaction, *J. Geophys. Res.*, 108(D23), 4717,
1069 doi:10.1029/2003JD003664, 2003.

1070 Nadykto, A.B. and Yu, F., Strong hydrogen bonding between atmospheric nucleation precursors
1071 and common organics. *Chemical physics letters*, 435(1), pp.14-18, 2007a.

1072 Nadykto, A.B., Du, H. and Yu, F., Quantum DFT and DF–DFT study of vibrational spectra of
1073 sulfuric acid, sulfuric acid monohydrate, formic acid and its cyclic dimer. *Vibrational*
1074 *spectroscopy*, 44(2), pp.286-296, 2007b.

1075 Nadykto, A. B., F. Yu, and J. Herb, Theoretical analysis of the gas-phase hydration of common
1076 atmospheric pre-nucleation (HSO₄⁻)(H₂O)_n and (H₃O⁺)(H₂SO₄)(H₂O)_n cluster ions, *Chemical*
1077 *Physics*, 360, 67-73, doi:10.1016/j.chemphys.2009.04.007, 2009.

1078 Nadykto, A.B., Herb, J., Yu, F. and Xu, Y., Enhancement in the production of nucleating clusters
1079 due to dimethylamine and large uncertainties in the thermochemistry of amine-enhanced
1080 nucleation. *Chemical Physics Letters*, 609, 42-49, 2014.

1081 Nadykto, A.B., Herb, J., Yu, F., Nazarenko, E.S. and Xu, Y., Reply to the ‘Comment on
1082 “Enhancement in the production of nucleating clusters due to dimethylamine and large
1083 uncertainties in the thermochemistry of amine-enhanced nucleation”’ by Kupiainen-Maatta et al.
1084 *Chemical Physics Letters*, 624, 111-118, 2015.

1085 Napari, I, Noppel, M, Vehkamäki, H., Kulmala, M., An improved model for ternary nucleation of
1086 sulfuric acid–ammonia–water. *J. Chem. Phys.*, 116: 4221-4227, DOI: 10.1063/1.1450557, 2002.

1087 Olenius T., O. Kupiainen-Määttä, I. K. Ortega, T. Kurtén, and H. Vehkamäki, Free energy barrier
1088 in the growth of sulfuric acid–ammonia and sulfuric acid–dimethylamine clusters, *The Journal*
1089 *of Chemical Physics* 2013 139:8, 2013.

1090 Ortega, I. K., Kupiainen, O., Kurtén, T., Olenius, T., Wilkman, O., McGrath, M. J., Loukonen, V.,
1091 and Vehkamäki, H., From quantum chemical formation free energies to evaporation rates,
1092 Atmos. Chem. Phys., 12, 225-235, 2012.

1093 Payzant, J.D.; Cunningham, A.J.; Kebarle, P., Gas - Phase Solvation of Ammonium Ion by NH₃
1094 and H₂O and Stabilities of Mixed Clusters NH₄⁺(NH₃)_n(H₂O)_w, Can. J. Chem., 51, 19, 3242,
1095 1973.

1096 Peng, X.Q., Liu, Y.R., Huang, T., Jiang, S. and Huang, W., Interaction of gas phase oxalic acid
1097 with ammonia and its atmospheric implications, Physical Chemistry Chemical Physics, 17(14),
1098 9552-9563, 2015.

1099 Raes, F., A. Janssens, and R. V. Dingenen, The role of ion-induced aerosol formation in the lower
1100 atmosphere, J. Aerosol Sci., 17, 466–470, 1986.

1101 Schnitzhofer, R., et al., Characterisation of organic contaminants in the CLOUD chamber at
1102 CERN, Atmos. Meas. Tech., 7, 2159–2168, doi:10.5194/amt-7-2159-2014, 2014.

1103 Schobesberger, S., et al., On the composition of ammonia–sulfuric-acid ion clusters during aerosol
1104 particle formation, Atmos. Chem. Phys., 15, 55-78, <https://doi.org/10.5194/acp-15-55-2015>,
1105 2015.

1106 [Sipilä, M., Berndt, T., Petäjä, T., Brus, D., Vanhanen, J., Stratmann, F., Patokoski, J.,](#)
1107 [Mauldin, R. L., Hyvärinen, A. P., Lihavainen, H., and Kulmala, M.: The Role of](#)
1108 [Sulfuric Acid in Atmospheric Nucleation, Science, 327, 1243,](#)
1109 <https://doi.org/10.1126/science.1180315>, 2010.

1110 Sorokin, A., Arnold, F. and Wiedner, D., Formation and growth of sulfuric acid–water cluster ions:
1111 Experiments, modelling, and implications for ion-induced aerosol formation, Atmospheric
1112 Environment, 40, 2030-2045, 2006.

1113 Temelso, B., Morrell, T.E., Shields, R.M., Allodi, M.A., Wood, E.K., Kirschner, K.N.,
1114 Castonguay, T.C., Archer, K.A. and Shields, G.C., Quantum mechanical study of sulfuric acid
1115 hydration: Atmospheric implications. The Journal of Physical Chemistry A, 116(9), 2209-2224,
1116 2012a.

1117 Temelso, B., Phan, T.N. and Shields, G.C., Computational study of the hydration of sulfuric acid
1118 dimers: Implications for acid dissociation and aerosol formation, Journal of Physical Chemistry
1119 A, 116(39), pp.9745-9758, 2012b.

1120 Thomson, J. J., Applications of Dynamics to Physics and Chemistry, 1st ed., Cambridge University
1121 Press, London, 1888.

1122 Torpo, L., Kurtén, T., Vehkamäki, H., Laasonen, K., Sundberg, M.R. and Kulmala, M.,
1123 Significance of ammonia in growth of atmospheric nanoclusters. The Journal of Physical
1124 Chemistry A, 111(42), pp.10671-10674, 2007.

1125 Vehkamäki H., Kulmala, M., Napari, I., Lehtinen, K. E. J., Timmreck, C., Noppel, M., and
1126 Laaksonen, A., An improved parameterization for sulfuric acid–water nucleation rates for
1127 tropospheric and stratospheric conditions, *J. Geophys. Res.*, 107 (D22), 4622,
1128 doi:10.1029/2002JD002184, 2002.

1129 Warner, J. X., Wei, Z., Strow, L. L., Dickerson, R. R., & Nowak, J. B.. The global tropospheric
1130 ammonia distribution as seen in the 13-year AIRS measurement record. *Atmospheric Chemistry*
1131 *and Physics*, 16(8), 5467-5479. <https://doi.org/10.5194/acp-16-5467-2016>, 2016.

1132 Wilhelm, S., Eichkorn, S., Wiedner, D., Pirjola, L. and Arnold, F.: Ion-induced aerosol formation:
1133 new insights from laboratory measurements of mixed cluster ions, $\text{HSO}_4^-(\text{H}_2\text{SO}_4)_a(\text{H}_2\text{O})_w$ and
1134 $\text{H}^+(\text{H}_2\text{SO}_4)_a(\text{H}_2\text{O})_w$, *Atmos. Environ.*, 38, 1735-1744, 2004.

1135 Włodek, S., Z. Łuczyński, H. Wincel, Stabilities of gas-phase $\text{NO}_3^- (\text{HNO}_3)_n$, $n \leq 6$, clusters, In
1136 *International Journal of Mass Spectrometry and Ion Physics*, 35, 1–2, 1980, 39-46, 1980.

1137 Xu, W. and Zhang, R., A theoretical study of hydrated molecular clusters of amines and
1138 dicarboxylic acids, *Journal of chemical physics*, 139(6), p.064312, 2013.

1139 Xu, W. and Zhang, R., Theoretical investigation of interaction of dicarboxylic acids with common
1140 aerosol nucleation precursors, *Journal of Physical Chemistry A*, 116(18), 4539-4550, 2012.

1141 Yu, F., and Turco, R. P., The role of ions in the formation and evolution of particles in aircraft
1142 plumes, *Geophys. Res. Lett.*, 24, 1927-1930, 1997.

1143 Yu, F., and Turco, R. P., Ultrafine aerosol formation via ion-mediated nucleation, *Geophys. Res.*
1144 *Lett.*, 27, 883-886, 2000.

1145 Yu, F., and R. P. Turco: From molecular clusters to nanoparticles: The role of ambient ionization
1146 in tropospheric aerosol formation, *J. Geophys. Res.*, 106, 4797-4814, 2001.

1147 Yu, F. and Turco, R. P., The size-dependent charge fraction of sub-3-nm particles as a key
1148 diagnostic of competitive nucleation mechanisms under atmospheric conditions, *Atmos. Chem.*
1149 *Phys.*, 11, 9451–9463, doi:10.5194/acp-11-9451-2011, 2011.

1150 Yu, F., Modified Kelvin-Thomson equation considering ion-dipole interaction: Comparison with
1151 observed ion-clustering enthalpies and entropies, *J. Chem. Phys.*, 122, 084503, 2005.

1152 Yu, F., Effect of ammonia on new particle formation: A kinetic $\text{H}_2\text{SO}_4\text{-H}_2\text{O-NH}_3$ nucleation model
1153 constrained by laboratory measurements, *J. Geophys. Res.*, 111, D01204,
1154 doi:10.1029/2005JD005968, 2006a.

1155 Yu, F., From molecular clusters to nanoparticles: Second-generation ion-mediated nucleation
1156 model, *Atmos. Chem. Phys.*, 6, 5193-5211, 2006b.

1157 Yu, F., Improved quasi-unary nucleation model for binary $\text{H}_2\text{SO}_4\text{-H}_2\text{O}$ homogeneous nucleation,
1158 *J. Chem. Phys.*, 127, 054301, 2007.

1159 Zhang, R, Khalizov, AF, Wang, L, Hu,M, Wen,X., Nucleation and growth of nanoparticles in the
1160 atmosphere, Chem. Rev. 112: 1957-2011, DOI: 10.1021/cr2001756, 2012.

1161 Zhang, R., Wang, L., Khalizov, A.F., Zhao, J., Zheng, J., McGraw, R.L. and Molina, L.T.,
1162 Formation of nanoparticles of blue haze enhanced by anthropogenic pollution, Proceedings of
1163 the National Academy of Sciences, 106(42), 17650-17654, 2009.

1164 Zhang, Y., P. H. McMurry, F. Yu, and M. Z. Jacobson, A Comparative Study of Homogeneous
1165 Nucleation Parameterizations, Part I. Examination and Evaluation of the Formulations, J.
1166 Geophys. Res., 115, D20212, doi:10.1029/2010JD014150, 2010.

1167 Zhu, Y.P., Liu, Y.R., Huang, T., Jiang, S., Xu, K.M., Wen, H., Zhang, W.J. and Huang, W.,
1168 Theoretical study of the hydration of atmospheric nucleation precursors with acetic acid, Journal
1169 of Physical Chemistry A, 118(36), 7959-7974, 2014.

1170 Zollner, J. H., W. A. Glasoe, B. Panta, K. K. Carlson, P. H. McMurry, and D. R. Hanson, Sulfuric
1171 acid nucleation: Power dependencies, variation with relative humidity, and effect of bases,
1172 Atmos. Chem. Phys., 12(10), 4399–4411, doi:10.5194/acp-12-4399-2012, 2012.

1173

1174 **Table A1.** Number of isomers successfully converged at 6-311 level for selected clusters, along
 1175 with the enthalpy (H), entropy (S), and Gibbs free energy (G) of the most stable isomers.

1176

Cluster Formula	6-311++ conv.	Enthalpy (Hartree) H	Entropy (cal/K·mol)	Gibbs free energy (Hartree)
S ₄	56	-2801.256008	179.461	-2801.341276
S ₄ A ₁	169	-2857.820795	187.395	-2857.909833
S ₄ A ₂	84	-2914.388489	193.997	-2914.480663
S ₄ A ₃	68	-2970.94645	209.77	-2971.046119
S ₄ A ₄	38	-3027.500303	225.959	-3027.607663
S ₄ A ₅	34	-3084.050337	237.758	-3084.163303
S ⁻ S ₃	97	-2800.835072	168.993	-2800.915366
S ⁻ S ₃ A ₁	122	-2857.389946	184.899	-2857.477797
S ⁻ S ₃ A ₂	21	-2913.941409	192.489	-2914.032867
S ⁻ S ₃ A ₃	13	-2970.490814	195.627	-2970.583762
S ⁻ S ₄	138	-3501.162655	200.525	-3501.257931
S ⁻ S ₄ A ₁	71	-3557.727072	208.015	-3557.825907
S ⁻ S ₄ A ₂	22	-3614.287482	213.397	-3614.388874
S ⁻ S ₄ A ₃	23	-3670.836831	226.504	-3670.94445
S ⁻ S ₄ A ₄	18	-3727.385956	237.152	-3727.498634
H ⁺ A ₂	16	-113.413269	68.478	-113.445805
H ⁺ A ₂ W ₁	42	-189.845603	94.248	-189.890384
H ⁺ A ₂ W ₂	56	-266.276653	113.49	-266.330576
H ⁺ A ₂ W ₃	63	-342.706301	132.722	-342.769362
H ⁺ A ₂ W ₄	114	-419.133157	160.449	-419.209391
H ⁺ A ₂ W ₅	116	-495.567408	161.447	-495.644117
H ⁺ A ₂ W ₆	70	-571.994961	175.085	-572.078149
H ⁺ A ₂ W ₀ S ₁	40	-813.745253	107.764	-813.796455
H ⁺ A ₂ W ₁ S ₁	173	-890.181285	121.33	-890.238933
H ⁺ A ₂ W ₂ S ₁	103	-966.618165	130.584	-966.680209
H ⁺ A ₂ W ₃ S ₁	169	-1043.047622	154.145	-1043.120861
H ⁺ A ₂ W ₄ S ₁	188	-1119.476882	177.051	-1119.561004
H ⁺ A ₂ W ₅ S ₁	178	-1195.90253	200.029	-1195.99757
H ⁺ A ₂ W ₆ S ₁	85	-1272.330781	215.117	-1272.43299

1177

1178 **Table A2.** QC-based stepwise Gibbs free energy change (in kcal/mol) for the addition of one
 1179 water (ΔG_{+W}°), ammonia (ΔG_{+A}°), or sulfuric acid (ΔG_{+S}°) molecule to form the given positively
 1180 charged clusters under standard conditions, and the corresponding experimental data or semi-
 1181 experimental estimates.

	ΔG_{+W}°		ΔG_{+A}°		ΔG_{+S}°	
	QC	experimental	QC	experimental	QC	experimental
$H^+W_1S_1$					-28.59	-24.65 ^f
$H^+W_2S_1$	-15.66				-15.33	-13.76 ^f
$H^+W_3S_1$	-9.40				-10.12	-11.93 ^f
$H^+W_4S_1$	-7.83				-9.18	-9.71 ^f
$H^+W_5S_1$	-6.77	-5.79 ^a			-9.52	-9.82 ^f
$H^+W_6S_1$	-5.32	-4.24 ^a			-9.70	-9.94 ^f
$H^+W_7S_1$	-3.18	-3.28 ^a			-9.64	-9.96 ^f
$H^+W_8S_1$	-2.80	-2.67 ^a			-9.84	-10.10 ^f
$H^+W_9S_1$	-2.30	-2.12 ^a			-10.24	-10.86 ^f
$H^+A_1W_1$	-13.47	-13.01 ^b , -11.43 ^c	-52.08			
$H^+A_1W_2$	-9.85	-7.14 ^b , -8.17 ^c	-33.02			
$H^+A_1W_3$	-6.60	-5.92 ^b , -5.88 ^c	-25.01			
$H^+A_1W_4$	-3.50	-3.94 ^b , -4.06 ^c	-19.73			
$H^+A_1W_5$	-2.50	-2.55 ^b , -3.02 ^c	-15.80			
$H^+A_1W_6$	-2.26	-2.54 ^b	-12.93			
$H^+A_1W_7$	-1.15	-1.84 ^b	-10.84			
$H^+A_1W_8$	-1.02		-9.26			
$H^+A_1W_9$	0.25		-8.32			
H^+A_2			-22.97	-18.25 ^c		
$H^+A_2W_1$	-7.04	-6.85 ^c	-16.53	-11.54 ^c , -12.75 ^d		
$H^+A_2W_2$	-4.29	-5.25 ^c	-10.97	-9.13 ^c , -9.50 ^d		
$H^+A_2W_3$	-3.41	-3.70 ^c	-7.78	-6.83 ^c , -7.02 ^d		
$H^+A_2W_4$	-3.08		-7.36			
$H^+A_2W_5$	-1.97		-6.82			
$H^+A_2W_6$	-0.42		-4.99			
$H^+A_1W_1S_1$	-8.99		-33.14		-9.65	-8.3 ^d
$H^+A_1W_2S_1$	-8.11		-25.59		-7.90	-7.1 ^d
$H^+A_1W_3S_1$	-6.09		-22.28		-7.40	-6.7 ^d
$H^+A_1W_4S_1$	-4.25		-18.71		-8.15	-6.9 ^d
$H^+A_1W_5S_1$	-1.92		-13.85		-7.56	-7.5 ^d
$H^+A_1W_6S_1$	-2.04		-10.57		-7.34	-8.0 ^d
$H^+A_2W_0S_1$			-22.09	-22.14 ^e	-13.35	-16.8 ^d

H ⁺ A ₂ W ₁ S ₁	-5.72	-18.92	-12.03	-15.8 ^d
H ⁺ A ₂ W ₂ S ₁	-4.97	-15.78	-12.71	-15.9 ^d
H ⁺ A ₂ W ₃ S ₁	-4.58	-14.27	-13.89	-16.3 ^d
H ⁺ A ₂ W ₄ S ₁	-4.26	-14.27	-15.06	-17.3 ^d
H ⁺ A ₂ W ₅ S ₁	-2.01	-14.37	-15.11	-18.8 ^d
H ⁺ A ₂ W ₆ S ₁	-1.29	-13.63	-15.98	-19.9 ^d

1183 ^a Froyd and Lovejoy, 2003; ^b Meot-Ner (Mautner) et al., 1984; ^c Payzant et al., 1973; ^d Froyd, 2002; ^e
1184 Froyd and Lovejoy, 2012. ^f The ΔG_{+S}° values given here were calculated based on experimental ΔG_{+S}°
1185 values at T=270 K from Froyd and Lovejoy (2003) and ΔS values from quantum calculation.

1186

1187
1188

Table A3. Same as Table A2 except for neutral clusters.

	ΔG_{+W}°		ΔG_{+A}°		ΔG_{+S}°	
	QC	experimental	QC	experimental	QC	experimental
S1A1			-7.77 ^a (-7.29 ^b , -7.61 ^c , -6.60 ^d)	-8.2 ^e	-7.77 ^a (-7.29 ^b , -7.61 ^c , -6.60 ^d)	-8.2 ^e
S1A1W1	-1.39 ^a		-6.88 ^a			
S1A1W2	-2.30 ^a		-6.18 ^a			
S1A1W3	-1.52 ^a		-5.81 ^a			
S1A2			-4.75			
S1A2W1	-0.78		-4.15			
S2A1			-13.84 ^a		-11.65 ^a	
S2A1W1	-2.31 ^a		-12.77		-12.59 ^a	
S2A1W2	-1.21 ^a		-11.00		-11.52 ^a	
S2A1W3	-2.04 ^a		-9.69		-12.04 ^a	
S2A2			-8.75		-15.65	
S2A2W1	-1.96		-8.37		-16.83	
S2A2W2	-1.19		-8.35		-15.49	
S2A2W3	0.60		-5.71		-14.42	
S2A3			-4.19			
S3A1			-16.14		-7.08	
S3A2			-13.84		-12.17	
S3A3			-8.93		-16.92	
S3A4			-7.42			
S4A1			-15.74		-4.16	
S4A2			-17.16		-7.48	
S4A3			-13.79		-12.34	
S4A4			-11.34		-16.26	
S4A5			-7.63			

1189 ^a Nadykto and Yu, 2007; ^b Torpo et al., 2007; ^c Ortega et al., 2012; ^d Chon et al., 2007; ^e Kurten et al.,
1190 2015.
1191

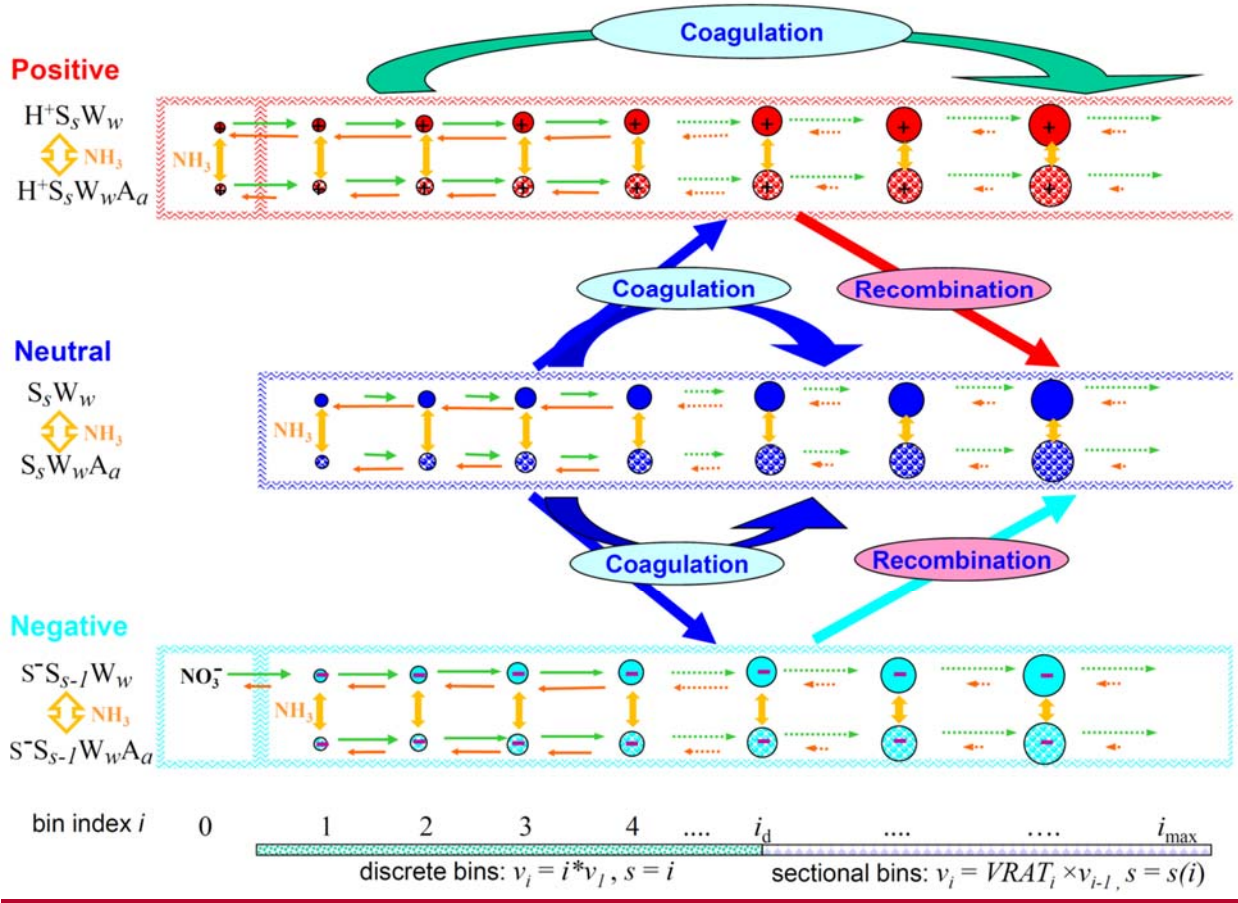
1192
1193

Table A4. Same as Table A2 except for negatively charged clusters.

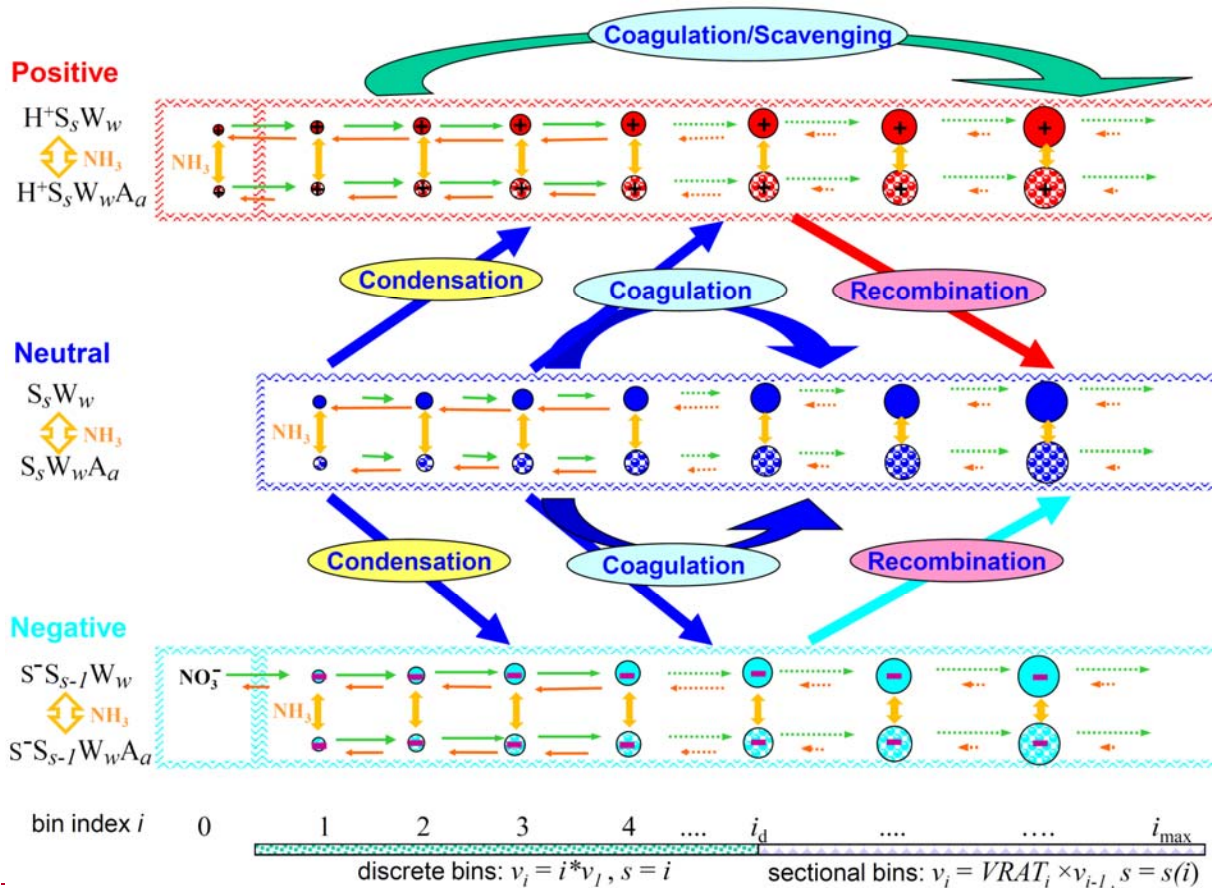
	ΔG_{+W}°		$\Delta G_{+\Delta}^{\circ}$		ΔG_{+S}°	
	QC	experimental	QC	experimental	QC	experimental
S ⁻ A ₁			2.81			
S ⁻ S ₁ W ₀					-32.74	-29.10 ^a
S ⁻ S ₁ W ₁	-0.61				-28.12	
S ⁻ S ₁ W ₂	-1.06				-25.36	
S ⁻ S ₁ A ₁			0.08		-35.47	
S ⁻ S ₂ W ₀					-15.06	-17.14 ^a
S ⁻ S ₂ W ₁	-1.83				-16.28	
S ⁻ S ₂ A ₁			-4.85		-19.99	
S ⁻ S ₃ W ₀					-10.58	-13.28 ^a
S ⁻ S ₃ W ₁	-2.92	-2.73 ^a			-11.67	-14.29 ^a
S ⁻ S ₃ W ₂	-2.03	-1.53 ^a			-11.12	-13.80 ^a
S ⁻ S ₃ W ₃	-2.01	-1.93 ^a			-11.52	-14.72 ^a
S ⁻ S ₃ W ₄	-1.73					
S ⁻ S ₃ A ₁ W ₀			-11.89		-17.62	
S ⁻ S ₃ A ₁ W ₁	0.52		-8.45		-14.90	
S ⁻ S ₃ A ₁ W ₂	0.39		-6.03		-13.06	
S ⁻ S ₃ A ₂			-7.27		-18.36	
S ⁻ S ₃ A ₃			-4.66			
S ⁻ S ₄ W ₀					-8.28	-10.96 ^a
S ⁻ S ₄ W ₁	-3.50	-2.61 ^a			-8.86	-10.71 ^a
S ⁻ S ₄ W ₂	-3.17	-2.79 ^a			-9.99	-12.10 ^a
S ⁻ S ₄ W ₃	-2.65	-2.41 ^a			-10.64	-12.48 ^a
S ⁻ S ₄ W ₄	-2.25	-2.14 ^a			-11.16	-12.77 ^a
S ⁻ S ₄ A ₁ W ₀			-15.37		-11.76	
S ⁻ S ₄ A ₁ W ₁	-2.21		-14.09		-14.49	
S ⁻ S ₄ A ₁ W ₂	-0.74		-11.66		-15.62	
S ⁻ S ₄ A ₂			-12.23		-16.71	
S ⁻ S ₄ A ₃			-7.59		-19.65	
S ⁻ S ₄ A ₄			-6.72			

1194 ^a Froyd and Lovejoy, 2003.

1195



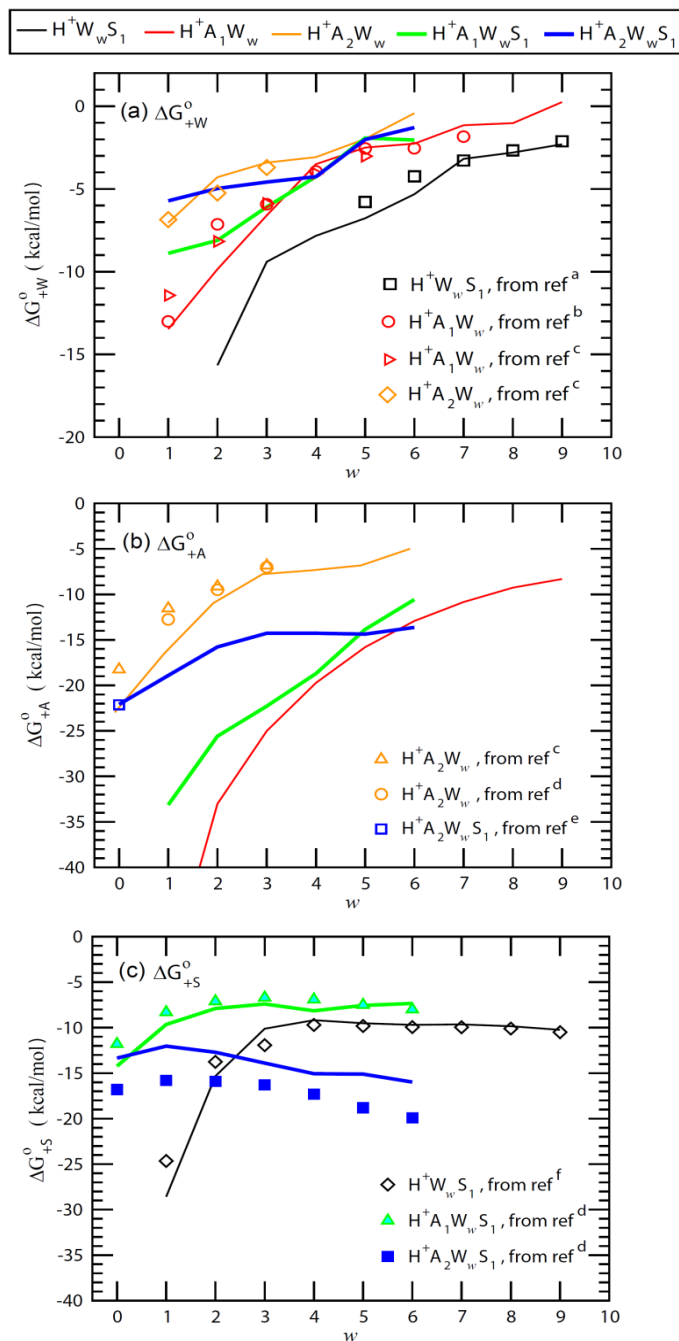
1197



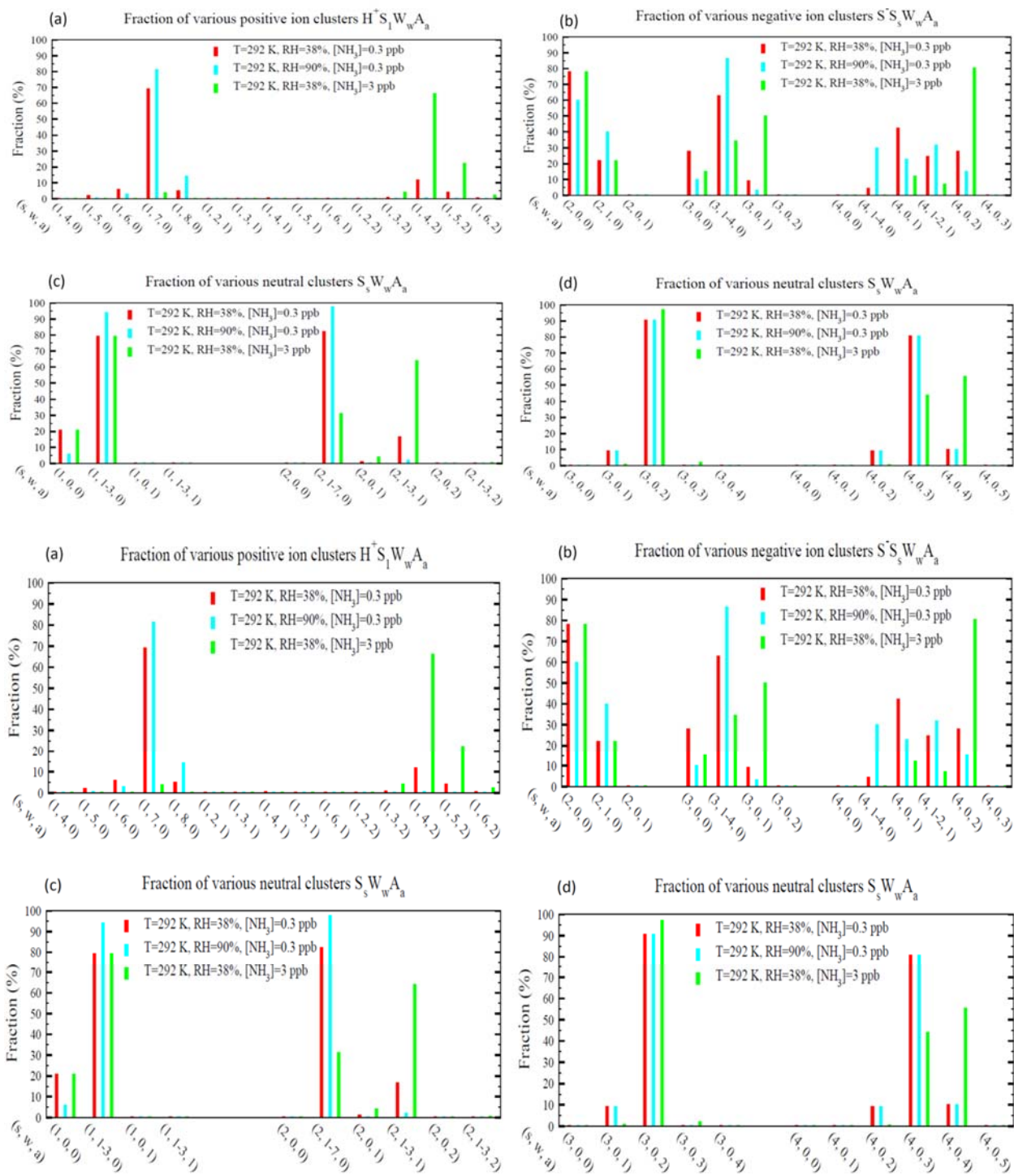
1198
1199

1200 **Figure 1.** Schematic illustration of kinetic processes controlling the evolution of positively
 1201 charged ($H^+S_sW_wA_a$), neutral ($S_sW_wA_a$), and negatively charged ($S^-S_{s-1}W_wA_a$)
 1202 clusters/droplets that are explicitly simulated in the ternary ion-mediated nucleation (TIMN)
 1203 model. Here S, W, and A represent sulfuric acid (H_2SO_4), water (H_2O), and ammonia (NH_3)
 1204 respectively, while s , w , and a refer to the number of S, W, and A molecules in the clusters/droplets,
 1205 respectively. The TIMN model has been extended from an earlier version treating binary IMN
 1206 (BIMN) by adding NH_3 into the nucleation system and using a discrete-sectional bin structure to
 1207 represent the sizes of clusters/particles starting from a single molecule up to background particles
 1208 larger than a few micrometers.

1209



1210
 1211 **Figure 2.** Stepwise Gibbs free energy change under standard conditions for the addition of a water
 1212 (ΔG°_{+W}), ammonia (ΔG°_{+A}), or sulfuric acid (ΔG°_{+S}) molecule to form the given positively charged
 1213 clusters as a function of the number of water molecules in the clusters (w). Lines are QC-based
 1214 values, and symbols are experimental results or semi-experimental estimates (see notes under
 1215 Table [A2](#) for the references).



1216

1217

1218

1219 **Figure 3.** Relative abundance (or molar fraction) of small clusters containing a given number of

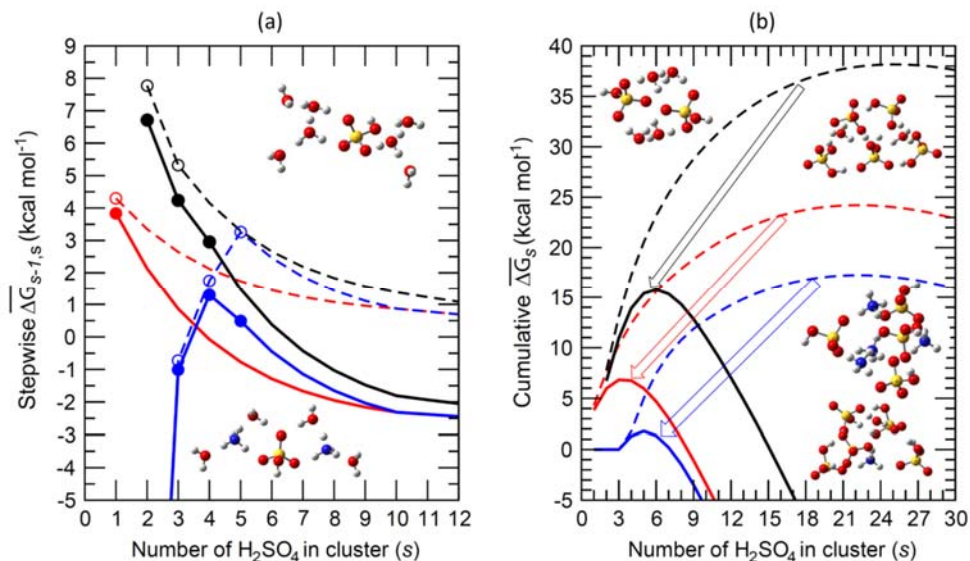
1220 H₂SO₄ molecules for positive, negative, and neutral cluster types at a temperature of 292 K and

1221 three different combinations of RHs (38% and 90%) and [NH₃] (0.3 and 3 ppb). Some clusters
1222 with different numbers of water molecules were grouped together to make the plot more clear and
1223 neat. For the clusters shown in panel (d), there is no hydrate data and thus hydration for these
1224 clusters were not calculated.

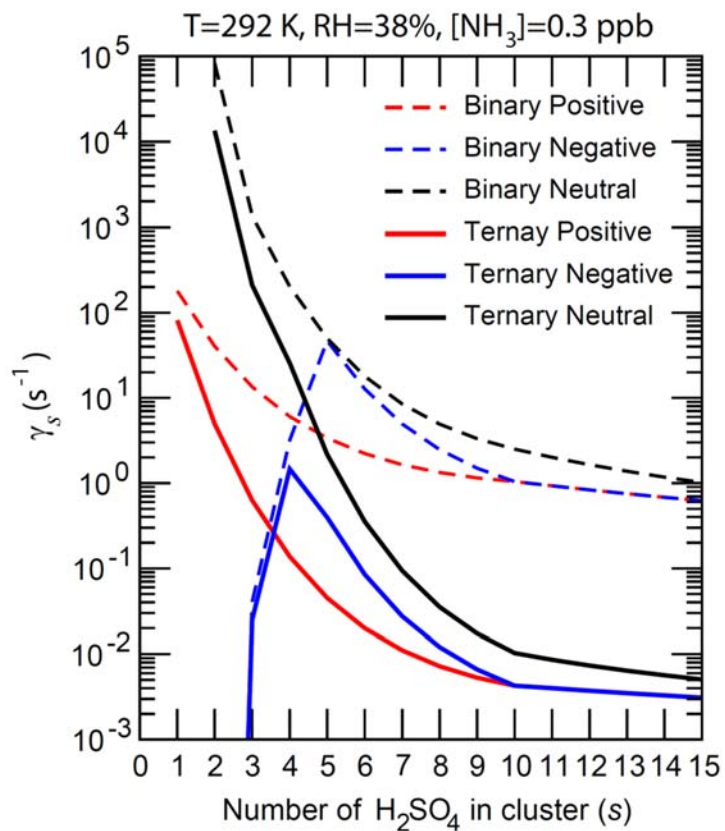
1225

1226

1227



1229 **Figure 4.** (a) Average stepwise Gibbs free energy change for the addition of one H₂SO₄ molecule
 1230 to form a neutral (black), positively charged (red), or negatively charged (blue) binary H₂SO₄-H₂O
 1231 (dashed lines or empty circles) or ternary H₂SO₄-H₂O-NH₃ (solid lines or filled circles) cluster
 1232 containing s H₂SO₄ molecules ($\overline{\Delta G}_{s-1,s}$); (b) Same as (a) but for the cumulative (total) Gibbs free
 1233 energy change in each case. Filled and empty circles in (a) refer to $\overline{\Delta G}_{s-1,s}$ obtained using
 1234 measurements and/or quantum-chemical calculations. $\overline{\Delta G}_{s-1,s}$ for larger clusters with $s \geq 10$, which
 1235 approach the properties of the equivalent bulk liquid (20), are calculated using the capillarity
 1236 approximation. Interpolation is used to calculate $\overline{\Delta G}_{s-1,s}$ for clusters up to $s=10$ (Eq. 11).
 1237 Calculations were carried out at $T=292$ K, $RH=38\%$, $[H_2SO_4]=3 \times 10^8 \text{ cm}^{-3}$ and $[NH_3]= 0.3$ ppb.
 1238 The inset diagrams represent equilibrium geometries for the most stable isomers of selected binary
 1239 clusters ($(H_3O^+)(H_2SO_4)(H_2O)_6$, $(H_2SO_4)_2(H_2O)_4$, and $(HSO_4^-)(H_2SO_4)_4(H_2O)_2$), and ternary
 1240 clusters ($(NH_4^+)(H_2SO_4)(NH_3)(H_2O)_4$, $(HSO_4^-)(H_2SO_4)_4(H_2O)(NH_3)$, $(H_2SO_4)_4(NH_3)_4$).

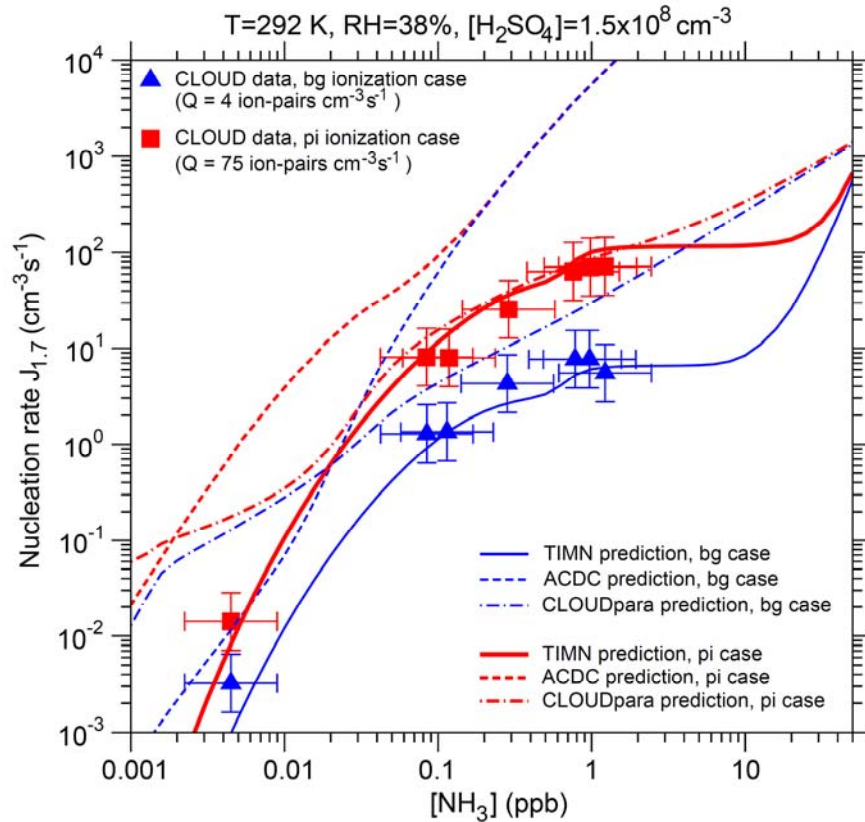


1243
 1244 **Figure 5.** The number-concentration-weighted mean evaporation rates ($\bar{\gamma}$) of H_2SO_4 molecules
 1245 from neutral clusters (black), positively charged clusters (red), and negatively charged clusters
 1246 (blue) for binary ($\text{H}_2\text{SO}_4\text{-H}_2\text{O}$, dashed lines) and ternary ($\text{H}_2\text{SO}_4\text{-H}_2\text{O-NH}_3$, solid lines) nucleating
 1247 systems containing s H_2SO_4 molecules ($\overline{\Delta G_{s-1,s}}$). $T=292$ K, $\text{RH}=38\%$, and $[\text{NH}_3] = 0.3$ ppb for
 1248 the ternary system.

1249

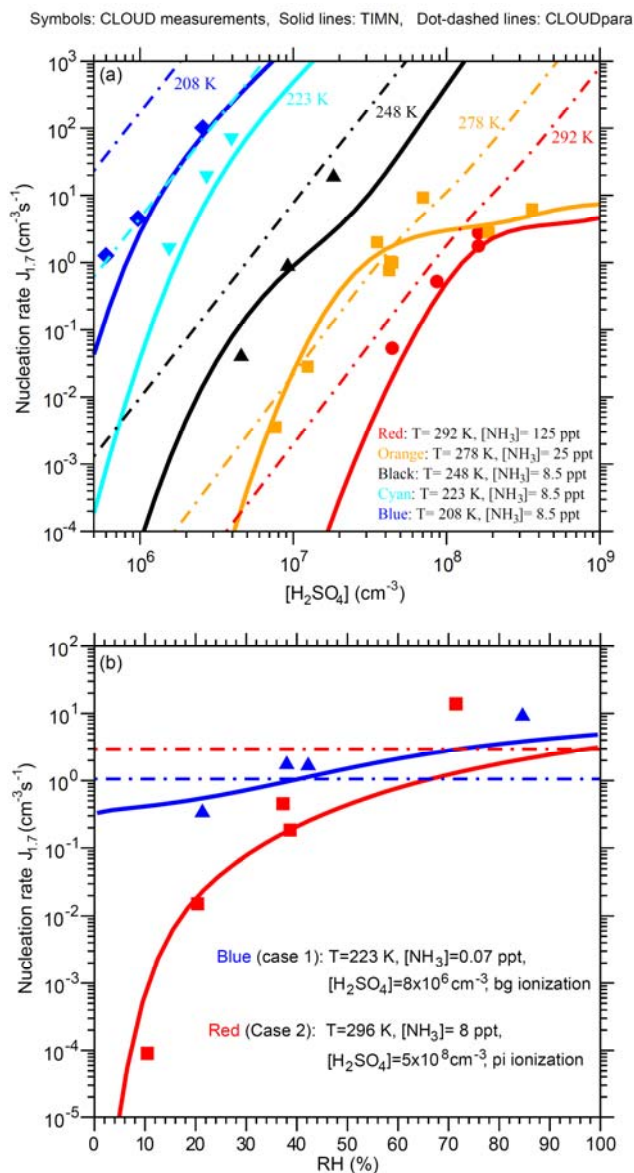
1250

1251



1252

1253 **Figure 6.** Effect of ammonia concentrations ($[\text{NH}_3]$) on effective nucleation rates calculated at a
 1254 cluster mobility diameter of 1.7 nm ($J_{1.7}$, lines) under the stated conditions with two ionization
 1255 rates (Q) – background ionization, bg (blue), and ionization enhanced by a pion beam, pi (red).
 1256 Also shown are predictions from the TIMN model, the Atmospheric Cluster Dynamics Code
 1257 (ACDC) with thermochemistry obtained using RI-CC2//B3LYP method (McGrath et al., 2012;
 1258 Kurten et al., 2016), and an empirical parameterization of CLOUD measurements (CLOUDpara)
 1259 (Dunne et al., 2016) are indicated by solid, dashed, and dot-dashed lines, respectively. The symbols
 1260 refer to CLOUD experimental data (Kirkby et al., 2011; Dunne et al., 2016), with the uncertainties
 1261 in measured $[\text{NH}_3]$ and $J_{1.7}$ shown by horizontal and vertical bars, respectively. To be comparable,
 1262 the CLOUD data points given in Dunne et al. (2016) under the conditions of $T=292$ K and
 1263 $\text{RH}=38\%$ with $[\text{H}_2\text{SO}_4]$ close to $1.5 \times 10^8 \text{ cm}^{-3}$ have been interpolated to the same $[\text{H}_2\text{SO}_4]$ value
 1264 ($=1.5 \times 10^8 \text{ cm}^{-3}$).

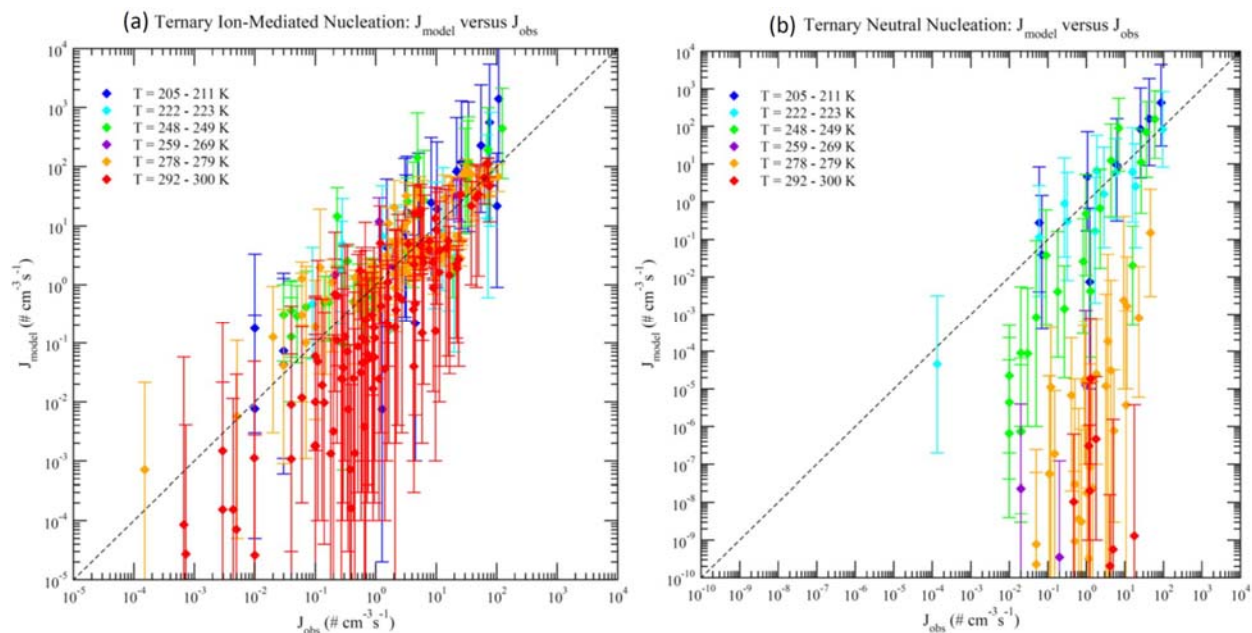


1265

1266 **Figure 7.** Comparison of TIMN simulations (solid lines), CLOUDpara predictions (Dunne et al.,
 1267 2016) (dot-dashed lines) and CLOUD measurements (symbols, data from Dunne et al. (2016) of
 1268 the dependences of nucleation rates on (a) $[\text{H}_2\text{SO}_4]$ at five different temperatures ($T = 292, 278,$
 1269 $248, 223,$ and 208 K) and (b) RH at two sets of conditions as specified. $[\text{NH}_3]$ is in ppt (parts per
 1270 trillion, by volume). Error bars for the uncertainties in measured $[\text{H}_2\text{SO}_4]$ (-50%, +100%), $[\text{NH}_3]$
 1271 (-50%, +100%), and $J_{1.7}$ (overall a factor of two) are not shown. To be comparable, the CLOUD
 1272 data points given in Dunne et al. (2016) under the conditions ($T, \text{RH},$ ionization rate) with $[\text{NH}_3]$
 1273 or $[\text{H}_2\text{SO}_4]$ close to the corresponding values specified in the figure legends have been interpolated
 1274 to the same $[\text{NH}_3]$ (Fig. 7a) or $[\text{H}_2\text{SO}_4]$ (Fig. 7b) values.

1275

1276



1277

1278 **Figure 8.** Model predicted (J_{model}) versus observed (J_{obs}) nucleation rates under various conditions
 1279 of all 377 data points of CLOUD measurements reported in Table S1 of Dunne et al. (2016), with
 1280 (a) and without (b) the presence of ionization. The data points are grouped according to
 1281 temperatures as specified in the legend. Vertical error bars show the range of J_{model} calculated at
 1282 50% and 200% of measured $[\text{H}_2\text{SO}_4]$, corresponding to the uncertainties in measured $[\text{H}_2\text{SO}_4]$ (-
 1283 50%, +100%). Error bars associated with the uncertainties in measured $[\text{NH}_3]$ (-50%, +100%), and
 1284 J_{obs} (overall a factor of two) are not shown.